NOTE TO USERS

CO_2 Capture and Bioconversion to Biogas in an Anaerobic System using an UASB Reactor

Mahmood Alimahmoodi

A thesis in

Department of Building, Civil and Environmental Engineering

Presented in Partial Fulfillment of the Requirements

For the Degree of Master of Applied Science at Concordia University

Montreal, Quebec, Canada

March 2004

Your file Votre référence
ISBN: 0-612-90990-5
Our file Notre référence
ISBN: 0-612-90990-5

ABSTRACT

CO_2 Capture and Bioconversion to Biogas in an Anaerobic System using an UASB Reactor

Mahmood Alimahmoodi

Carbon dioxide is the most dominant component of greenhouse gases and its increasing level in the atmosphere has been of growing concern for many years. There have been many methods to reduce carbon dioxide emissions in the form of CO_2 capture and storage, for example, through its injection into underground waters, saline waters or aquifers in which, CO_2 is transferred from one place to another. However, with these approaches there is always the risk of CO_2 release to the environment.

In this research, a new method for capture and conversion of carbon dioxide in an anaerobic system with an UASB (Upflow Anaerobic Sludge Blanket) reactor (1 L working volume) at 35°C is developed. Acetic acid and mixed VFAs (Volatile Fatty Acids) were tested as sources of hydrogen. The system performance was evaluated based on CO_2 and COD (Chemical Oxygen Demand) removals. Values of 68.7%-85.78% were obtained for CO_2 removal and the overall efficiency values were above 50% for loading rates up to 25 gCOD/L.d with a high methane content (>70%) in the biogas.

Also, in a set of batch experiments, kinetic parameters were obtained using experimental data and a numerical method that was developed in this study to solve the differential equations for substrate utilization and biomass growth.

The method can be applied to reduce CO_2 emitted to the atmosphere from a wide variety of industrial point sources with a value added product, methane.

AKNOWLEDGEMENTS

"Problems can not be solved at the same level of awareness that created them"

Albert Einstein

First and foremost, I would like to express my gratitude to my supervisor Dr. Catherine Mulligan for her expert guidance and suggestions for this thesis.

I would like to thank Mr. Ron Parisella for his cooperation, help and guidance in the laboratory.

Also, I would like to acknowledge the financial support provided by Concordia University to do this work.

TABLE OF CONTENTS

CHAPTER 5: CONCLUSIONS AND RECOMMENDATIONS

LIST OF TABLES

LIST OF FIGURES

List of Symbols

BOD	Biological Oxygen Demand
b	Death rate (1/d)
C	Concentration
COD	Chemical Oxygen Demand
c	centi (1/100)
D	Dilution rate (1/d)
d	day
EP	Enzyme-Product Complex
EPA	Environmental Protection Agency
h	hour
Hac	Acetic acid
HBu	Butyric acid
HPr	Propionic acid
HRT	Hydraulic Retention Time
K	Reaction constant- Reaction rate ($gCOD/m^3.d$)
k_{max}	Maximal reaction rate ($gCOD/m^3.d$)
k_d	Biomass death rate (1/d)
K_m	Michaelis constant (same unit as S)
K_s	Half-saturation constant (same unit as S)
L	Liter
m	meter
M	Molecular weight - Molar (mole/L)
η	Efficiency

μ	Growth rate (1/d)
μ_{max}	Maximum growth rate (1/d)
ν	Specific substrate utilization rate (1/d)
OLR	Organic Loading Rate
P	Pressure- Product
pH	power of Hydrogen
S	Substrate - Substrate concentration
t	time
T	Temperature
TA	Total Alkalinity
TSS	Total suspended solids
UASB	Upflow Anaerobic Sludge Blanket
V	Volume
V_{max}	Maximum velocity (or reaction rate with the unit of K_m/t)
VFA	Volatile Fatty Acid
VSS	Volatile suspended solids
X	Biomass concentration (g/L or mg/L)

CHAPTER 1

INTRODUCTION

1.1 Problem Statement

1.1.1 Global Warming

Global mean surface temperatures of the Earth have increased 0.4-1.0°C since the late 19th century. The last 15 years of the 20th century, were the warmest years of the century. Of these, 1998 was the warmest year on record. The snow cover in the Northern Hemisphere and floating ice in the Arctic Ocean have decreased. Globally, sea level has risen 10-20 cm over the past century. Worldwide precipitation over land has increased by about one percent (http://yosemite.epa.gov/oar/globalwarming.nsf/content).

Increasing concentrations of greenhouse gases are likely to accelerate the rate of climate change. Scientists expect that the average global surface temperature could rise

0.6-2.5°C in the next fifty years, and 1.4-5.8°C in the next century, which would have the following circumstances:

- significant regional climate variations

- continental heartlands will dry out more in summer

- declining soil moisture in many regions

- increasing evaporation and average global precipitation, which can increase sea levels and cause intense rainstorms. This will in turn increase flooding in coastal areas and river estuaries.

- storms and hurricanes will become more frequent and stronger as oceans heat up causing more water to evaporate.

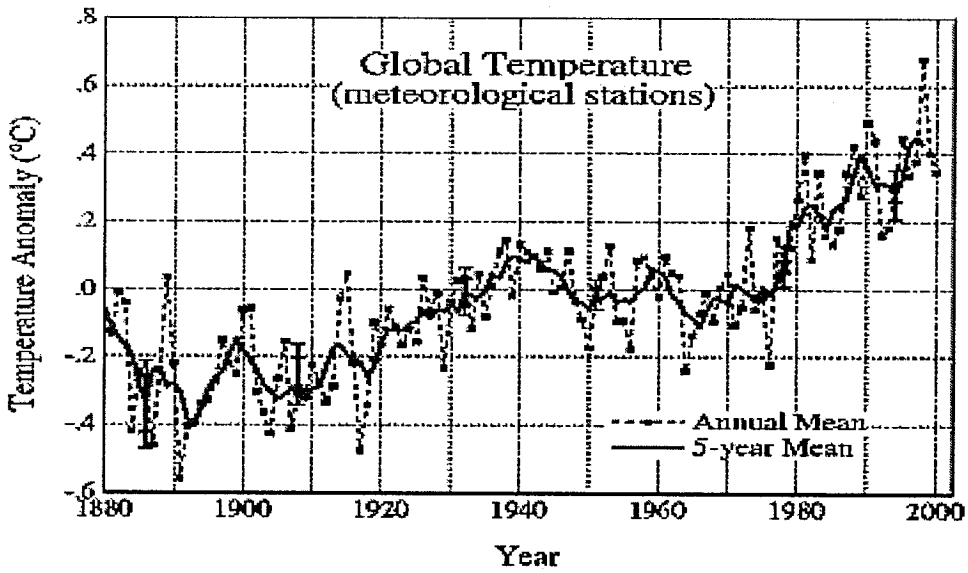

Figure 1.1 Variation of the global temperature (1880-2000) [source: http://www.swales.wea.org.uk/myweb2/Desktop/what%20is.htm]

1.1.2 Greenhouse Gases and their effect

Atmospheric greenhouse gases as shown in Figure 1.2, consist of water vapor, carbon dioxide, and other gases. Energy from the sun drives the Earth's weather and

climate, and heats the Earth's surface; in turn, the Earth radiates energy back into space. Greenhouse gases trap some of the outgoing energy, retaining heat as in a greenhouse.

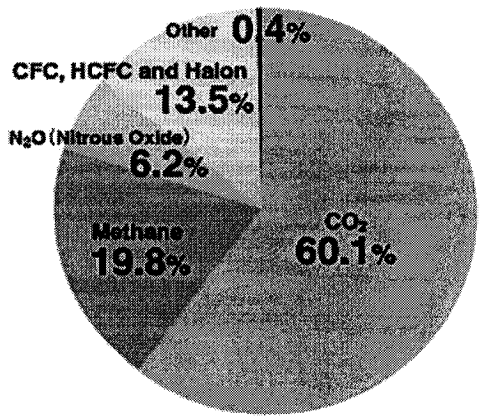

Figure 1.2 The percentage of the Greenhouse Gases in the atmosphere (http://www.virtualglobe.org/en/info/env/01/gw05.html)

They allow visible light to reach the Earth's surface, but then trap the resulting long-wavelength heat radiation that would otherwise escape to space. Figure 1.3 shows a schematic of this phenomenon.

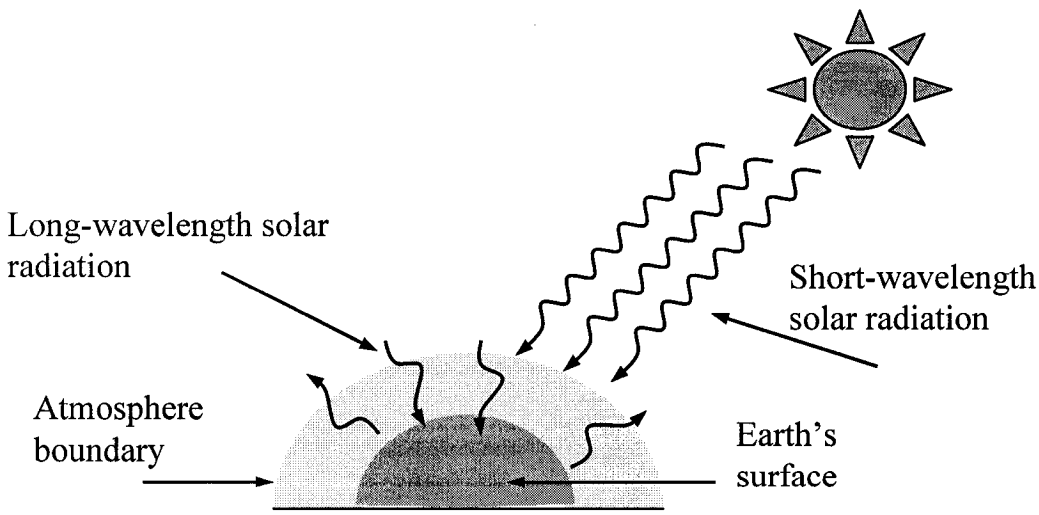

Figure 1.3 Schematic of heat-trapping function of GHGs

Without this natural "greenhouse effect," temperatures would be much lower than they are now, and life as it is known today would not be possible. Due to this phenomenon, the Earth's average temperature is about 16°C. However, problems arise when the atmospheric concentration of greenhouse gases increases. Regulations to limit some greenhouse gases (GHGs) have gone into effect in many countries around the world. Attempts have been made to reduce the production of GHGs on a global scale. In the Kyoto conference on climate change in 1997, countries from around the world agreed to reduce their annual GHG emissions to a target level of minus 6% in 2010 relative to the 1990 level, estimated to have been equivalent to 526 megatons of CO_2 (Reeve, 2000).

1.1.3 Carbon Dioxide

Carbon dioxide is the most dominant component of greenhouse gases and its increasing level in the atmosphere has been of growing concern for many years. Since the beginning of the industrial revolution, atmospheric concentrations of carbon dioxide have increased nearly 30%, methane concentrations have more than doubled, and nitrous oxide concentrations have risen by about 15%. These increases have enhanced the heat-retaining capacity of the Earth's atmosphere. As shown in Figure 1.4, the level of carbon dioxide in the world's atmosphere has increased from about 280 ppm in 1850 to approximately 350 ppm in 2000.

It is generally known that the combustion of fossil fuels and other human activities are the primary reasons for the increased concentration of carbon dioxide.

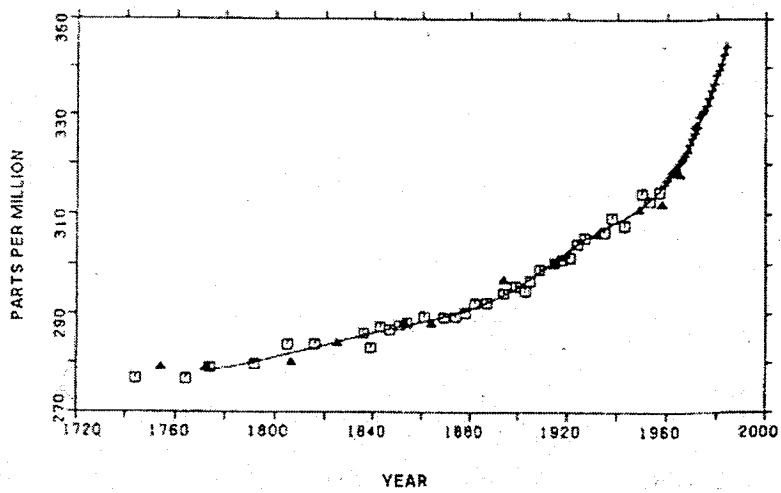

Figure 1.4 Trends of atmospheric carbon dioxide content (ppm).
(Source: http://www.iitap.iastate.edu/gcp/chem/gases/gases_lecture.html)

Although plant respiration and the decomposition of organic matter release more than 10 times the CO_2 released by human activities, until the industrial revolution, these emissions have generally been in balance during the centuries with carbon dioxide absorbed by terrestrial vegetation and the oceans. Figure 1.5 shows a block diagram of the sources and sinks of carbon dioxide in nature.

(http://yosemite.epa.gov/oar/globalwarming.nsf/webprintview/Climate.html)

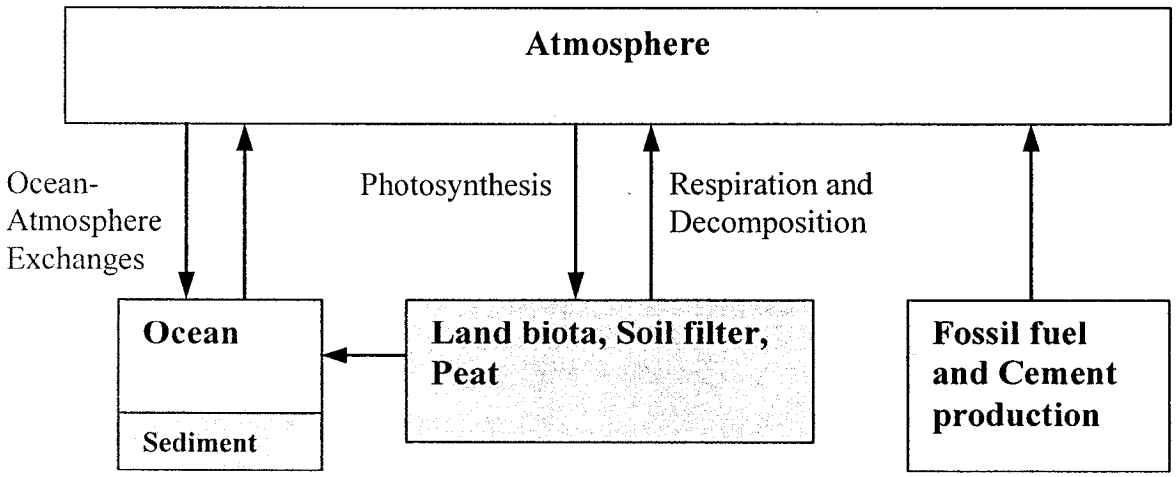

Figure 1.5 Block diagram of the sinks and sources in carbon cycle

Natural sources and sinks of carbon dioxide are respiration by plants (source), photosynthesis by plants (sink), and physico-chemical diffusion in the oceans (source and sink), which have remained in balance for thousands of years. The population growth and change in life style have increased the combustion of fossil fuels and the deforestation of tropical areas, which in turn, have resulted in an exponential increase in the carbon dioxide levels in the atmosphere.

1.2 Carbon Dioxide Mitigation

Carbon dioxide mitigation has been the subject of much research. The underground disposal technology for carbon dioxide is a method of reducing atmospheric emissions of carbon dioxide to prevent global warming. In this technology, which will be discussed more in Chapter 2, carbon dioxide is separated from emission sources like power plants, and then is stored in some reservoirs such as aquifers, or depleted gas and oil reservoirs.

The efforts to reduce CO_2 emissions in power plants can be classified in three categories:

1. Improvements in fuel utilization to reduce CO_2 emissions and increase efficiency.
2. Using biofuels in power generation systems with traditional power cycles or developing new technologies.
3. Using CO_2 separation methods as pre- or post-treatment techniques.

CO_2 separation methods are generally divided to two major groups:

1) Physical and /or chemical techniques. These techniques can be employed separately or all in one process. Using absorption and regeneration towers (Tontiwachwuthikul, 1996), application of liquid membranes to separate CO_2 from flue gas (Chakma, 1995) and CO_2 capture using integrated air separation and flue gas recycling (Shao and Golomb, 1997) are several examples of these techniques.

2) Biological techniques. Several biological techniques to capture or convert CO_2 in the flue gas from power generation units have been proposed. Examples of these techniques are summarized as follows:

- Photosynthetic systems in which cyanobacteria consume CO_2 for their growth using sunlight (Otaguchi *et al.*, 1997).
- Carbon fixation through conversion of CO_2 to inorganic carbonates using special types of microalgae that can withstand harsh conditions associated with the flue gas (Maeda *et al.*, 1995).
- CO_2 reduction to methane and/or acetate in a bio-electro reactor where the immobilized bacteria on the cathodic electrodes, convert CO_2 to CH_4/acetate using H_2 gas produced by the electrolysis of water on the cathode side (Kuroda and Watanabe, 1995).

1.3 Objectives of this study

Special types of bacteria called methanogens are able to convert carbon dioxide to methane under anaerobic condition using hydrogen. In an anaerobic process, which will

be discussed more in Chapter 2, several types of microorganisms are involved in converting complex molecules to simpler ones along with hydrogen and carbon dioxide.

Methanogens are involved in the final step of an anaerobic process to convert simple organic molecules, CO_2 and H_2 to methane. Therefore, it is possible to provide methanogens with the required chemicals and nutrients in order to convert CO_2 to methane.

In this work, a method to capture and convert CO_2 to biogas with high methane content in an anaerobic system is developed. The main objectives of this study were:

1- to establish an anaerobic system to convert CO_2 to methane,

2- to investigate kinetic characteristics of the system and methanogenic activity of the microorganisms,

3- to investigate the system performance under different conditions and evaluate its overall efficiency.

CHAPTER 2

LITERATURE REVIEW

2.1 Anaerobic treatment and methanogenesis

2.1.1 Introduction

In 1776, Alessandro Volta performed some experiments on combustible air that were reported to him by a friend, Father Carlo Campi. On a little boat in Lake Maggiore he started to poke and stir the bottom of an area covered with reeds. Upon doing this, Volta noticed a lot of air emerging and decided to collect some in a large glass container. Upon analysis of the air he noted that it burned a beautiful blue flame. Nearly half a century later it was shown that the methane formation in these habitats was by a microbial process (Ferry, 1993).

2.1.2 Anaerobic digestion

Anaerobic digestion refers to various reactions and interactions that take place among the *methanogens*, *non-methanogens* and substrates fed into a digester as inputs. As shown schematically in Figure 2.1, this is a complex physio-chemical and biological process involving different stages and factors.

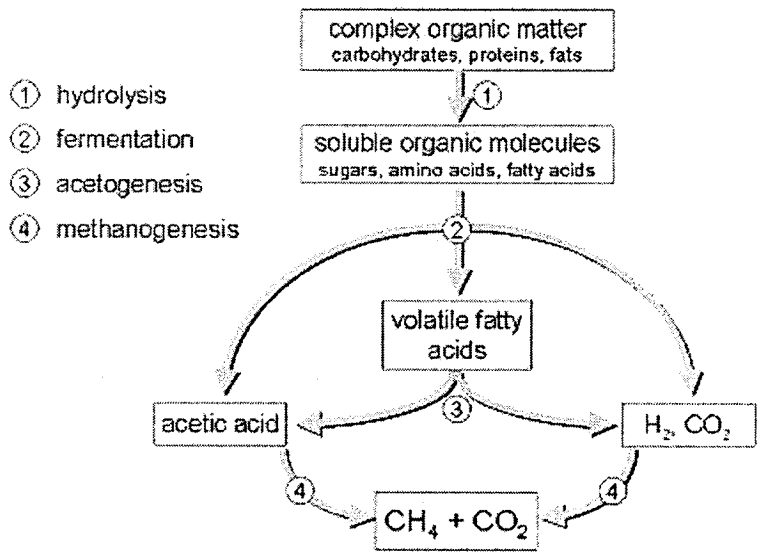

Figure 2.1 Schematic of the pathway of anaerobic digestion (http://www.biotank.co.uk/anaerobic_digestion.htm)

Input materials that are complex organic compounds are broken down through 4 stages (as described below).

2.1.2.1 Hydrolysis

The waste materials of plant and animal origin consist mainly of carbohydrates, lipids, proteins and inorganic materials. Large molecular complex substances are solubilized into simpler ones with the help of extracellular enzymes released by the

bacteria. This stage is also known as the polymer breakdown stage. For example, the cellulose consisting of polymerized glucose is broken down to dimeric, and then to monomeric sugar molecules (glucose) by cellulolytic bacteria.

2.1.2.2 Fermentation or acidogenesis

In this step, the monomeric molecules such as glucose, which are produced in the previous step, are fermented under anaerobic conditions into various acids with the help of enzyme produced by the acid-forming bacteria. They break down molecules of six atoms of carbon (glucose) into molecules of fewer atoms of carbon (acids). The principal acids produced in this process are acetic, propionic and butyric acids.

2.1.2.3 Acetogenesis

In this step, the fermentation products are converted into acetate, hydrogen and carbon dioxide by so-called acetogenic bacteria.

2.1.2.4 Methanogenesis

In this step, methane (CH_4) is formed from acetate and hydrogen/carbon dioxide by a special group of anaerobic bacteria called *methanogens*.

2.1.3 Methanogens

Methanogenic archaea are all obligate anaerobes, in fact, they are the strictest anaerobes discovered (Harley *et al.*,1990, Holt *et al.*, 1994). *Methanogens*, as their name implies, produce methane (CH_4) as a byproduct of metabolism (Ingraham *et al.*, 1986,

Holt *et al.* 1994). No other known living things are methanogenic, and therefore their metabolic enzymes are unique (Holt *et al.*, 1994).

Methanogens can be found in a variety of waters from freshwaters to hypersaline waters. There are many types of *methanogens*, but a few known to be extremely halophilic are methylotrophs belonging to the *Methanosarcinaceae*. Sowers and Gunsalus (1988) reported a type of salt-adapted *Methanosarcina* (Ferry, 1993).

The catabolic pathways of *methanogens* can be divided into three groups: CO_2-reducing, methyltrophic, and acetoclastic pathways. Most *methanogens* can grow using H_2 as a source of electrons via hydrogenase. H_2 is a major fermentation product in many species of anaerobic bacteria, fungi and protozoa. In many methanogenic environments, this H_2 is utilized rapidly even when it is present at very low concentrations (Wolin, 1976). Many H_2-using *methanogens* also can use formate as an electron donor for the reduction of CO_2 to CH_4. Like H_2, formate may be an important substrate for methanogenesis even though its concentration in methanogenic environments is low, because it is rapidly produced and consumed (Boone *et al.*, 1989; Hungate *et al.*,1970; Thiele and Zeikus, 1988).

A limited number of *methanogens* can also utilize secondary alcohols for CO_2 reduction to methane, and an even smaller number can use some primary alcohols (Bleincher *et al.*, 1989; Maestrojuan *et al.*, 1990; Widdel, 1986; Widdel *et al.*, 1988; Zellner and Winter, 1987a).

Methylotrophic pathways catabolize compounds that contain methyl groups, such as methanol (Schnellen, 1947), trimethylamine (Hippe *et al.*, 1979), and dimethyl sulfate (Kiene *et al.*, 1986; Mathrani *et al.*, 1988; Oremland *et al.*, 1989). Typically the methyl

group is transferred to a methyl carrier (ultimately to coenzyme M) and reduced to methane. Electrons for this methyl reduction may be obtained by oxidizing a fraction of methyl groups to CO_2 or by using H_2 as an electron donor.

Acetate is degraded by many methylotrophic *methanogens* and by some rod-shaped *methanogens*. This catabolic pathway (called the acetoclastic pathway) splits acetate, oxidizes the carboxyl group to CO_2 and reduces the methyl group to methane. The most widespread catabolic reactions carried out by *methanogens* are shown in Table 2.1. Acetate is the ultimate product of many fermentative pathways and can be an important CH_4 precursor in many habitats (Ferry, 1993).

Table 2.1 Energy-yielding reactions of *methanogens* (From Ferry, 1993)

Reaction			**$\Delta G°$(kJ/mol CH_4)**
$4\ CO + 2\ H_2O$	⟶	$CH_4 + 3\ CO_2$	-211
$4\ H_2 + CO_2$	⟶	$CH_4 + 2\ H_2O$	-130.4
$CH_3OH + H_2$	⟶	$CH_4 + H_2O$	-112.5
$4\ CH_3OH$	⟶	$3\ CH_4 + CO_2 + 2\ H_2O$	-106
$4\ CH_3NH_2 + 2H_2O$	⟶	$3\ CH_4 + CO_2 + 4\ NH_3$	-76.7
$4\ (CH_3)_3N + 6H_2O$	⟶	$9\ CH_4 + 3\ CO_2 + 4\ NH_3$	-75.8
$2\ (CH_3)_2NH + 2H_2O$	⟶	$3\ CH_4 + CO_2 + 2\ NH_3$	-74.8
$(CH_3)SH + H_2$	⟶	$CH_4 + H_2S$	-69.3
$2(CH_3)_2S + 2H_2O$	⟶	$3\ CH_4 + CO_2 + 2\ H_2S$	-52.1
$4(CH_3)SH + 2H_2O$	⟶	$3\ CH_4 + CO_2 + 4\ H_2S$	-51.0
$CH3COO^- + H^+$	⟶	$CH_4 + CO_2$	-36.0

There are two types of acetate-consuming *methanogens*: *Methanosarcina* and *Methanothrix*. The latter is able to grow on several substrates and grows faster than the

former at high acetic acid concentrations although it is very sensitive to changes in those concentrations (Grady, 1999). The family *Methanothrix* (or *Methanosaeta*) that only uses acetate is not influenced so strongly by the acetic acid concentration and can compete effectively when it is low.

Many attempts have been made to formulate expressions to describe the methabolism kinetics of microorganisms and estimate their kinetic parameters. Most of these studies have been based on two famous models: Michaelis Menten or Monod models.

2.1.3.1 Kinetics of the biodegradation reactions

The kinetics of the biodegradation reactions are empirically driven and are mostly described by the following general expressions:

$$\frac{dC_A}{dt} = -k_0 \qquad \text{Zero order} \qquad (2\text{-}1)$$

$$\frac{dC_B}{dt} = -k_1 C_A \qquad \text{First order} \qquad (2\text{-}2)$$

$$\frac{dC_B}{dt} = -k_2 C_A C_B \qquad \text{Second order} \qquad (2\text{-}3)$$

k_0, k_1, k_2 = rate constants mol/1.sec, 1/sec, 1/mol.sec, respectively

C_A, C_B = some reacting species

t = time

This can be applied to the reaction of the compounds with a surface such as a metal catalyst, a soil surface or an enzyme. Two extreme cases can be considered; the first is when there are few molecules of reactant, C_A, compared to many of the surface. In this case, a few of the available sites will be covered, so the reaction rate dC_A/dt is

proportional to the concentration of C_A (first order reaction above). Secondly, when C_A is so large that every site is saturated with A, the rate is constant (zero order reaction above). Therefore, in a general case, the rate expression can be written;

$$\frac{dC_A}{dt} = \frac{-k_0 C_A}{k' + C_A} \qquad (2\text{-}4)$$

where $k' = \frac{k_0}{k_1}$

This is the very common biological form of the equation for growth on a substrate as the concentration of the substrate is increased. It leads to Michaelis-Menten (or Monod-) type kinetics.

An enzymatic reaction can be written in a general form as below:

$$S \longrightarrow P \qquad (2\text{-}5)$$

where S and P represent substrate and product. This reaction takes place in several steps: First the substrate (S) binds to the enzyme (E), to form the enzyme-substrate complex (ES), the substrate is converted to the product (P), and a new enzyme-product complex (EP) is formed. Finally, the latter dissociates to the enzyme and free product (P). The whole process can be expressed as follows:

$$S + E \rightleftharpoons ES \longrightarrow EP \longrightarrow E + P \qquad (2\text{-}6)$$

The Michaelis-Menten model leads to the conclusion that the relationship between the rate of reaction (v) and the concentration of (S) in the reaction follows the following equation:

$$-\frac{dS}{dt} = v = \frac{v_{max}.S}{K_m + S} \qquad (2\text{-}7)$$

where: v_{max} = maximal reaction rate ($gCOD/m^3.d$)

S = Substrate concentration ($gCOD/m^3$)

t = time (d) and

v = substrate utilization rate

A typical curve resulting from this equation is shown in Figure 2.2. The parameter K_m is a is the value of S when $v = v_{max}/2$ and indicates the tightness of binding of E to S and therefore, the substrate affinity of the enzyme.

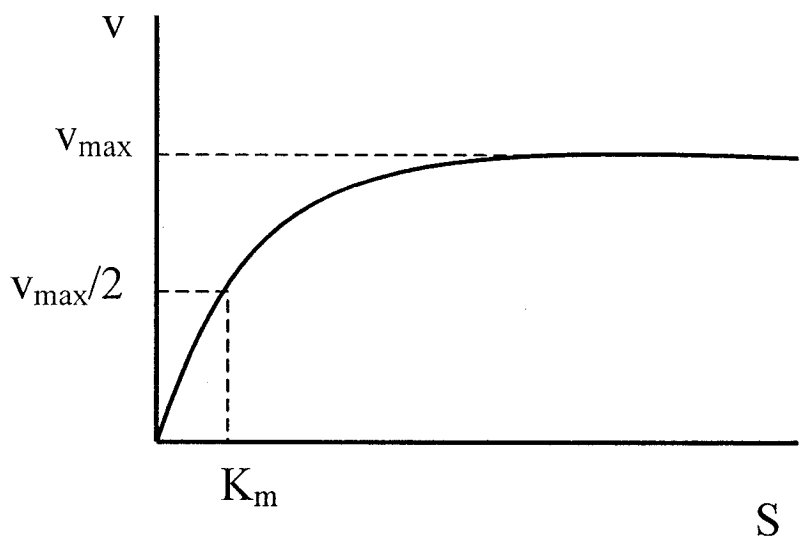

Figure 2.2 Relation between substrate utilization rate and substrate concentration in Michelis-Menten model.

Michelis-Menten equations often can be used to estimate kinetic parameters of biological processes. Michaelis-Menten kinetics were formulated on the basis of constant catalyzing material (enzymes), and are applicable to a situation in which the growth of microbial cells participating in the degradation is not significant. In other words, the value of v_{max} should not change during substrate consumption (De Zeeuw, 1984).

Bacterial growth kinetics are slightly more complex and follow the classical kinetics proposed by Monod (1950), who studied the fermentation of grape sugars to alcohol.

In this case, the rate of substrate utilisation is proportional to the concentration of the microorganisms present, X, and is a function of the substrate concentration. The Monod bacterial growth kinetics are traditionally written as:

$$\mu = \mu_{\max} \frac{S}{K_s + S} \tag{2-8}$$

where

S = Substrate concentration

μ = Specific growth rate of microorganisms (1/d)=Relative increase of mass per time unit

μ_{max} = Maximum specific growth rate (1/d)

K_s = Monod constant (at which the rate of growth is half the maximum rate) (gCOD/L)

In this case, K_s is the value of S when $\mu = \mu_{max}/2$. Monod model yields an S-shaped (sigmoidal) substrate depletion curve in batch experiments (Robinson and Tiedje, 1983). Since $\frac{dX}{dt} = \mu X$ and $Y = \frac{dX}{dS}$, where Y= growth yield factor (gVSS/gCOD), it can be derived that:

$$-\frac{dS}{dt} = \frac{\mu_{\max} S}{K_s + S} \cdot \frac{X}{Y} \tag{2-9}$$

In the present work, the Monod model is employed for the growth rate of the microorganisms. Also, a 1st- order death rate is considered which is proportional to the microbial population. The basic equations used in this work can be summarized as follows:

$$(\frac{dX}{dt})_g = Y(\frac{dS}{dt}) = X\mu = \frac{X\mu_m S}{S + K_s} \tag{2-10}$$

$$(\frac{dX}{dt})_d = -k_d X \tag{2-11}$$

where:

k_d = Death rate constant (1/d)

Indices "g " and "d" = " growth" and " death" respectively.

Table 2.2 shows the values of specific growth rate and half-saturation constant for two types of *methanogens*.

Table 2.2 Specific growth rate and half-saturation constant in Monod model for *Methanotrix* and *Methanosarcina* (T = 33°C- From Ferry, 1993)

Parameter	**Culture**	
	Methanosarcina	***Methanotrix***
μ_{max} **(1/d)**	**0.3**	**0.1**
K_s **(mg/L)**	**200**	**30**

The maximum specific growth rates of these acetate-consuming microorganisms are μ_m =0.1 and 0.3 (1/d), respectively. The specific growth rate is at half its maximum value when the substrate concentration is equal to the parameter K_s, which for that reason, is called the half-saturation constant (Van Haandel and Lettinga, 1994).

Therefore, the manner in which an anaerobic operation is designed and operates will determine the predominant acetoclastic *methanogens* (Boone *et al.*,1993).

Methanogens have different shapes regarding their morphology. Figure 2.3 shows some micrographs of these microorganisms.

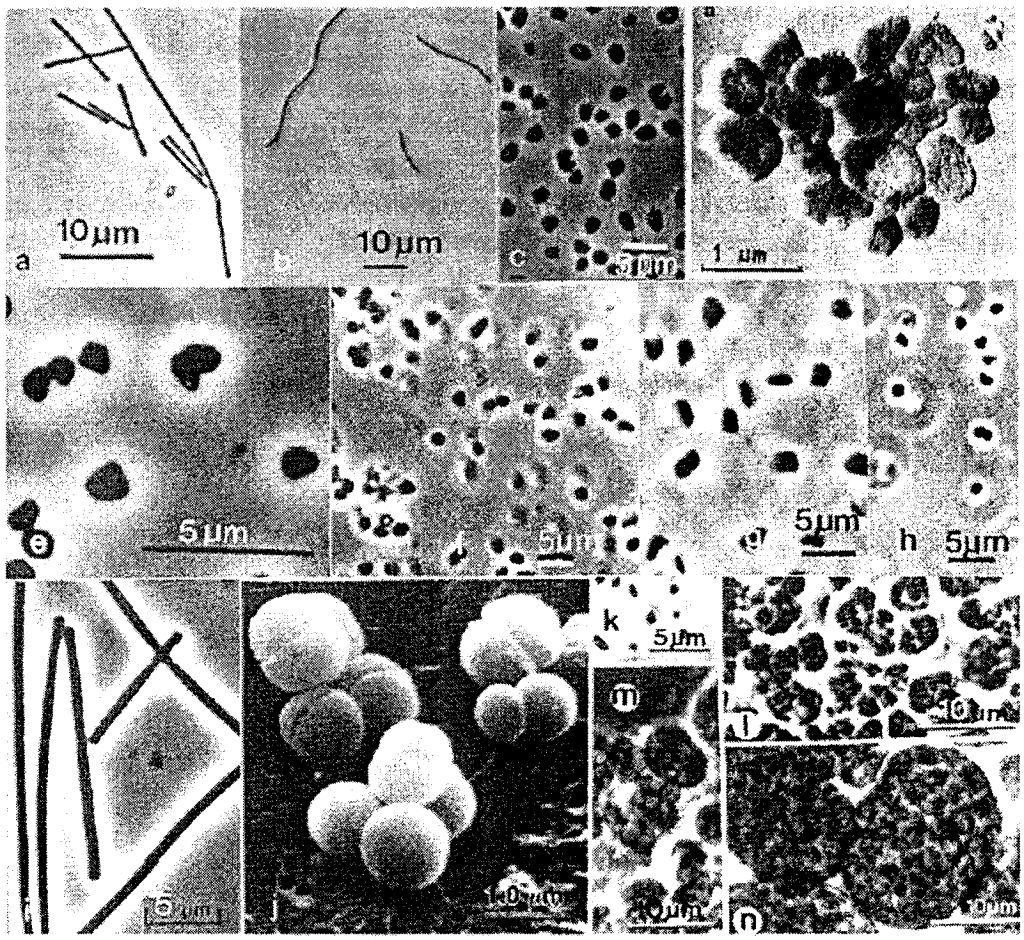

Figure 2.3 Morphology of methanogen cells (Ferry, 1993)

Rod-shaped *methanogens* are illustrated by *Methanobacterium spp.* or *Methanopyrus kandleri* (Figure 2.3a). Some *methanogens* have such a distinctive shape that they can be tentatively identified by light microscopy even in mixed cultures. These are *Methanospirillum* (long thin spirals, Figure 2.3b), *Methanosaeta* ("*Methanothrix*") (Patel, 1992) (also long but thicker filaments, Figure 2.3i), and *Methanosarcina* (clusters of round cells, Figure 2.3, l-n). Examples of the round-shaped or coccoid *methanogens* are *Methanogenium* (Figure 2.3 c), *Methanococcus* (Figure 2.3 h), *Methanocorpusculum* (Figure 2.3 d), *Methanococcoides* (Figure 2.3e), *Methanolobus* (Figure 2.3f), *Methanohalophilus* (Liu *et al.*, 1990), and *Methanoculleus* (Blotevogel *et al.*, 1991).

2.1.4 Environmental growth factors

Many environmental factors may affect the activity of *methanogens* and therefore the performance of the whole system. So it is importance to know how they affect the system.

2.1.4.1 Temperature

Methanogens are found in a vide variety of temperatures. They are generally divided into mesophilic *methanogens* with an optimum temperature of about 35°C and themophilic *methanogens* with optimum temperatures of about 65°C. There are also special types like marine *methanogens* living at 2°C and geothermal *methanogens* living at temperatures above 100°C (Ferry, 1993).

2.1.4.2 pH

The optimum pH for most *methanogens* is near neutrality (Jones *et al.*, 1987). Some *methanogens* like those in peat bogs can produce methane at pH values of 4.0 or below. There are also some alkaliphilic *methanogens* that can grow at pH values of 8 and 9 (Blotevogel *et al.*, 1985).

In order to achieve a pH around 7 in a reactor at a carbon dioxide concentration of 30% in the biogas, roughly, 40 equivalents of bicarbonate per cubic meter of wastewater must be present in the reactor (Kleerebezem and Macarie , 2003).

2.1.4.3 Oxygen

Methanogens are known to be strict anaerobes. They are unable to grow or produce methane in aerobic media, but they can tolerate certain amounts of dissolved oxygen. In a study by Kiener and Leisinger (1983), it was found that there is a wide range of oxygen tolerance for *methanogens* from 3 to 24 hours, before dying because of peroxides and toxic byproducts. Meanwhile, some adaptations to oxygen peroxides have been reported (Kiener *et al.*, 1988).

2.1.4.4 Toxicity

Mineral ions, heavy metals and detergents are some of the toxic materials that inhibit the normal growth of bacteria in a digester. Small quantities of mineral ions (e.g. sodium, potassium, calcium, magnesium and sulfur) also stimulate the growth of bacteria, while very high concentrations of these ions will have a toxic effect.

For example, NH_4 concentrations of 50 to 200 mg/l stimulate the growth of microbes, whereas concentrations above 1500 mg/l produce toxicity. Similarly, heavy metals such as copper, nickel, chromium, zinc, lead, etc. in small quantities are essential for the growth of bacteria but higher concentrations have toxic effects.

Likewise, detergents including soap, antibiotics, organic solvents, etc. inhibit the activities of methane producing bacteria and addition of these substances in the digester should be avoided. Although there is a long list of substances that produce toxicity on bacterial growth, the inhibiting levels of some of the major ones are given in Table 2.3.

Table 2.3 Toxic levels of various inhibitors for *methanogens*
Source: The Biogas Technology in China, BRTC, China (1989)-
(http://www.fao.org/sd/EGdirect/EGre0022.htm)

Inhibitor	Inhibiting Concentration
Sulphate (SO_4^{2-})	5000 ppm
Sodium Chloride or Common salt (NaCl)	40000 ppm
Nitrate (Calculated as N)	0.05 mg/ml
Copper (Cu^{++})	100 mg/l
Chromium (Cr^{+++})	200 mg/l
Nickel (Ni^{+++})	200 - 500 mg/l
Sodium (Na^{+})	3500 - 5500 mg/l
Potassium (K^{+})	2500 - 4500 mg/l
Calcium (Ca^{++})	2500 - 4500 mg/l
Magnesium (Mg^{++})	1000 - 1500 mg/l
Manganese (Mn^{++})	Above 1500 mg/l

2.2 Carbon Dioxide Capture and Conversion

Carbon dioxide capture and storage (Reeve, 2000, Hitchon, 1996) is a relatively new method to reduce CO_2 emissions as compared to the others e.g., reducing energy consumption, increasing energy efficiency, using lower or zero carbon fuels and reducing greenhouse gases from non-energy sources. As an example, it has a particular application in western Canada where large fossil fuel users are located close to suitable underground reservoirs (Reeve, 2000).

Figure 2.4 shows a schematic for underground storage and disposal of CO_2. In this method, carbon dioxide is transferred from the source to the geological reservoirs for storage or reuse.

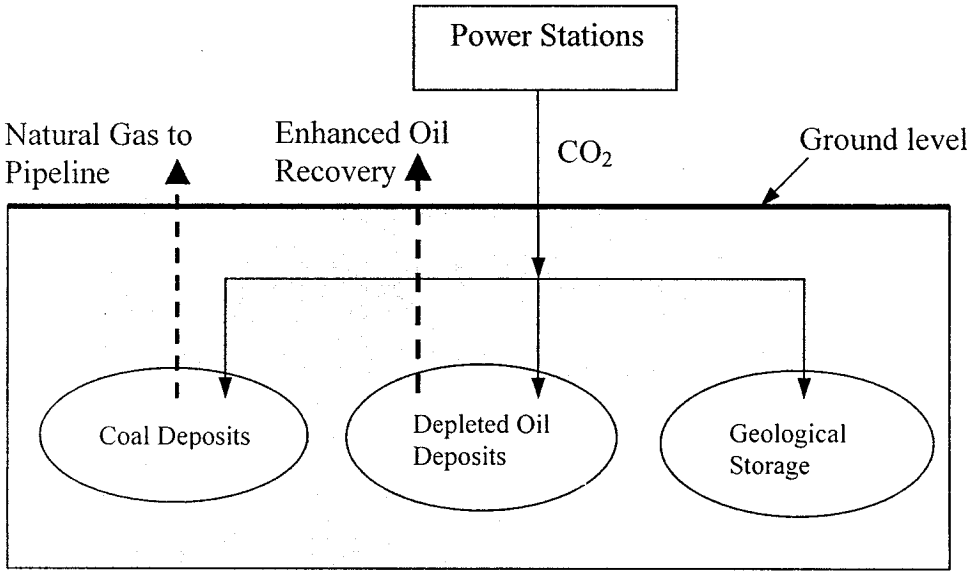

Figure 2.4 Carbon dioxide capture and storage (http://www2.nrcan.gc.ca/es/oerd/english/View.asp?x=649&oid=18)

Injection of CO_2 into local geologic formations or sea floors may be a reasonable component of the carbon management strategy (Herzog *et al.*, 1991; Bachu *et al.*, 1994), Riemer and Ormerod (1995) suggested that deep ocean injection is not immediately applicable due to a lack of information about the physiological effects of dissolved CO_2 on marine life.

Carbon dioxide can be converted to methane either chemically or biologically. It can be catalytically activated in the presence of hydrogen, which fully hydrogenates the adsorbed carbon species to methane:

$$CO_2 + 4H_2 \rightarrow CH_4 + 2H_2O \qquad H° = -165 \text{ kJ/mol} \qquad (2\text{-}12)$$

This reaction is moderately exothermic. Some experiments in microchemical catalytic reactors at 250°C have been done with about 90% CO_2 conversion (Vanderwiel *et al.*, 1999).

In one study (Roh *et al*, 2000) biogeochemically facilitated carbon sequestration processes using metal-rich fly ash in the presence of CO_2 atmosphere as well as in HCO^-_3 buffered media were tested. Biological conversion of CO_2 into sparingly soluble carbonate minerals such as calcite ($CaCO_3$) and siderite ($FeCO_3$) have been studied using Fe(III)-reducing bacteria in conjunction with metal containing fly ash and lime. In this process, fly ash is stabilized into carbonate solid conglomerates that could potentially be useful as fill materials or road construction aggregates.

Another system is proposed (Pal, 1999) to capture and use CO_2 for growing photosynthetic algae. The bioreactor slurry along with algae will be passed to a separation system, where the liquid will be strained and recycled to the reactor. Figure 2.5 shows the schematic of this system.

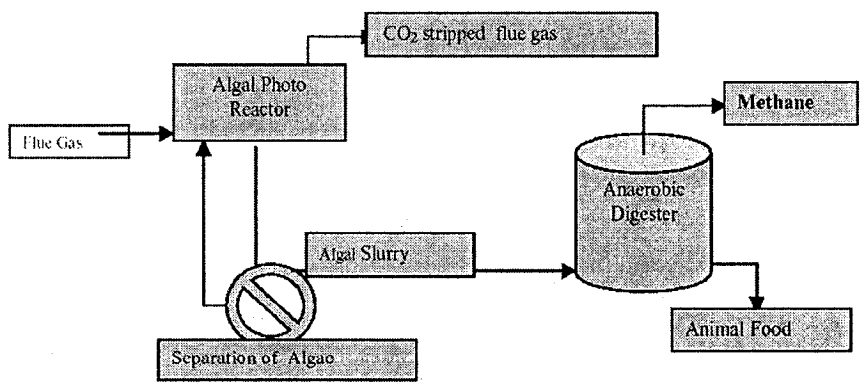

Figure 2.5: Schematics of the proposed technology by Pal (1999)

The concentrated algal slurry will be transferred to an anaerobic digester tank, where the fungal biomass will be digested and methane will be used to generate

electricity. After digestion is complete, the semi-solid byproduct can be dried and then used as animal feed or as a soil amendment or fertilizer.

2.3 UASB (Upflow Anaerobic Sludge Blanket) Reactors

Developed at Wageningen Agricultural University, Netherlands (Lettinga, 1978), an UASB reactor (Fig.2.6) employs anaerobic bacteria especially *methanogens*, which form self-immobilized granular structures with good settling properties inside the reactor.

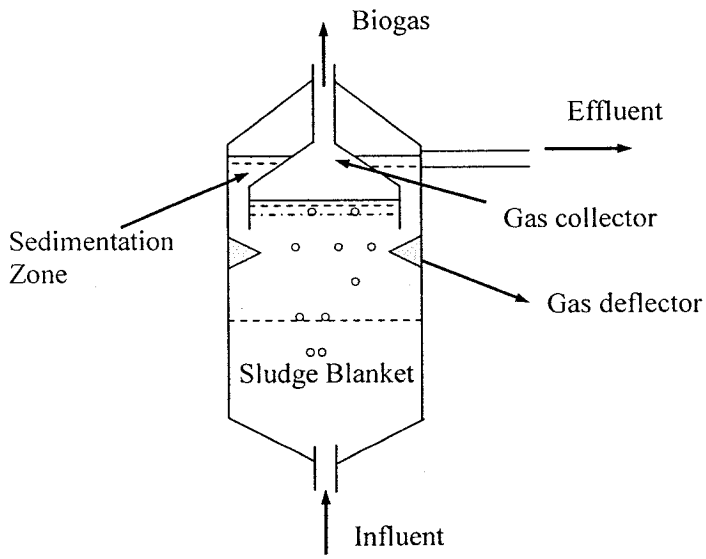

Figure 2.6 Schematic of an UASB reactor

These anaerobic bacteria granules make a "blanket" through which the effluent flows up the reactor. The substrate present in the effluent diffuses into the sludge granules where it is degraded by the anaerobic route. Thus, these reactors due to their high biomass concentrations can achieve conversions higher than that possible by conventional anaerobic processes and tolerate fluctuations in influent feed, temperature and pH (Kosaric & Blaszcyk, 1991). Moreover, since no support medium is required for attachment of the biomass it decreases the capital cost and minimizes the possibility of

plugging. The energy requirement also is small because there is no mechanical mixing within the reactor, no recirculation of sludge, and no high recirculation of effluent (Praveen and Ramachandran, 1993).

The Upflow Anaerobic Sludge Blanket reactor process utilizes a combined anaerobic reactor-solids separation unit from which clarified liquid (effluent) overflows from the reactor. The design and operation of the system depends on maintaining a granular, flocculent biomass which will provide the necessary organic removal while at the same time, allowing solid and liquid separation and growth control (Corbit, 1999).

2.3.1 Factors affecting the granulation process in anaerobic treatment

A granular type of sludge develops on mainly soluble types of wastewater (Van Haandel and Lettinga, 1994). The granulation process has been studied by several workers (De Zeeuw 1984; Hulshoff Pol and Lettinga 1986; Hulshoff Pol *et al.* 1987). Characteristics of well-developed granules are:

- High settleability
- High methanogenic activity

According to Hulshoff *et al.* (1983), several factors including environmental factors, the type of seed sludge and the process conditions during start-up affect the granulation process in anaerobic treatment.

2.3.1.1 Environmental conditions

Environmental conditions that affect this process may include:

1) the availability of essential nutrients, because growth conditions should be optimal,
2) the temperature, since the specific activity of methanogenic sludge is highly temperature dependent,
3) the pH, which should be in the optimal range (pH 6.5-7.8),
4) the type of wastewater, with regard to the composition of the waste, the biodegradability of the organic matter, the presence of finely dispersed non-biodegradable organic and inorganic matter, the ionic-composition (concentration of uni- and divalent cations) and the presence of inhibitory compounds.

The composition of the wastewater plays a rather dominant role in formation of granules with high methanogenic activity.

2.3.1.2 The type of the seed sludge

The type of the seed sludge and its specific activity, its settleability and the nature of the inert fraction affect its settleability.

2.3.1.3 The process conditions applied during the start-up

1) The procedure to increase the organic loading rate, e.g., the extent of overloading and allowed wash-out of suspended solids
2) The amount of seed sludge used.

Granulation is very successful with high carbohydrate or sugar wastewaters but less so with wastewaters high in proteins, resulting in a more fluffy floc instead (Thaveesri *et al.* 1994).

Hulshoff Pol *et al.* (1983) showed that for a system fed with fatty acid mixtures, the granulation occurs at organic loading rate higher than $0.6\frac{kgCOD}{kgVSS-day}$ (Grotenhuis *et al.*, 1991).

2.3.2 Typical design values for UASB reactors

Table 2.3 shows some design values for an UASB reactor. Depending on characteristics of the wastewater and operating conditions, the values are different and are site-specific.

Table 2.4 Some design values for UASB reactors.

Parameter	Value
Maximum biomass conc.(gVSS/L)	25[1]
Max. upflow velocity (m/h)	1.0[1] 1.0-3.0[2] 0.6-0.9[3]
Reactor height (m)	6[1]
Hydraulic retention time (HRT-h)	6-8[2] 4-12[3] 5-48[4]
Organic loading rate (OLR)	18[2] 4-12[3] 2-25[4]

1- Kleerebezem and Macarie (2003).
2- Metcalf and Eddy (2002)
3- Qasim (1999)
4- Grady *et al.* (1999)

CHAPTER 3

MATERIALS AND EXPERIMENTAL METHODS

3.1 Materials used

3.1.1 Substrate

Substrate solutions were made based on acetate and the recommended media for methanogens in the reference books (Atlas, 1997). The main constituent of the solutions was acetate since about 72% of the methane produced during anaerobic digestion of a complex substrate results from acetic acid (Ince, 2001). Acetic, propionic and butyric acids used as volatile fatty acids (VFAs) and two types of solutions were made: solutions containing acetic acid and those with mixed VFAs. There are also necessary components and elements for the cell growth that were included in the solutions. Ammonium chloride (crystalline 99.5%) and potassium hydrogen phosphate (100% dry basis) purchased from Fisher Scientific Ltd., served as sources of nutrients, and other inorganic components and

trace mineral solutions were also included. Table 3.1 shows the amounts of these components per 1L of solution (all chemicals were supplied from Fisher Scientific Ltd.).

Table 3.1 Composition of the solution used in the experiments

Component	Purity (%)	Amount (g/L)
NaCl	99.7	0.6
KH_2PO_4	100	0.44
$MgCl_2$	99.8	0.2
$CaCl_2$	98.6	0.2
NH_4Cl	99.5	1.2
Trace mineral solution	-	10 ml

The composition of the solution containing trace elements necessary for bacterial growth is shown in Table 3.2. This solution was made in 1 L and each time a certain amount of it according to Table 3.1, was added to the main solution.

Table 3.2 Composition of the trace mineral solution (from Fisher Scientific Ltd.)

Minerals	Purity (%)	Amount (g/L)
$MnSO_4.xH_2O$	98	0.1
$CoCl_2$	97	0.0131
$CaCl_2$	98.6	0.076
$CuCl_2$	99	0.02
$ZnCl_2$	97-100.5	0.1
NaCl	99.7	1.0
$NiCl_2.6H_2O$	99.88	0.12
$FeCl_3.6H_2O$	100	1.34

Other components used in the solutions are peptone and yeast extract containing vitamins, amino acids and coenzymes. The amount of these components and acetate concentrations were different for each solution depending on the required initial COD.

Based on many solutions that were made, approximate amounts of the acids, sodium acetate, peptone and yeast extract (Supplied from Fisher Scientific Ltd.) as shown in Table 3.3 were obtained to make a solution with a certain COD. The amounts of these components were approximately in proportion for different solutions.

Table 3.3 Approximate concentrations of basic components and corresponding COD values of the solutions.

Component	COD (g/L)		
	3.2	**6.0**	**8.5**
Sodium acetate (g/L)	1.5	2.8	4.0
Acetic acid (ml/L)	0.75	1.4	2.0
Acetic acid +Propionic acid +Butyric acid (ml/L)	0.25+0.25+0.25	0.5+0.5+0.5	0.7+0.7+0.7
Propionic acid + Butyric acid (mL/L)	0.5+0.5	0.75+0.75	1.1+1.1
Yeast extract (g/L)	0.8	1.5	2.0
Peptone (g/L)	0.4	0.75	1.0

A 1 N KOH (from 86.9% solid KOH) solution was made and added to bring the pH up to a desired value between 6 and 7. The initial values of pH will be discussed in sec. 4.1.4.

3.1.2 Carbon Dioxide

A carbon dioxide gas tank with industrial purity of 99% purchased from Praxair Inc. was used as a source of CO_2. The tank pressure was reduced from 50 atmosphere to the ambient pressure with a gas regulator to permit low gas flow rates.

3.1.3 Nitrogen Gas

An industrial grade nitrogen gas tank purchased from Praxair Inc. was used as the source of N_2. Nitrogen pressure was reduced from 70 atmosphere to the ambient pressure with a gas regulator in order to inject it into water and make it free from dissolved oxygen and chlorine for solution preparation.

3.2 Experimental Set-up

As shown in Figure 3.1 and the schematic in Figure 3.2, the experimental set-up used, has several sections which can be classified as follows:

3.2.1 The Reactor System

The reactor system consisted of external and internal compartments as illustrated below:

1- A translucent plastic cylinder with 40 cm height and 7cm diameter was used as an UASB reactor. This cylinder was basically a part of an artificial aquarium. It had an air diffuser at the bottom, which could efficiently be used as an influent distributor. So, it was decided to use this tube as an UASB reactor. The dent around the diffuser was filled with small glass beads to avoid dead zones having no liquid flow. This cylinder was

graduated and a few holes were made in its cap to install necessary probes and measuring devices. Figure 3.3 shows the top-view of the reactor.

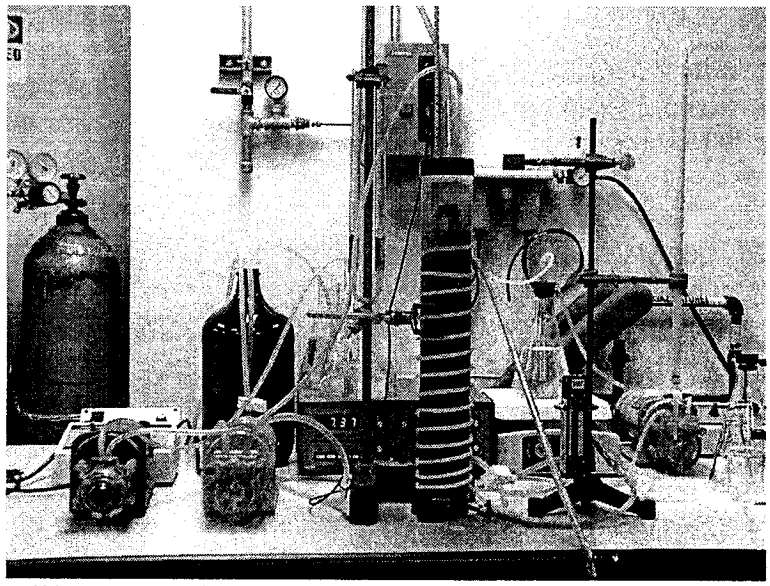

Figure 3.1 The experimental set-up used in this thesis.

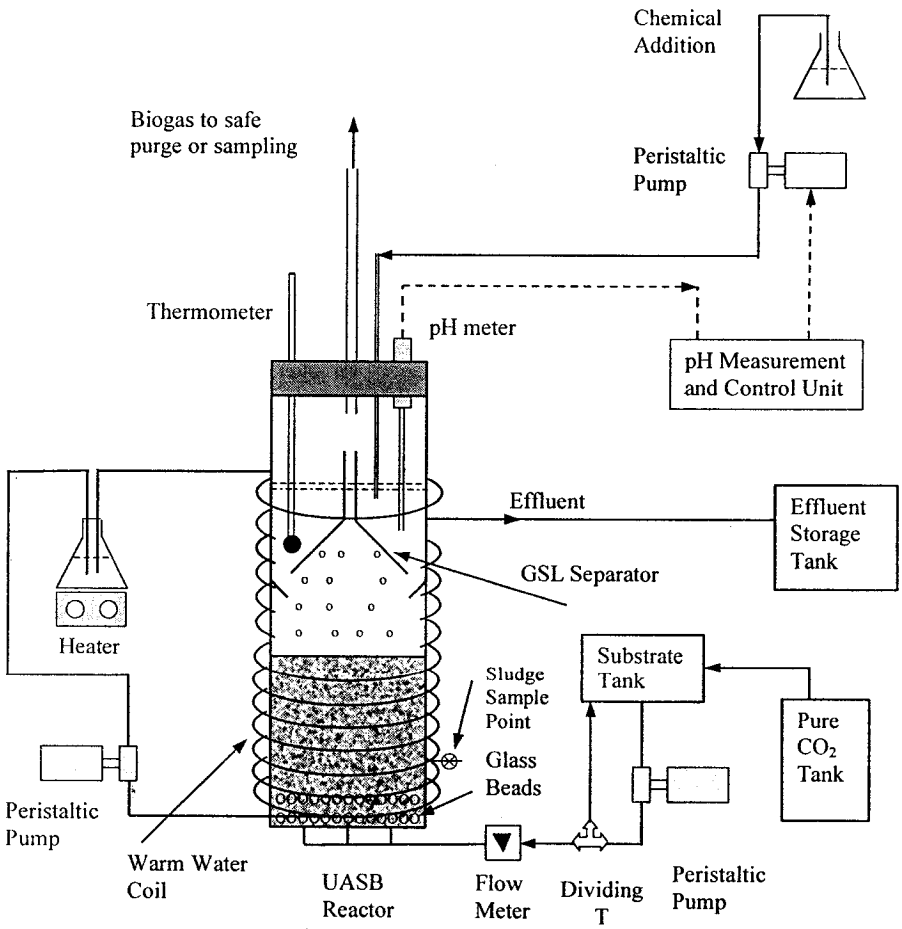

Figure 3.2 Schematic of the experimental set-up used in this thesis.

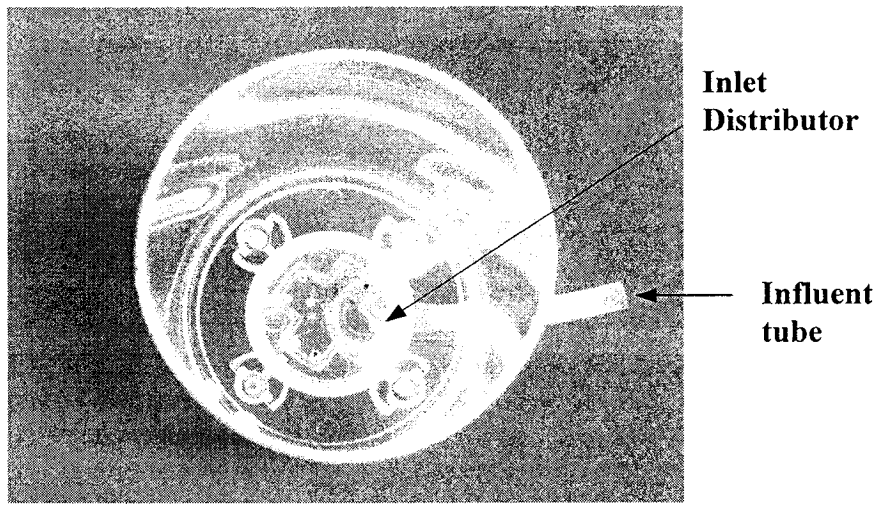

Figure 3.3 Top view of the cylindrical vessel used as an UASB reactor in this work.

2- A heating source for the reactor. To maintain the operating temperature of the reactor at 35°C, a closed circulation system was used. It consisted of a Masterflex peristaltic pump with variable speed controller, a 1-L Erlenmeyer containing warm water, an adjustable heater and a coil which was made using a ½ mm diameter plastic tube wrapped around the reactor. Warm water with a controlled temperature was circulated through the coil to maintain the reactor temperature at 35°C. A thermometer was installed in the reactor above the GSL separator to monitor the temperature.

3- Internal Gas-Liquid-Solid (GSL) separator to separate sludge particles from upflowing liquid and gas streams and send them back to the sludge section. It also conducted the biogas to the reactor headspace. The GSL separator was made using two plastic funnels that are modified for this purpose and were installed in the upper section of the reactor as shown in Figure 3.4. the upper funnel served as a gas collector and the lower one as a side-baffle to conduct liquid and gas streams.

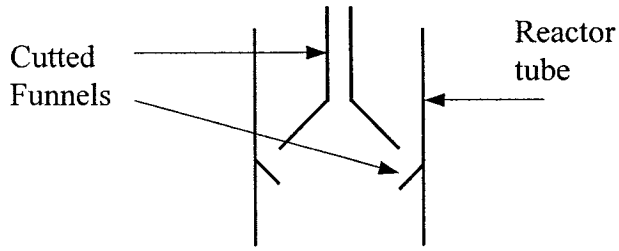

Figure 3.4 Schematic of the GSL separator.

3.2.2 pH Measuring and Control Unit

pH was measured and controlled by a pH meter probe (purchased from Fisher Scientific Inc.), which was installed in the reactor and was connected to a pH meter and controller (Chemocadet from Cole-Parmer). This unit was used to measure and compare the pH value to a set point and based on their difference, to send a signal to an injection pump (a Masterflex peristaltic pump) to inject acid or base solutions into the reactor and to adjust the pH. To avoid problems caused by the accumulation of fine biomass particles on the pH probe, every week the pH probe was cleaned with 2% hydrogen peroxide solution and then recalibrated with standard pH solutions.

3.2.3 Biogas Discharge

A piece of 10-cm of a 10-ml glass pipette installed in the reactor cap, served as a gas discharge tube and was connected to a safe purge line or a sampling port.

3.2.4 Biogas Measurement

To measure the rate of biogas flow, a U-shape device as shown in Figure 3.5, was made and used as a manometer. It consisted of two pieces of plastic pipettes whose bottoms were connected with a plastic tube.

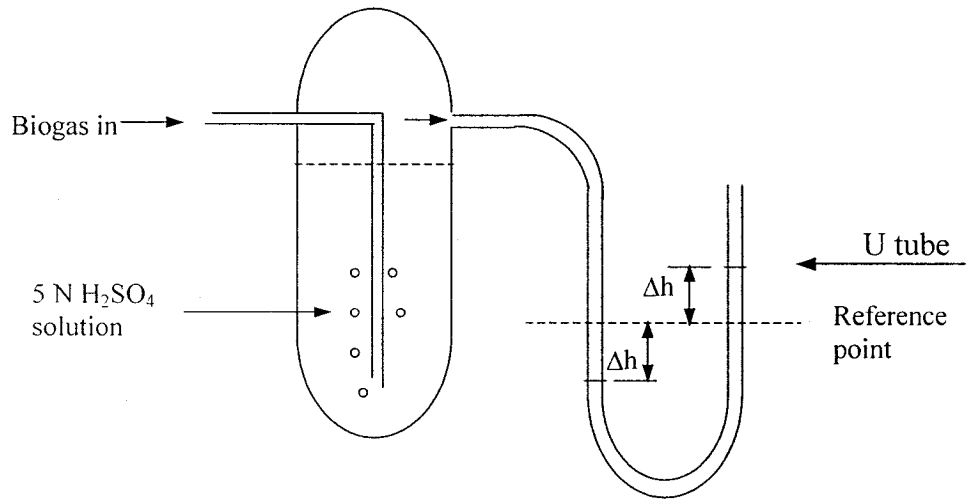

Figure 3.5 Schematic of measuring device for the biogas rate and its connection to the biogas-washing device.

The biogas discharge tube was connected to a Dudley Bubbling Tube containing concentrated (5N) sulfuric acid to absorb any moisture in it and the discharge tube was connected to the manometer inlet. The biogas rate was measured with the liquid displacement method: The displacement of the liquid column in time measured by a stopwatch, was recorded as the biogas rate. The formula 3-1 was used to calculate the biogas rate (in L/d).

$$\text{Biogas rate} = \Delta h/t \qquad (3\text{-}1)$$

3.2.5 Biogas Sampling

A special sampling device was made to take samples from the reactor headspace. As shown in Figure 3.6, it consists of a plastic syringe, a small globe valve and a plastic head to connect to the gas discharge pipe as shown in Figure 3.7.

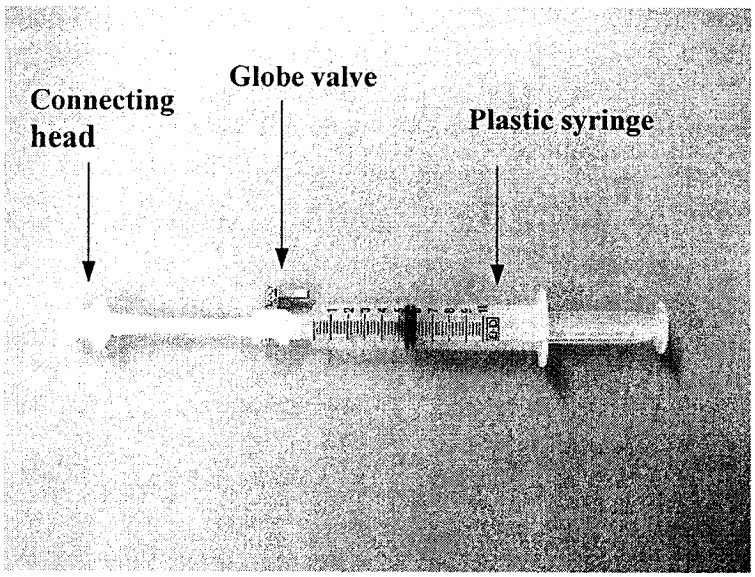

Figure 3.6 Gas sampling device.

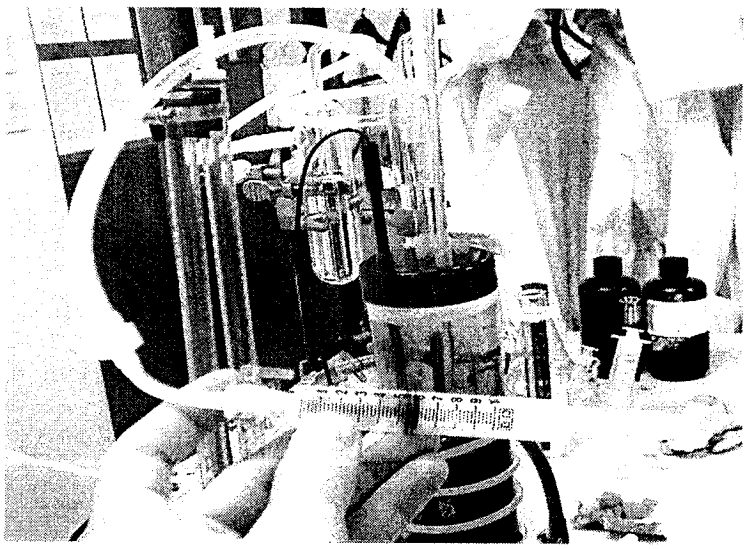

Figure 3.7 Taking gas samples from the reactor headspace with the sampling device.

3.2.6 Solution storage tank

Because the solutions were prone to aerobic decay and there was no special vessel to store them anaerobically for a long time, it was decided to make them in small amounts as needed in each individual test.

3.2.6.1 Batch experiments

For every run, 1 L of the reactor solution was made in an Erlenmeyer Flask with N_2-purged water and after heating up to 35°C, it was immediately pumped to the reactor. The amount of dissolved oxygen (DO) was measured by a special device (AQUACHECK, Model 51600), which can also measure pH, temperature and conductivity. The values of DO were always below 0.5 ppm.

3.2.6.2 Continuous experiments

For this, the system was run on a continuous basis using a 4 L dark glass bottle to store the solutions during each run. Because the solutions served as the media to absorb carbon dioxide as well, pure CO_2 from a storage tank was injected into the storage bottle until saturation conditions and a positive pressure was maintained above the liquid level. The benefits of this procedure are:

-The substrate is always at its maximum capacity to capture CO_2

-The substrate is deoxygenated, and

-The storage tank is under anaerobic conditions and air is not going into it as the liquid level goes down.

This bottle is shown in Figures 3.1 and 3.2. Influent flowrate was monitored by a flow meter.

3.3 Analytical Methods

3.3.1 COD Test

Values of COD were measured according to a colorimetric method [Standard Method (1998) - Method 5220B] using a Perkin Elmer Lambda 40 UV/VIS spectrometer at 600 nm wavelength. In this method, a hot mixture of chromic and sulfuric acidic is used to oxidize most types of organic matter. A sample is refluxed in a strongly acid solution containing an excess amount of potassium dichromate ($K_2Cr_2O_7$) through which Cr^{6+} is reduced to three-valence chromium Cr^{3+}.

The density of the green color of the chromium ion is measured against a known value in the standard calibration curve.

3.3.1.1 Solution Preparation

A standard potassium hydrogen phthalate (KHP) was first made according to the following procedure:

1- Lightly crush 450 g of KHP ($HOOCC_6H_4COOK$).

2- Dry crushed KHP in the oven (Linderberg/Blue Gravimetric Oven) at 120°C to constant weight.

3- Dissolve 425 mg of KHP in distilled water (made in the laboratory) and dilute the solution to 1000 ml. This solution has a theoretical COD of 500 mgO_2/L.

3.3.1.2 Test Procedure

In the standard COD test procedure, twist-cap vials purchased from Bioscience Inc. were used. This test is approved by the EPA as a micro-COD test. The total volume of the COD reagent is 5 ml. The procedure to prepare the standard curve is as follows:

1- Preheat a COD block heater (do not use oven) to 150°C.

2- Remove the cap from a COD twist-cap vial.

3- Carefully add 2.5 ml of sample down the side of the vial such that it forms a layer on top of the reagents.

4- Replace the twist cap.

5- Thoroughly mix the contents of the sealed vial by shaking.

6- Process standards and blanks exactly as the samples.

7- Place the twist-cap vial in a COD heater block capable of maintaining 150°± 2°C for 2 hours.

8- Remove the vial from the heater block and allow it to cool.

9- Allow any suspended precipitate to settle and wipe the outside of the twist cap clean.

10- Set the wavelength of the spectrophotometer to 600 nm, and, using a procedural blank, zero the absorbance reading.

11- Read the absorbance of each standard and sample on the spectrophotometer.

12- Prepare a graphic calibration curve by plotting the absorbance of the standards versus their known concentrations. Compare sample absorbance to the graphic calibration curve to determine COD concentration.

3.3.1.3 Standard Curve

The standard curve was prepared using five standard concentrations as shown in table 3.4. COD values of these vials were measured according to the test procedure.

Table 3.4 Standard sample concentrations for COD standard curve.

COD Value (mg/L)	Amount of KHP solution (ml)	Amount of Distilled Water (ml)
500	2.5	0
400	2.0	0.5
300	1.5	1.0
200	1.0	1.5
100	0.5	2.0

3.3.2 Volatile Fatty Acids (VFA)

Concentrations of VFAs in the samples was measured using a Beckman-Coulter system gold HPLC (high pressure liquid chromatography) analyzer. A YMC 8476 HPLC column was used to process the samples. The analyzer settings are shown in Table 3.5.

Each sample was tested in triplicate. For single and mixed VFAs, standard solutions were made with different concentrations. As an example, for a standard solution containing 1ml/L acetic acid (density 1.05 g/L), 1ml of acetic acid was added to 1 L HPLC water. Then a small amount of the solution was filtered through a 0.45 μm Whatman syringe filter into a 2 ml vial of the HPLC analyzer.

The solvent was a 50 mM solution of ammonium phosphate (pH=2.4) which was prepared by adding 66 g of dry crystalline ammonium phosphate diabasic, $(NH_4)_2HPO_3$ (purity 98%-101%), to 1L of HPLC water and adjusting the pH to 2.4 using O-phosphoric acid (85%) (All the chemicals were from Fisher Scientific Ltd.).

Table 3.5 Operating conditions for VFA tests with the HPLC analyzer.

Parameter	Setting
Solvent type	Ammonium phosphate
Solvent concentration (mM)	50
Solvent flow-rate (ml/min)	0.5
Solvent pH	2.4
Run time (min)	15
Column temperature (°C)	30
Injection volume (μL)	10
UV detection wavelength (nm)	210

The resulting peak was compared with those of the standards to determine the unknown VFA concentration. The concentration of the sample is determined using the following relationship:

$$\frac{(Area)_S}{(Area)_r} = \frac{C_S}{C_r} \qquad (3\text{-}2)$$

where indices "s" and "r" represent "sample" and " reference" respectively.

3.3.3 Total Alkalinity (TA)

Alkalinity refers to the capacity of water to neutralize acids. This parameter is determined by the abundance of four ions: carbonate (CO_3^{2-}), bicarbonate (HCO_3^-), hydroxyl (OH^-), and hydrogen (H^+). For many engineering purposes, the alkalinity is defined as follows:

$$A = [OH^-] + [HCO_3^-] + 2[CO_3^{2-}] - [H^+] \quad (3\text{-}3)$$

where the concentrations of ionic species are measured in mole per liter and alkalinity is expressed in equivalent per liter (Nazaroff and Alvarez-Cohen, 2001).

The alkalinity was measured by titration and according to the method No.2320 B (Standard Method, 1998). The indicator was Bromcresol green solution, which has a color change at pH 4.5. To prepare the solution, 100 mg dry Bromcresol green was dissolved in 100 ml distilled water.

The standard used was sulfuric acid (0.02 N). Each ml of this acid is equivalent to total alkalinity of 1 ppm $CaCO_3$. The end point for the titration test was determined based on changing the solution color from blue to pale green.

3.3.4 Dissolved Carbon Dioxide

Dissolved carbon dioxide concentration in the reactor influent and effluent for the continuous operation was measured based on the total alkalinity (TA) and pH values and using the equilibrium relationship among carbonate species. It also was measured in the influent by measuring the rate of injected CO_2 using a flowmeter and the time to reach a constant pH.

When carbon dioxide is dissolved in water, it is converted to its dissolved form $CO_2(aq)$ or carbonic acid (a weak acid) and its conjugate base, bicarbonate (an even weaker acid). $CO_2(aq)$ then dissociates in water and the equilibrium reactions are as follows:

$$CO_2(aq) \Leftrightarrow H^+ + HCO_3^- \qquad K_1 = \frac{[H^+][HCO_3^-]}{[CO_2(aq)]} = 4.47 \times 10^{-7} M \quad (3\text{-}4)$$

$$HCO_3^- \Leftrightarrow H^+ + CO_3^{2-} \qquad K_2 = \frac{[H^+][CO_3^{2-}]}{[HCO_3^-]} = 4.68\times10^{-11} M \qquad (3\text{-}5)$$

By combining two equations, we have:

$$K_1 K_2 = \frac{[H^+]^2[CO_3^{2-}]}{[CO_2(aq)]} = 2.1\times10^{-17} \qquad (3\text{-}6)$$

By definition of pH, we can calculate $[H^+]$ as:

$$[H^+] = 10^{-pH} \qquad (3\text{-}7)$$

By measuring the alkalinity and calculating the concentration of $[OH^-]$ from the following equation for water dissociation,

$$K_w = [H^+][OH^-] \qquad (3\text{-}8)$$

the concentrations of species CO_3^{2-} and HCO_3^- were calculated from equations (3-3) and (3-5). Then expression (3-6) was used to determine the concentration of dissolved $CO_2(aq)$. All calculations were programmed into Excel with pH, alkalinity and temperature as the input data (see appendix B).

3.3.5 Purity (Methane Content) of the Biogas

At first and during the acclimation period, because the gas chromatograph (GC) was not working, methane content of the biogas was measured by washing the biogas with a concentrated acid to absorb traces of saturated water in it and then with a concentrated base solution to absorb carbon dioxide, which is the main impurity in the biogas stream.

For batch experiments and continuous operation, gas samples were analyzed using the GC. The operating conditions and column specification are shown in Table 3.6.

Table 3.6 Test conditions for gas chromatography.

Parameter	Setting or type
Column (30mm×0.53mm)	CARBOXEN 1010 PLOT (Capillary Column) from SUPELCO
Carrier gas	Helium
Detector	TCD
Injector temperature (°C)	225
Column oven temperature (°C)	50-100 (5°C/min)
Injection flow (ml/min.)	5
Gas retention time (min.)	15

3.3.5.1 Biogas washing method

For the batch experiments, biogas purity was measured using the apparatus as shown in Figure 3.9. For acid solution, 5 N H_2SO_4 and for base solution, 10 N KOH solutions were made.

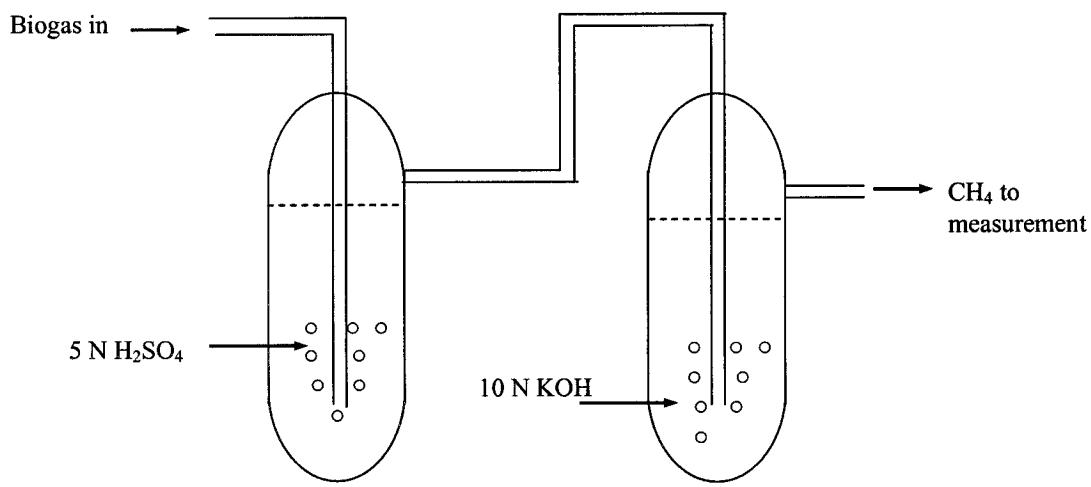

Figure 3.9 Schematic of the Dudley Bubbling tubes used for measurement of the biogas purity

3.3.5.2 Methane content of the biogas

To measure the methane content of the biogas using the GC analyzer, a reference curve was made. For this purpose, samples containing known compositions of pure carbon dioxide and methane were injected to the GC analyzer and for each one, the peak ratio of CH_4/CO_2 was measured and plotted against the methane content. The resulted curve is shown in appendix A.

3.3.6 Volatile suspended solids (VSS) and total suspended solids (TSS)

TSS is a measure of the total suspended solids in water, both organic and inorganic, and VSS is the organic portion of the TSS that is lost after ignition. Both are expressed in mass per volume as g/L or mg/L in this work. These tests were done according to the Standard Method (Clesceri *et al.*,1998), to measure the concentration of the sludge in the reactor and effluent. Test procedure was as follows:

1- Pre-dry a gooch crucible with Whatman GF/C filter paper in a furnace (here, Fisher Scientific Isotemp muffle furnace) at 550°C± 2°C for 1 hour and allow it to cool down in a desiccator (Sanpla Dry Keeper, automatic dehumidifying desiccator) for 30 min. Then weight it immediately and record it as weight "A".

2- Take a sample from the reactor sample point (here, with a 1ml sample) and transfer it to the gooch crucible and filter it by vacuum filteration.

3- Put the gooch crucible in the oven (here, Linderberg/Blue Gravimetric Oven) and let it dry at 105°C ± 2°C for 1 hour and allow it to cool down in the desiccator for 10 min. Then weigh it and record it as weight " B".

The TSS can be determined using the following relationship:

$$TSS = \frac{A-B}{1(mL)} \times 1000 \quad (\frac{g}{L}) \tag{3-9}$$

4- Put the gooch crucible in the muffle furnace at 550°C±2°C for 2 hours, and then allow it to cool down in a dessicator for 30 min. Weigh the crucible and record it as weight "C".

5- Calculate the VSS from the following expression:

$$VSS = \frac{B-C}{1(mL)} \times 1000 \quad (\frac{g}{L}) \tag{3-10}$$

The residual material in the gooch crucible, represents the ash content of the biomass, and can be calculated per mass of dry solids as follows:

$$Ash = 1 - \frac{VSS}{TSS} \quad (\frac{g}{g}) \tag{3-11}$$

The test procedure for the effluent was as above and each week, 3 samples were taken from the processed solutions (for the batch experiments) or the effluent streams (for the continuous experiments to measure VSS concentrations.

3.3.7 Methanogenic activity measurement

Sludge activity, usually referred to as methanogenic or specific methanogenic activity (MA or SMA respectively), is an important parameter for an anaerobic system which determines the system tolerance to organic loadings. For start up of a new reactor, the amount and activity of seeding sludge are important factors to determine applicable

organic loading rates. Any decrease in this quantity may be a sign of inhibitory conditions due to either toxic or increasing amount of non (or slowly)- biodegradable organic matter.

This parameter is usually measured in a SMA test reactor (Ince *et al.*, 1994, James *et al.*, 1990) using known amounts of biomass and substrate solution. SMA can be expressed in several units based on rate of methane production or substrate consumption and the amount of biomass present. Methane production rate is usually expressed as volumetric rate or calculated COD equivalent.

SMA also can be measured from *in situ* experiments with an UASB (De Zeeuw, 1984). In this work, SMA is expressed as gCH_4-COD/gVSS.

3.3.7.1 Calculation of COD for known components

For known components, COD was calculated based on the theoretical amount of oxygen required for their oxidation. For example, for methanol and acetic, propionic and butyric acid COD was calculated as follows:

$$CH_3OH + 2O_2 \longrightarrow CO_2 + 2H_2O \qquad (3\text{-}12)$$

Each gram of methanol = $(\frac{1}{32})(2)(32) = 2.0$ g O_2 or 2.0 g COD

$$CH_3COOH + 2O_2 \longrightarrow 2CO_2 + 2H_2O \qquad (3\text{-}13)$$

Each gram of acetic acid = $(\frac{1}{60})(2)(32) = 1.07$ g O_2 or 1.07 g COD

And so for propionic and butyric acids:

Each gram of propionic acid = $(\frac{1}{74})(3.5)(32) = 1.51$ g O_2 or 1.51 g COD

Each gram of butyric acid = $(\frac{1}{88})(5)(32) = 1.82$ g O_2 or 1.82 g COD

The amount of methane produced was expressed as COD based on the following reaction:

$$CH_4 + 2O_2 \longrightarrow CO_2 + 2H_2O \qquad (3\text{-}14)$$

Each gram of methane = $(\frac{1}{16})(2)(32) = 4.0$ g O_2 or 4.0 g COD

The mass of methane at any temperature and pressure was calculated using ideal gas law as:

$$m = \frac{MPV}{RT} \qquad (3\text{-}15)$$

where (units in CGS system):

m = mass of the gas (g)

M = Molecular weight of the gas $(\frac{g}{gmole})$

P = Gas pressure (atm)

T = Gas temperature (°C)

V = Gas volume (litre)

R = Universal gas constant $(82.05 \frac{litre.atm}{gmole°K})$

The equation (3-15) should preferably be used at low to moderate pressures to better represent the ideal gas behavior (which is usually the case in anaerobic reactors).

3.4 Sampling schedule

For each part of this work, routine samples were taken according to a time schedule summarized below to monitor the operations and evaluate the system performance.

3.4.1 Acclimation period

The reactor sludge was first acclimated in batch runs using acetate-based substrates made with distilled water. The objective of this period was to activate the biomass to start consuming the substrate and producing biogas. The substrate composition was previously described in Table 3.1.

Before feeding the biomass, it was stored under the desired operating temperature, 35°C, for about 1 month in order to acclimate to the new temperature. The tests and sampling intervals for this period are shown in Table 3.7.

Table 3.7 Tests and their time schedule for the acclimation period.

Test	Frequency
Dissolved oxygen (DO)	After purging the water with N_2 and before loading the solutions into the reactor
COD	Every 2 hours
Biogas rate	Every ½ hour
Methane content of the biogas	Every hour
pH	Online measurement
TA	Every 2 hours

3.4.2 Batch experiments

For this stage, the tests and their time schedule are shown in Table 3.8. Every week the reactor was fed batch-wise with a solution of certain COD value and every day the results were compared to check if they are close enough (within 5% error) to assume a steady condition for that load. For the reactor sludge, samples were taken from a point located about 1/3 height of the sludge bed from the reactor bottom (see Fig. 3.2).

Table 3.8 Tests and their time schedule for the batch experiments.

Test	Frequency
COD	Every 2 hours
VFA	Every 2 hours
Biogas rate	Every ½ or 1 hour
Methane content of the biogas	Every hour
pH	Online measurement
TA	Every 2 hours
VSS and TSS (reactor biomass)	Every week
VSS (effluent)	Every week

3.4.3 Continuous operation

The test schedule for the continuous operation is shown in Table 3.9. As mentioned before, every week the reactor was run at a certain organic loading rate and the tests were repeated until the results were within maximum 5% error (depending on the error expected form each test), which was regarded as a steady sate condition.

Table 3.9 Tests and their time schedule for the continuous operation.

Test	Frequency
COD	Every day
VFA	Every day
Biogas rate	Every hour
Methane content of the biogas	Every hour
pH	Online measurement
TA	Every hour
VSS and TSS (reactor biomass)	Every week
VSS (effluent)	Every week

3.5 Microscopic observations

During the whole work, the quality of the reactor biomass was monitored by taking samples and watching the biomass particles under the laboratory microscope (WILD Heerbrugg) to check possible changes in their structure and size. Photos were taken with a digital camera through the microscope eye tubes, since there were no special adaptors with it to take full frame pictures.

CHAPTER 4

RESULTS AND DISCUSSION

4.1 Acclimation of the sludge

4.1.1 Substrate loading and utilization

The reactor sludge was first acclimated in batch runs using acetate-based aqueous solutions made with deoxygenated distilled water. The objective was to acclimate the biomass in order to start consuming COD and producing biogas. The substrate composition was previously mentioned in Tables 3.1 and 3.3.

It was observed that despite the inactive period, the sludge started to produce biogas after 8 days with an increasing rate. Increasing the operating loading rate (OLR),

was based on COD removal from the influent at each load. Samples were taken from the effluent to check COD levels and when a satisfactory removal was measured (more than 50%), the OLR was increased. For each sample, COD was measured three times and it was found that the average values were within maximum 5% of the two extreme values. So, 5% error was considered for each test. Figure 4.1 shows the OLR profile for the acclimation period.

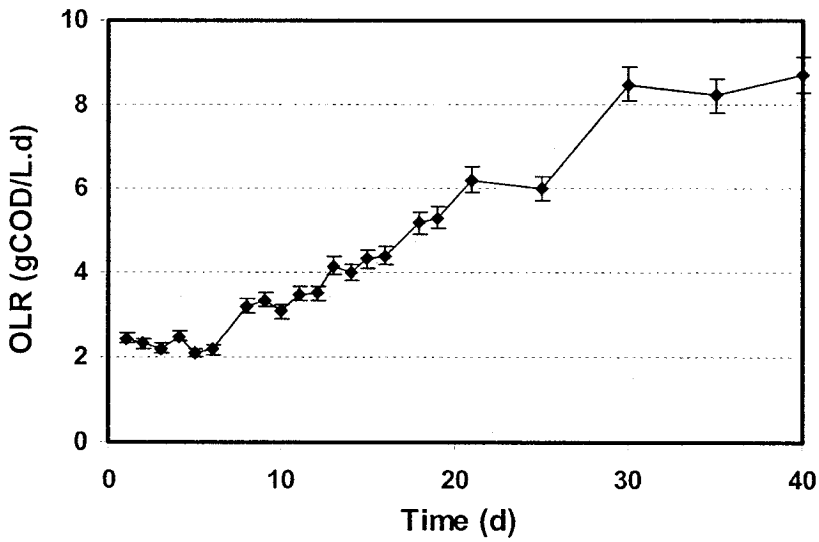

Figure 4.1 Increase of organic loading rate (OLR) during the acclimation period.

Figure 4.2 shows typical data of the COD removals for three solutions with different initial COD concentrations.

4.1.2 Biogas production and purity

Figure 4.3 shows the biogas production trends for the three solutions in Figure 4.2. As can be seen, the biogas production rate was at its maximum rate for the first 2-3 hours of substrate loading, therefore shorter measurement intervals for the biogas rate and purity were considered for the first few hours in each run.

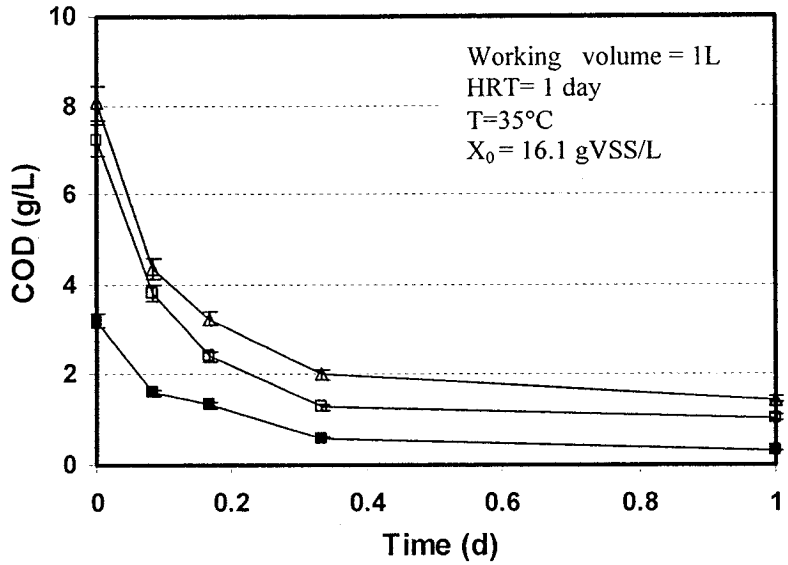

Figure 4.2 COD removal curves for three batch feedings with acetic acid solutions: (■) COD=3.2g/L, (□) COD= 7.2 g/L, (Δ) COD=8.1 g/L.

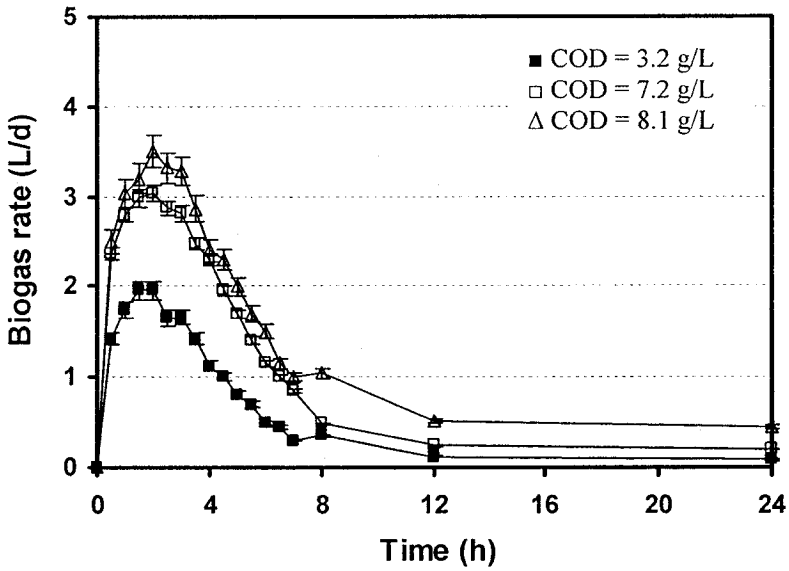

Figure 4.3 Biogas production rate for three batch feedings with acetic acid (conditions same as of Fig. 4.2).

Cumulative amounts of the biogas production were calculated from the surface area under the curves for biogas rate using the Simpson's Rule as described in appendix C. Figure 4.4 shows the calculated amounts of the biogas for the cases in Figure 4.3.

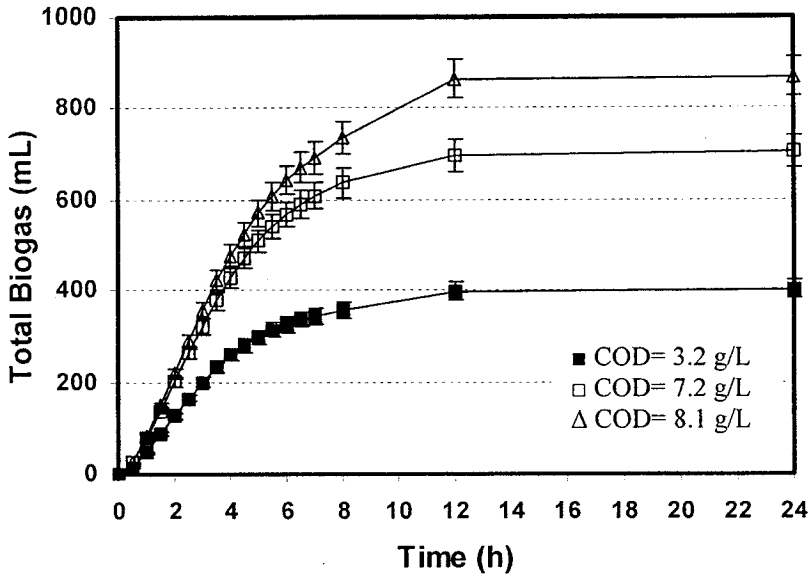

Figure 4.4 Cumulative amounts of the biogas calculated for three batch feedings with acetic acid solutions (based on data in the Figure 4.3).

4.1.3 Biogas Purity

In this stage the biogas purity was measured by washing the biogas with acid and base solutions as described earlier in Figure 3.9. Figure 4.5 shows the results for three cases in Figure 4.2, which are reported for the first 6 hours of the reactor operation.

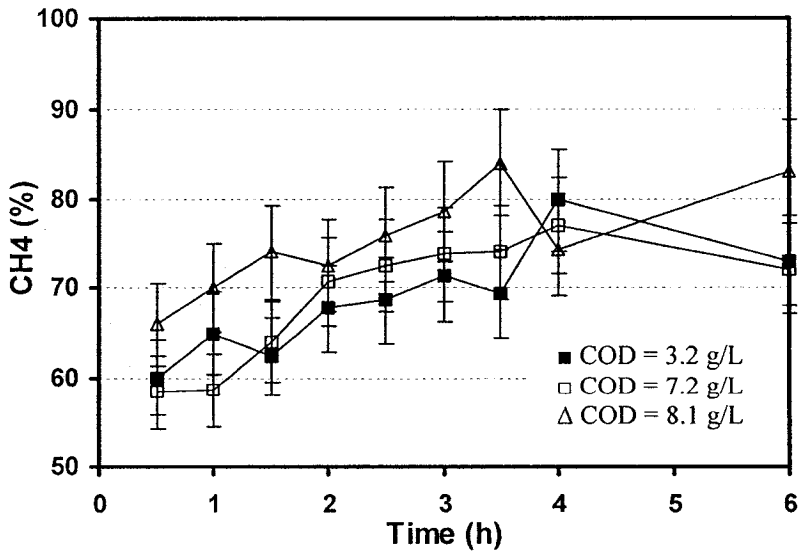

Figure 4.5 Results for methane content of the biogas measured from biogas washing for three batch feedings with acetic acid solutions (conditions same as of Fig. 4.2).

Each measurement was triplicated and an average value was considered for the purity. In this case, the measurement errors were within ±7% based on the average values, with some exceptions of ±10%. Although the acid and base solutions to wash the biogas, were frequently refreshed, the methane content of the washed biogas didn't follow the same pattern for the three cases, and some fluctuations were observed in the trends. However it was seen that the methane content was low at first (due to probably low initial activity of the biomass during this period) but increased with time.

4.1.4 pH trends

pH values of the first solutions were adjusted to around 7 with a 1 N KOH solution before feeding the reactor. After loading, it was realized that the pH was increasing due to conversion of acetic acid to methane by the methanogens, which subsequently increases the total alkalinity (TA) of the solution.

Then, other solutions with lower initial pH values were made. However in all cases, final pH values were about 1-1.5 unit higher than the initial values, so it was decided to start with the lowest recommended pH for methanogens, which is around 6.4, so that the final pH would be around 7.7, which is still in the recommended range. The sensitivity of the pH meter was up to 2 decimal digits and if a fixed value for pH was not legible on the digital indicator, an average value was recorded, which was within 0.5-1% of the two extreme values. Figure 4.6 shows the results for pH values of the three solutions.

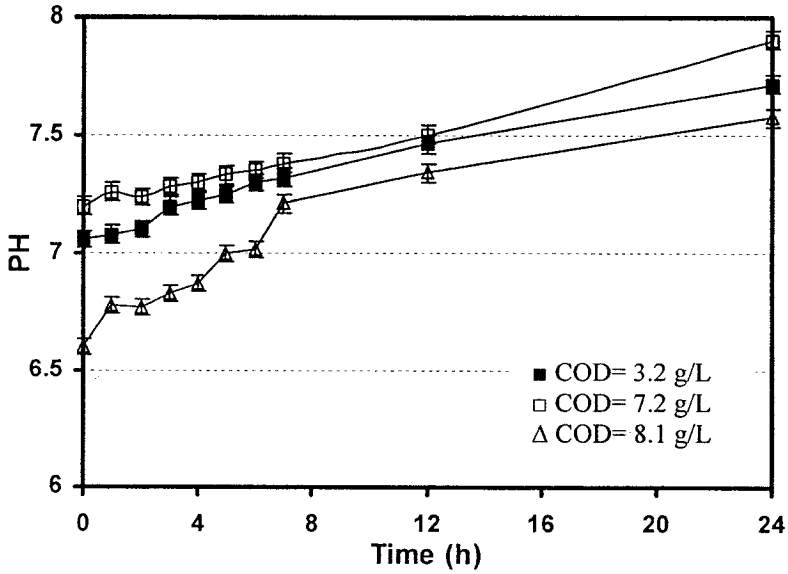

Figure 4.6 pH trends for batch feedings with acetic acid solutions (conditions as in Figure 4.2).

4.1.5 Total alkalinity (TA) trends

Figure 4.7 shows the TA trends for the solutions in Figure 4.7. TA was measured by a titration method as described in section 3.3.3. The values increased in all runs, which was an indication of the consumption of acetic acid by the methanogens and, therefore, a reduction of solution acidity. In all TA tests, end point determination by a visual check was easier for the dilute solutions than the concentrated ones and usually it took extra drops of 0.02 N H_2SO_4 to distinguish an obvious color change in the sample. So, based on these extra amounts, an estimated error in these tests, was about 2.2-5%.

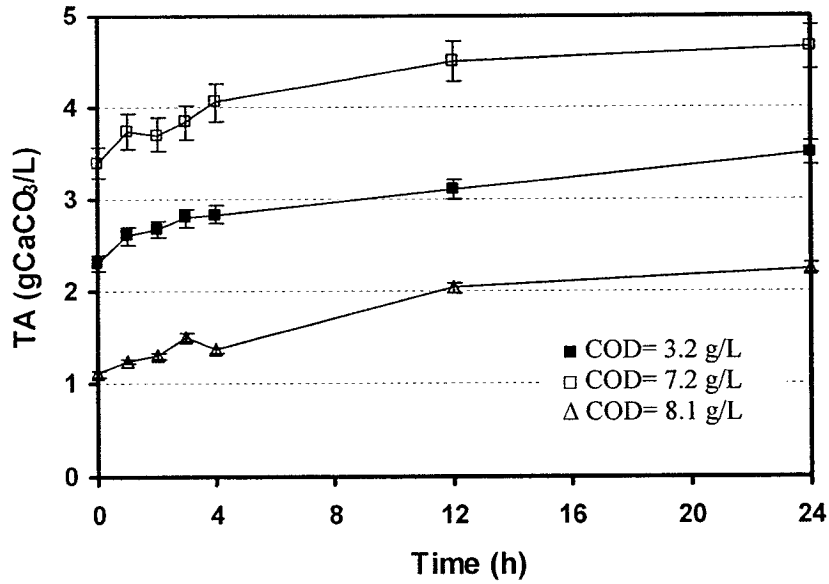

Figure 4.7 TA trends for batch feedings with acetic acid solutions (conditions as of Figure 4.2).

4.2 Batch experiments

The batch experiments were carried out using solutions with different concentrations of acetic acid and mixed VFAs at different OLRs and HRTs. The main objectives of this stage were:

1) to continue the acclimation process of the reactor biomass to new solutions,
2) to obtain kinetic parameters of the systems,
3) to measure methanogenic activity of the sludge.

It should be mentioned that at this stage, and regarding practicality of the method, the solutions were made using tap water instead of distilled water. So, before starting the experiments, the reactor was fed for 1 week with a dilute solution of acetic acid (3.0 gCOD/L) made with tap water. Before making solutions, tap water was purged with N_2 for about 15 minutes to remove dissolved oxygen and chlorine.

4.2.1 Substrate feeding

This part of the experiments includes two steps:

1) Experiments with acetic acid called the 1st system
2) Experiments with mixed VFAs called the 2nd system.

For each system, experiments started with dilute solutions and each week, the reactor was fed on a certain COD loading and the results for that load were finalized at the end of the week. Table 4.1 shows the initial test conditions for the two systems.

Table 4.1 Initial test conditions for two systems in the batch experiments.

System 1				
Parameter	**Amount**			
	Run 1	Run 2	Run 3	Run 4
Initial biomass concentration (gVSS/L)	13.4	13.1	12.7	12.8
Initial COD (g/L)	1.8	3.4	6.2	8.7
System 2				
Parameter	**Amount**			
	Run 1	Run 2	Run 3	Run 4
Initial biomass concentration (gVSS/L)	12.5	12.3	12.6	12.1
Initial COD (g/L)	2.3	4.5	7.6	8.8

Based on the results for COD reduction in the previous stage (Fig. 4.2) and since most of the COD reduction and biogas production were within 12 hours after each feeding, a hydraulic retention time of 12 hours was considered for each system. The initial pH for the solutions was adjusted at 6.5±0.2 and reactor temperature was

parameters for acetoclastic methanogenesis and for methanogenesis from hydrogen and carbon dioxide.

Table 4.2 Kinetic parameters obtained in this study for acetic acid and mixed VFAs in the batch experiments.

VFA(s) in Feed	Acetic acid				Mixed VFAs	
Concentration (g/L)	0.8	1.4	2.7	3.7	1.6	3.2
Initial Biomass (gVSS/L)	13.4	13.1	12.7	12.8	12.3	12.6
OLR (gCOD/L.d)	3.2	6.1	11.3	15.8	6.7	11.5
μ_{max} (1/d)	0.080	0.077	0.081	0.082	0.074	0.078
K_s (gCOD/L)	0.17	0.19	0.18	0.18	0.19	0.20
Y (gVSS/gCOD)	0.075	0.078	0.076	0.065	0.075	0.08
k_d (1/d)	0.037	0.0395	0.0375	0.04	0.038	0.033

A large number of studies have dealt with acetate conversion to methane, in which the kinetic data for acetate utilization are reported [Lawrence and McCarty (1969), Ahring and Westermann (1987), van den Berg (1977), Zinder and Mah (1979), Smith and Mah (1978), Kugelman and Chin (1971), Wandrey and Aivasidis (1983), Cappenberg (1975), Zehnder *et al.* (1980), Noike *et al.* (1985)].

Also, numerous studies have been undertaken on the kinetic values for methane production using H_2 and CO_2. Harper and Poland (1986) reviewed the kinetics and energetics of hydrogen gas in anaerobic wastewater treatment. Table 4.3 shows some of these data compared to those of this study.

Table 4.3 Summary of kinetic data for the aceticlastic methanogenesis and methanogenesis from H_2 and CO_2.

Culture	T (°C)	k (gCOD/gVSS.d)	K_s (mgCOD/L)	μ_{max} (1/d)	Y (gVSS/gCOD)	b (1/d)	Reference
B/Mixed Culture	30	2.6-5.1	-	-	0.02	-	Van den Berg (1977)
B/Mixed Culture	35	2.6-5.1	-	0.08-0.09	0.02	-	Van den Berg (1977)
B/Pure Culture	36	-	320	0.5-0.7	0.03-0.04	-	Smith and Mah(1978)
Methanobacterium sj	30	26.0	11	0.26	0.01	-	Cappenberg (1975)
Methanobrevibacter arboriphilus	33	-	0.6	1.4	0.04	-	Gujer and Zehnder (1983)
Rumen Bacteria	37	2-8[1]	0.016	-	-	-	Hungate et al.(1970)
Methanospirillum Hunguei JF-I[2]	37	1.92[3]	0.093-0.177	0.05	0.017-0.025	-	Robinson and Tiedje (1984)
B/Mixed Culture	35	1.0-1.14	0.17-0.2	0.074-0.081	0.065-0.08	0.033-0.04	This study

B = Batch; $k = \mu_{max}/Y$; b = Decay rate (equal to k_d in this study)
1 = Expressed as mg COD/g rumen liquid-day
2 = Batch grown on H_2-CO_2 gas mixture
3 = Assuming a protein content of 60% of dry weight

A large number of studies, especially those dealing with undefined, complex substrates, have yielded kinetic parameters which do not refer to the individual reactions in an anaerobic process but have assumed methanogenesis to be a one-step process. A summary of kinetic data from these studies has been complied by Henze and Harremoës (1983). Based on an extensive literature review, various researchers proposed a set of kinetic values for the acid-phase and the methane-phase of anaerobic digestion some of which are shown in Table 4.4. With the exception of the hydrolysis step, all other subprocesses of anaerobic treatment have been successfully modeled by Monod kinetics (Switzenbaum, 1991). Some reported values for the kinetic constants related to each subprocess along with the data obtained in this study are given in Table 4.4.

Table 4.4 Representative values of kinetic constants for anaerobic digestion in mesophilic range.

Process	k (gCOD/gVSS.d)	K_s (mgCOD/L)	μ_{max} (1/d)	Y (gVSS/gCOD)	b (1/d)
Acidogenesis[1]	13	200	2.0	0.15	-
Methanogenesis[1]	13	50	0.4	0.03	-
Overall[1]	2	-	0.4	0.18	-
Anaerobic oxidation[2]	6.2-17.1	12-500	0.13-1.2	0.025-0.047	0.01-0.027
Acetoclastic Methanogenesis[2]	2.6-11.6	11-421	0.08-0.7	0.01-0.054	0.004-0.037
Methanogenesis[3]	1.0-1.14	170-200	0.074-0.081	0.065-0.08	0.033-0.04

1 = Henze and Harremoës, 1983, t = 35°C
2 = Switzenbaum 1991
3 = This study

Some others like Kaspar and Wuhrmann (1978) studied the acetate degradation at 33°C and a retention time of 40 days in a lab-scale digester and obtained values of 13

mg/L to 29 mg/L (COD basis) for the half-saturated constant, which is in the range for K_s given in Table 4.4.

The kinetic parameters obtained in this work are very close to those of Switzenbaum (1991) for acetoclastic methanogenesis degradation in Table 4.4 and differences are probably due to different biomass cultures and measuring methods. A detailed microbiological study is needed to determine the methanogenic population of the biomass.

The results of the numeric method and the experimental data for VFA consumption are compared in Figures 4.11 and 4.12 for two systems.

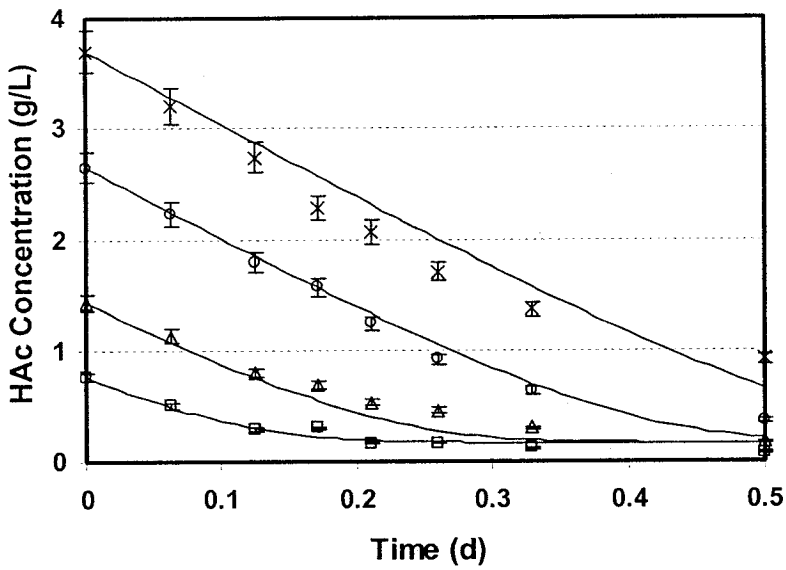

Figure 4.11 Comparison between the data and modeling results in each run for the first system [conditions as of system 1 in Table 4.1 for OLRs (gCOD/L.d): □ = 3.24, Δ = 6.1 ◊ = 11.3, x = 5.8].

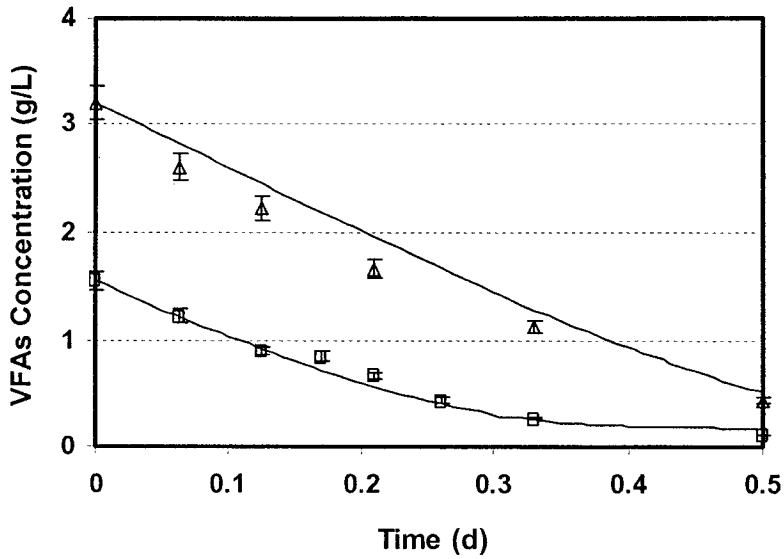

Figure 4.12 Comparison between the data and modeling results in each run for the second system [conditions as of system 2 in Table 4.1 for OLRs (gCOD/L.d): □ = 6.7, Δ = 11.5].

Results obtained from the numerical method are more consistent with the experimental data for lower COD loadings in both systems, and for higher loadings, an overestimation is observed from the method. This can be due to possible concentration-dependency of the kinetic parameters for concentrated solutions i.e. K_d and Y_g as mentioned by Chang *et al.* (1982).

4.2.4 Methane production

Total methane production and methane content of the biogas for the batch tests are shown in Figures 4.13 and 4.14. The results show that methane production increased with increasing loading rate, whereas the methane content of the biogas declined for higher loadings. Better results were obtained for the batch feedings with acetic acid solutions. For low loading rates, the amount of the methane produced is not very different for two systems, but for higher loadings, more methane is produced in the first system.

The biogas shows higher methane contents in all loadings for acetic acid feedings. An improvement in methane production can be seen when the organic load is increased for the batch runs using mixed-VFA solutions, since the results are closer to those for acetic acid. This could be a consequence of increasing adaptation of the reactor biomass to VFA feedings in the second system.

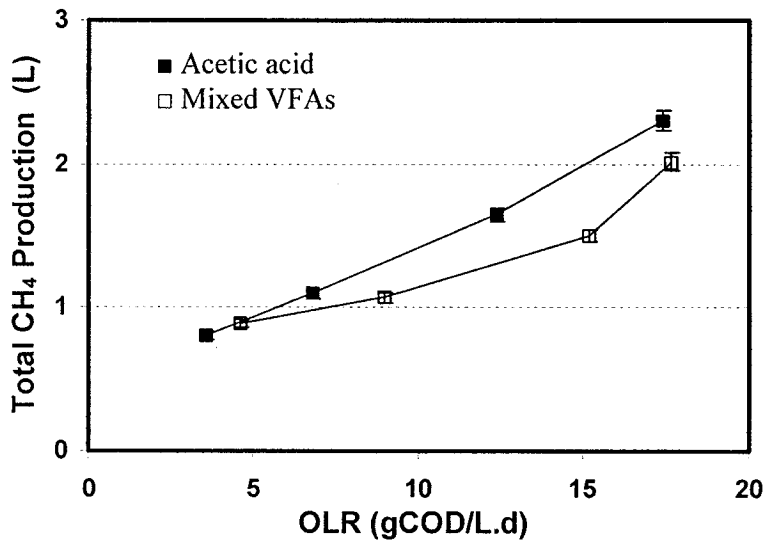

Figure 4.13 Variation of methane production rate with organic loading rate for the batch experiments.

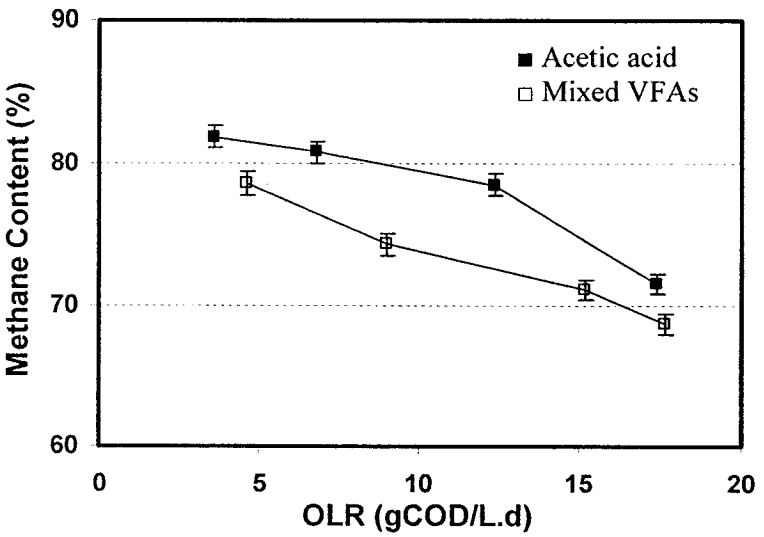

Figure 4.14 Results for methane content of the biogas at different organic loading rate for the batch experiments.

4.2.5 Methanogenic Activity

This parameter was calculated for each specific COD loading, based on the rate of methane production and the amount of biomass at the time, and was reported as $\frac{gCH_4 - COD/d}{gVSS}$. Calculation of methane production rate expressed in COD units is previously described in section 3.3.5. Starting with known concentrations of the biomass in each run, the amount of biomass at any time was calculated using the results from the numerical method and compensating for the washed-out biomass. Results for specific methanogenic activity are shown in Figure 4.15. Similar trends were obtained for both systems while better results were calculated for the first system.

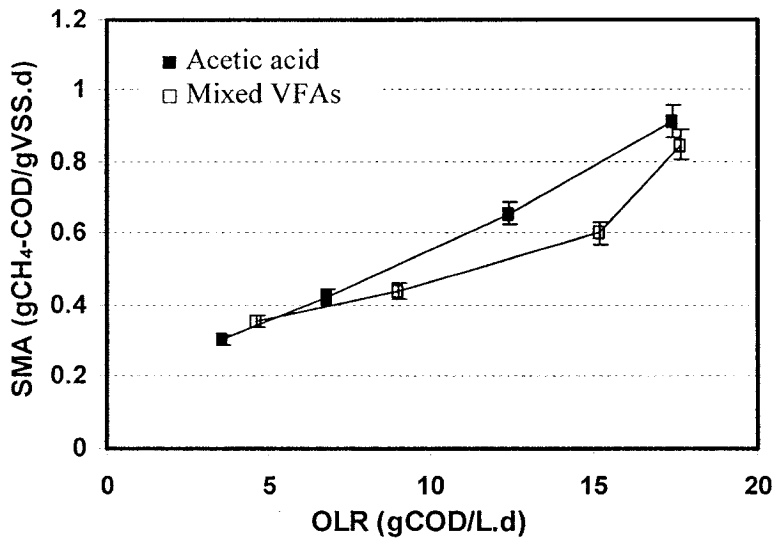

Figure 4.15 Specific methanogenic activity of the sludge as a function of organic loading rate for the batch experiments.

The maximum activity for the pure or enriched methanogenic culture is about 10 g COD removed/gVSS.d (Harper and Pohland, 1986), while the observed activity in both industrial and laboratory digesters ranges from 0.1 to 1.0 gCOD removed/gVSS (Dolfing and Bloemen, 1985; Field *et al.*, 1988; Guiot, 1991; Soto *et al.*, 1993). This can be due to the fact that in activity tests for a mixed culture, only a fraction of the inoculated

microorganisms will be able to produce methane. If the ratio between the actual activity and the maximum pure culture activity can be assumed as the fraction of acetoclastic bacteria in sludge, this fraction will range between 1 and 10% (Soto *et al.*, 1993). Expressing the values of SMA based on the volume of methane produced as $\frac{L(CH_4)}{gVSS.d}$, will result in Figure 4.16.

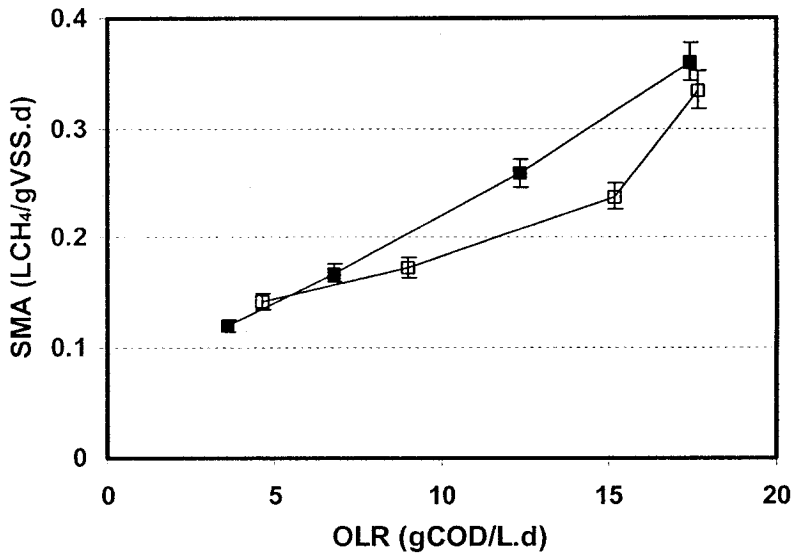

Figure 4.16 Values of specific methanogenic activity calculated based on methane volume as a function of organic loading rate for the batch experiments.

These values are in the range of those reported by James *et al.* (1991) at 35°C using a laborious method with a special respirometer. They used different solutions of acetic acid, mixed VFAs and sodium acetate as substrates with seed sludge from UASB reactors treating low to medium-strength wastewaters. Their values were mostly in the range of 0.2 - 0.4 $\frac{L(CH_4)}{gVSS.d}$.

Soto *et al.* (1993), used a simpler method using a 126 ml vial as described in Figure 4.17 with a VFA mixture (acetic, 2.0 g/L; propionic, and n-butyric acid, 0.5 g/L each) and also individual VFA, neutralized with NaOH. Seed sludge was from an

industrial processing of mussel (Lema *et al.*, 1987), whose most important carbon source was glucogen. They obtained values of 1.047 and 1.25 $\frac{gCH4-COD/d}{gVSS}$ for maximum methanogenic activity with a VFA mixture and acetic acid, respectively, at 37°C.

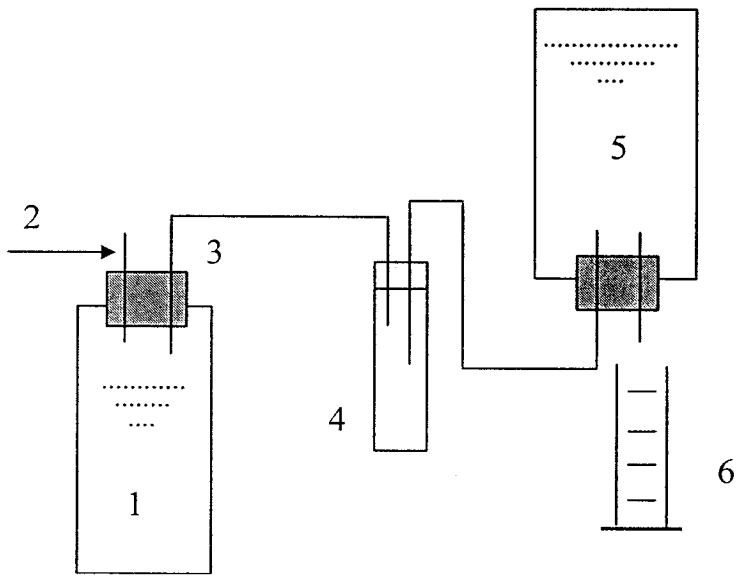

Figure 4.17 Digester of 126 mL connected to the alkaline solution displacement system, used for determination of specific methanogenic activity: (1) Culture medium (2) Sample point (3) Biogas circuit (4) Security vessel (5) Mariotte flask (6) Calibrated cylinder.

In another study, Ince *et al.* (2001) measured the acetoclastic methanogenic activity of a granular sludge to determine the potential loading of a pilot-scale UASB reactor. They used a SMA test reactor at 35°C with seed sludge from a fermentation-based pharmaceutical industry. They obtained a maximum value of 0.072 $\frac{L(CH_4)}{gVSS.d}$ at organic loading rate of 6.1 $\frac{gCOD}{L.d}$ for solutions of acetic acid. Gonzalez *et al.* (2001) obtained an average maximal value of 1.1 $\frac{gCH_4-COD/d}{gVSS}$ for SMA of a sludge sample from a unit treating brewery wastewater, fed on acetate at 31°C.

4.2.6 System efficiency

System efficiency was calculated based on a comparison between theoretical and calculated volumes of methane production for each unit mass of COD removal. A theoretical value of 0.35 L methane is expected for each gram of COD removal at standard temperature (0°C) and pressure (1atm). This value can be calculated for the actual test conditions. Because all experiments were done under atmospheric pressure and a temperature of 35°C, only a correction for temperature is needed for the theoretical value. Assuming the ideal gas law for methane, this correction can be done according the following T-V relationship:

$$\frac{V_s}{T_s} = \frac{V_a}{T_a} \qquad (4\text{-}8)$$

where V and T denotes volume and temperature and indices "s" and "a" refer to "standard "and "actual" conditions respectively. So, for the new temperature, we have:

$$V_a = V_s(\frac{T_a}{T_s}) = 0.35(\frac{273+35}{273+0}) = 0.395L \qquad (4\text{-}9)$$

The calculated results for the two systems are shown in Figure 4.18. Better performance was observed at lower loading rates, with a better efficiency for the first system. As the loading rate increased, two systems showed deviations from the theoretical value while for the final loadings, an improvement was observed which can be due to better adaptation and increasing the methanogenic activity of the reactor biomass.

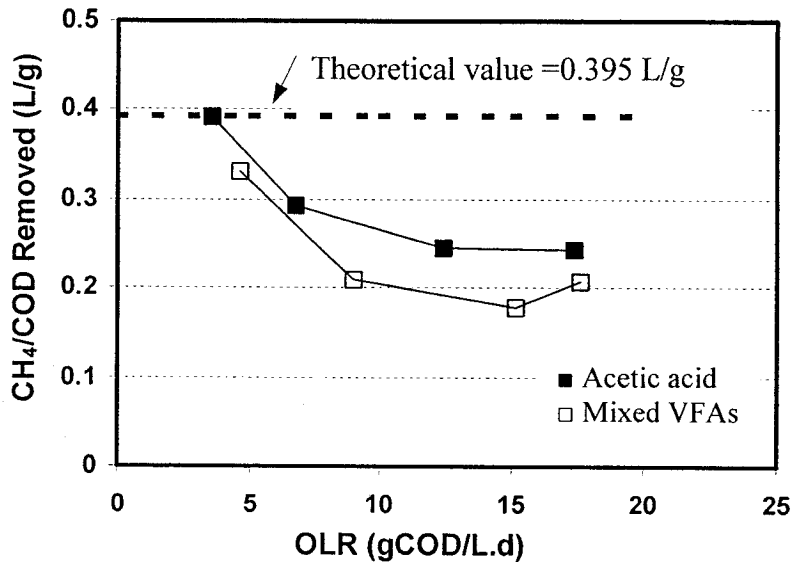

Figure 4.18 Calculated values of system efficiency as a function of organic loading rate for the batch experiments.

4.3 Continuous Operation

For this part of the experiments, a modified setup as illustrated in section 3.2 was used and three systems were considered:

1) System 1: experiments with solutions made with acetic acid as a single VFA.
2) System 2: experiments with solutions made with mixed VFAs including acetic acid
3) System 3: experiments with solutions made with mixed VFAs without acetic acid

Compositions of the solutions were as in Table 3.3. The operating temperature was 35 ± 1.5°C and the working volume was 1L in all experiments. Before starting the experiments, the reactor was fed with a dilute solution of acetic acid (3 gCOD/L) for 1 week for a better adaptation to the new method of feeding. It should be mentioned that throughout the continuous runs, the main operational problems were with the influent pump and flowmeter. It was very difficult to set a steady low flow on the pump because

of the nature of the flow associated with these pumps. Also, the inlet flowmeter was plugged frequently and in order to check the flow, effluent flow was measured using a graduated cylinder and a stopwatch. In this step and because of increased activity of the reactor biomass during the previous step, a hydraulic retention time of 8 h was considered for all experiments, but because of the above-mentioned problems to control the inlet flow, actual values were between 6.7-8.4 h. The initial conditions for each system are shown in Table 4.5.

Table 4.5 Initial test conditions for three systems in the continuous experiments.

System 1				
Parameter	**Amount**			
	Run 1	Run 2	Run 3	Run 4
Initial biomass concentration (gVSS/L)	12.7	13.1	12.9	12.2
Initial COD (g/L)	2.8	2.7	5.2	8.3
System 2				
Parameter	**Amount**			
	Run 1	Run 2	Run 3	Run 4
Initial biomass concentration (gVSS/L)	13.1	12.7	12.4	13.0
Initial COD (g/L)	3.5	3.6	5.8	8.4
System 3				
Parameter	**Amount**			
	Run 1	Run 2	Run 3	Run 4
Initial biomass concentration (gVSS/L)	13.5	13.2	13.5	13.6
Initial COD (g/L)	3.2	6.0	6.1	8.1

Based on recommended operating parameters for a UASB reactor (Table 2.4), it was decided that the maximum linear velocity in the reactor should not exceed 3 m/h to reduce losing the biomass through wash out. So, in order to increase the organic loading rate, whenever necessary, influent concentration instead of its flow rate was increased.

4.3.1 COD trends

The COD balance for the system can be written as follows:

$$COD_{rem.} = COD_i - COD_e = COD_m + COD_{loss} \qquad (4\text{-}10)$$

where:

$COD_{rem.}$ = COD removed (g/d)

COD_i = Influent COD (g/d)

COD_e = Effluent COD (g/d)

COD_m = COD converted to methane (g/d) = CH_4 production rate (L/d)/0.395

COD_{loss} = COD loss (g/d)

Table 4.6 shows the results and Figure 4.19 shows the COD removal trends for the three systems. The difference between theoretical and actual amounts of COD is the COD loss. The source of COD loss in the reactor could be the unmeasured methane that was lost through the piping connections and reactor cap, which were not well sealed. This effect is more significant in higher loading rates for which the methane production and therefore the reactor pressure were higher.

Table 4.6 COD balance values (in g/d) of the three systems for the continuous operation.

Parameter	System 1				System 2				System 3			
OLR (gCOD/L.d)	8.8	13.3	22.6	34.4	8.6	14.6	22.1	32.9	8.0	13.8	28.4	35.7
COD_i	8.1	12.2	20.8	31.7	7.9	13.5	20.3	30.2	7.4	12.7	26.1	32.8
COD_0	0.8	1.8	3.8	6.3	1.0	2.6	4.3	7.7	1.0	2.0	6.0	7.6
$COD_{rem.}$	7.3	10.4	17.0	25.3	7.0	10.9	16.0	22.5	6.3	10.7	20.1	25.2
COD_m	6.9	8.9	11.6	13.9	6.4	8.1	10.2	12.4	5.1	7.6	10.3	12.5
COD_{loss}	0.3	1.5	5.3	11.5	0.6	2.8	5.8	10.1	1.2	3.1	9.8	12.7

The same decreasing trends for COD, as those for the batch experiments were observed but with slightly lower values probably due to the new mode of operation. System 1 showed better results than the others and the results for systems 2 and 3 are in the same range.

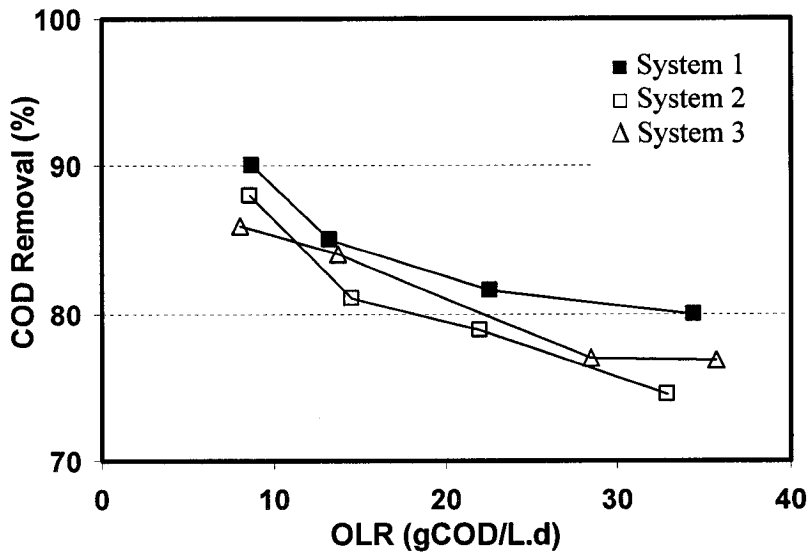

Figure 4.19 COD removal trends as a function of organic loading rate for the three systems during continuous operation.

4.3.2 VFA removal trends

The three systems showed good VFA removals as shown in Figure 4.20. As for COD trends, all VFA trends are decreasing with increasing OLR and similar trends were obtained for the three systems.

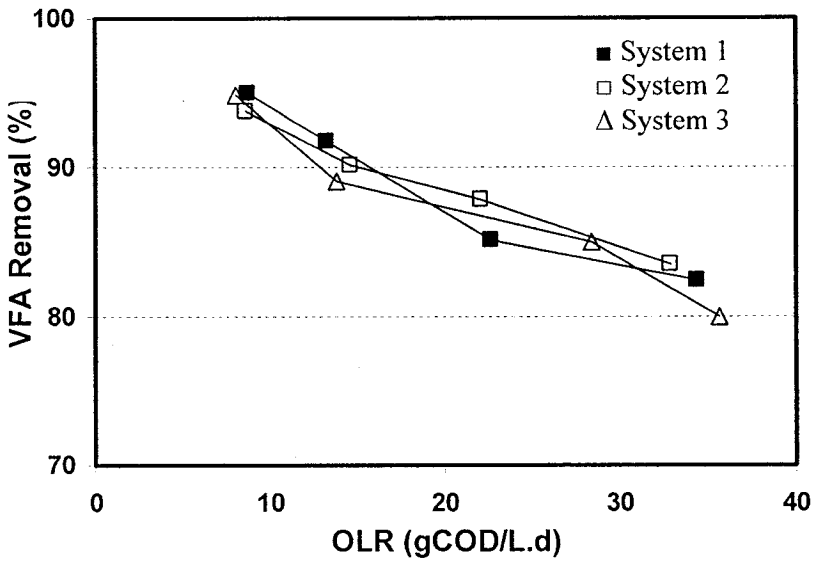

Figure 4.20 VFA removal trends as a function of organic loading rate for the three systems during continuous operation.

As shown in Table 4.7, based on the thermodynamics of VFA oxidation and net energy released from digestion of acetic, propionic and butyric acids (-31.0, -34.0 and -39.4 kJ/mol CH_4 respectively), the reaction preference is in the order of butyric acid > propionic acid > acetic acid. For lower organic loads which are usually associated with less concentrated solutions, this effect is not as significant as it probably is for higher loading rates. VFA analysis from reactor samples showed that acetic acid concentrations in the samples were higher than those of propionic and butyric acids with the minimum values for butyric acid (data not shown), which could be due to the possibility that the presence of the conjugate salt (sodium acetate) and lower concentrations of acetic acid in

VFA solutions (specially those without acetic acid) could accelerate the conversion of propionic and butyric acids to acetic acid by syntrophic bacteria in mixed VFA solutions.

Table 4.7 Standard Gibbs free energy for VFA degradation by methanogens (From Ferry, 1993).

Reaction	ΔG^0 (kJ/mole CH_4)
2 Butyrate$^-$ + HCO_3^- +H_2O ⟶ 4Acetate$^-$ + CH_4 + H^+	-39.4
4 Propionate$^-$ + $3H_2O$ ⟶ 4Acetate$^-$ + HCO_3^- + H^+ + $3CH_4$	-34.0
Acetate- + H_2O ⟶ HCO_3^- + CH_4	-31.0

On the other hand, as shown in Figure 4.21 (Björnsson, 2000), the hydrogen partial pressure plays an important role in the rate of propionate and butyrate oxidation and increasing the hydrogen partial pressure can have an inhibitory effect on the methane production from these acids.

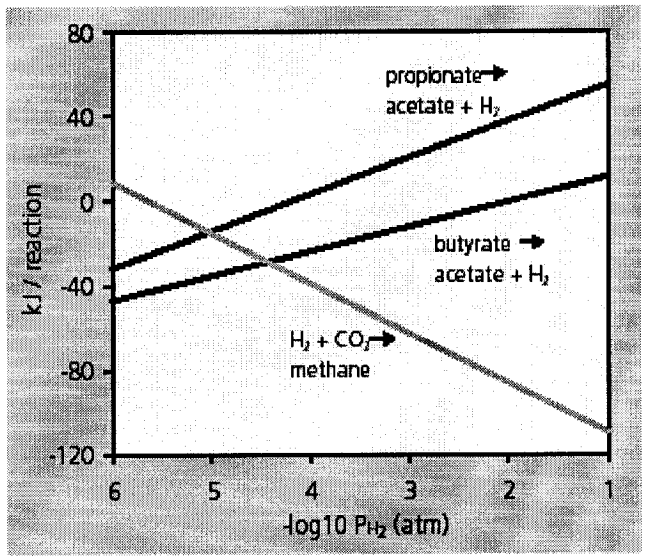

Figure 4.21 Thermodynamic dependency upon $P(H_2)$- Data derived from Archer (1983). Calculations based on standard values for free energies at pH 7, 25°C, 34 mM HCO_3^-, 1mM VFAs and $P(CH_4)$ 0.7 atm.

4.3.3 CO_2 trends

For the captured carbon dioxide, the mass balance (in g/d) was calculated as follows:

$$CO_2(aq)_i - CO_2(aq)_e - (CO_2)_b = (CO_2)_{rem.} = (CO_2)_m + (CO_2)_{abs} \quad (4\text{-}11)$$

where:

$CO_2(aq)_i$ = Dissolved carbon dioxide in the influent

$CO_2(aq)_e$ = Dissolved carbon dioxide in the effluent

$(CO_2)_b$ = Carbon dioxide in the biogas

$(CO_2)_{rem}$ = Removed carbon dioxide

$(CO_2)_m$ = Carbon dioxide converted to methane

$(CO_2)_{abs}$ = Carbon dioxide absorbed by the solution

The amount of dissolved carbon dioxide in the influent was higher for the concentrated solutions. Figure 4.22 shows the calculated vales of dissolved CO_2 at different COD values for the three systems.

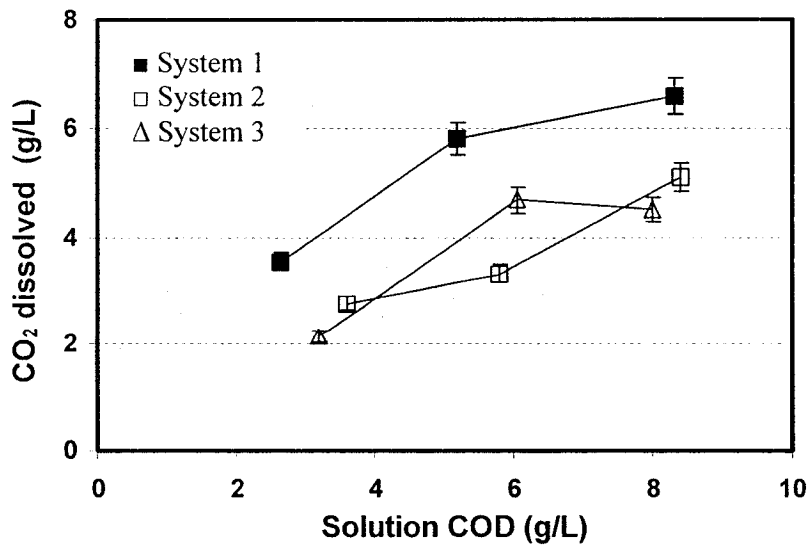

Figure 4.22 The amounts of dissolved carbon dioxide at different COD values for the three systems during continuous operation.

The values of dissolved carbon dioxide were calculated as described in section 3.3.4. Since the dissolved carbon dioxide took part in different reactions including its consumption (by hydrogentrophic methanogens) and production (see Table 4.7), or the reactions among the inorganic species, it was not possible to determine the contribution of each part to reduce dissolved carbon dioxide in the processed solutions. However, the values of removed carbon dioxide were calculated using the equation (4-11) and the removal efficiency was calculated (discussed in Section 4.3.5). Table 4.8 shows the CO_2 balance for the three systems.

Table 4.8 The CO_2 balance values (in g/d) of the three systems for the continuous operation.

Parameter	**System 1**				**System 2**				**System 3**			
OLR (gCOD/L.d)	8.8	13.3	22.6	34.4	8.6	14.6	22.1	32.9	8.0	13.8	28.4	35.7
$(CO_2)_i$	8.6	16.4	23.3	25.1	5.4	13.5	20.3	30.2	7.4	12.7	26.1	32.8
$(CO_2)_e$	0.5	0.7	0.7	0.3	0.2	2.6	4.3	7.7	1.0	2.0	6.0	7.6
$(CO_2)_b$	1.3	1.9	2.6	3.3	1.5	2.1	2.9	4.0	1.0	1.7	2.6	3.3
$(CO_2)_{rem.}$	6.7	13.8	19.9	21.4	3.7	7.9	8.5	14.0	3.6	7.8	17.1	14.8

The amounts of removed CO_2 at different organic loading rates are shown in Figure 4.23, which shows that the system 1 had a better removal rate.

4.3.4 Methane content of the biogas and methane production rate

The results for methane content and production rate for the three systems are shown in the Figure 4.24. For all systems, similar trends in each case are observed and better results are obtained compared to the batch experiments. The first system shows

better results than the others especially for higher loading rates. This behavior for two other systems could be due to lower methanogenic activity as a consequence of higher hydrogen partial pressure resulting from propionate and butyrate oxidation as discussed before.

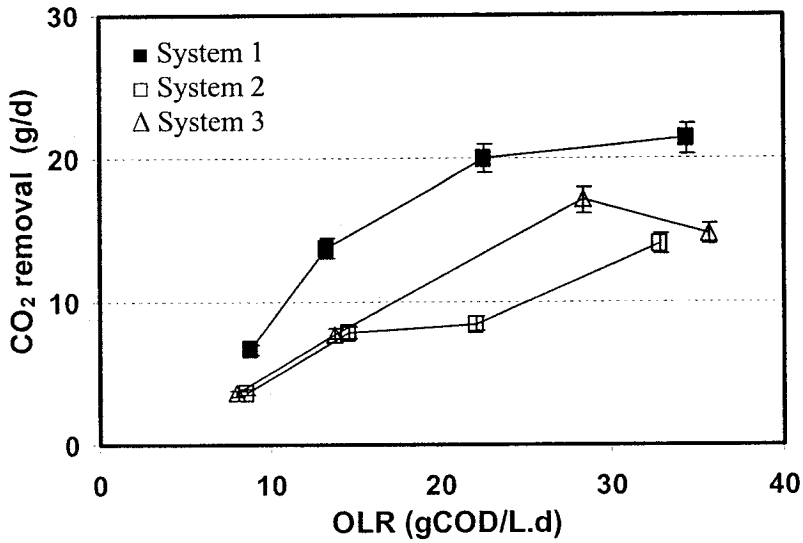

Figure 4.23 The amounts of CO_2 removal at different organic loading rates for the three systems during continuous operation.

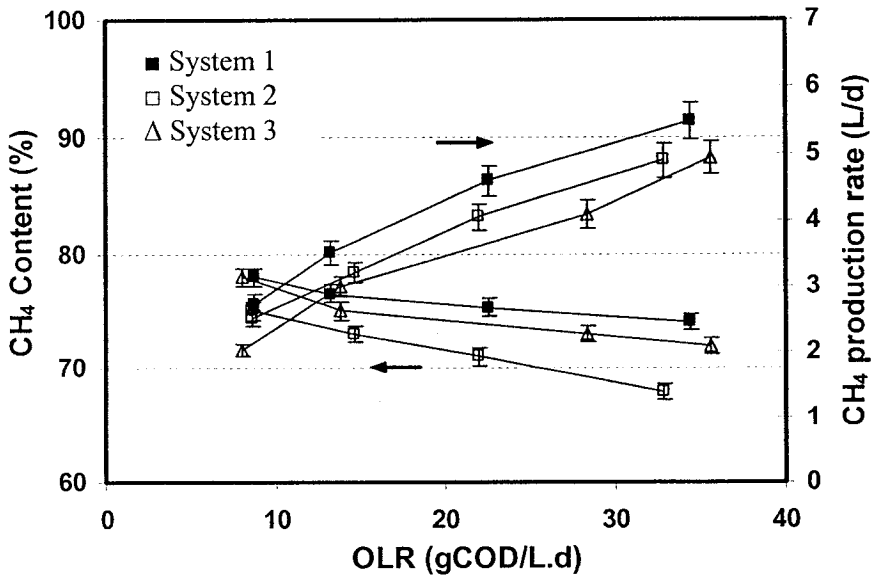

Figure 4.24 Results for methane content and methane production rate as a function of organic loading rate for three systems during continuous operation.

4.3.5 pH and total alkalinity (TA)

pH values of the reactor influent and effluent are shown in Figures 4.25. The pH values in the reactor were always increasing due to VFA digestion and CO_2 and H_2 consumption by the methanogenic reactions. Although it was beneficial to have a higher alkalinity in the initial solutions to absorb more injected CO_2, it was found that to maintain the reactor pH in the optimum range for the methanogens, the pH of the fed solutions after being saturated by CO_2, should be around 5.6 ± 0.15. Values for the effluent pH were then between 7.16-7.65.

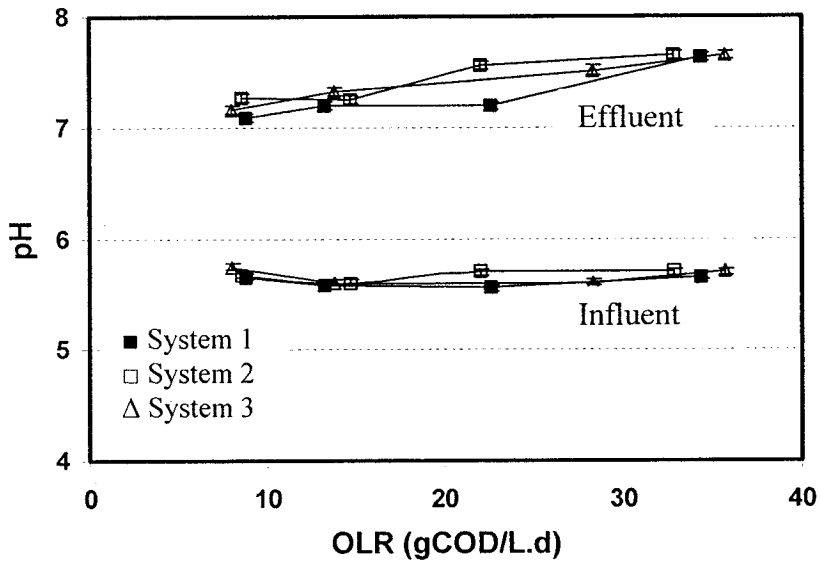

Figure 4.25 Values of influent and effluent pH at different organic loading rates for three systems during continuous operation.

Figure 4.26 shows the initial alkalinity of the solutions after being saturated by CO_2.

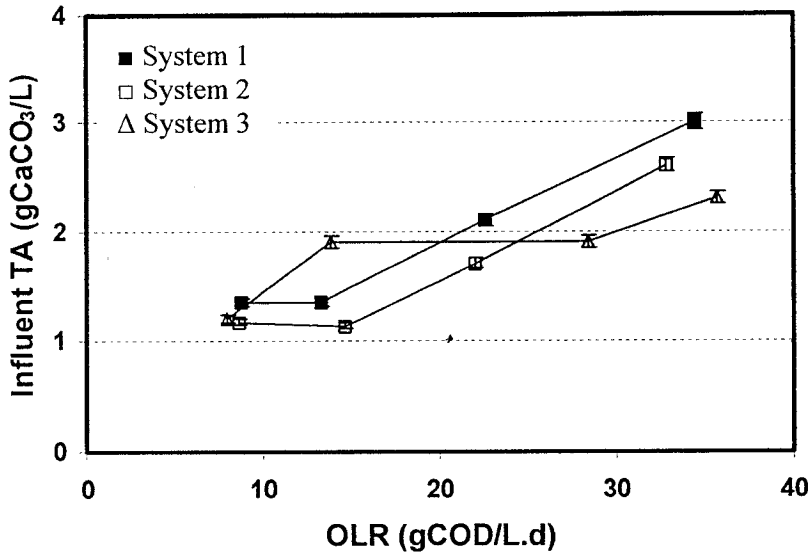

Figure 4.26 Values of influent total alkalinity (TA) at different organic loading rates for three systems during continuous operation.

The results for effluent alkalinity are shown in Figure 4.27. It was observed that due to digestion of the acids by the methanogens, the alkalinity values for the reactor effluents were higher than those for the influents and this increase was about 1-1.5 unit ($gCaCO_3/L$).

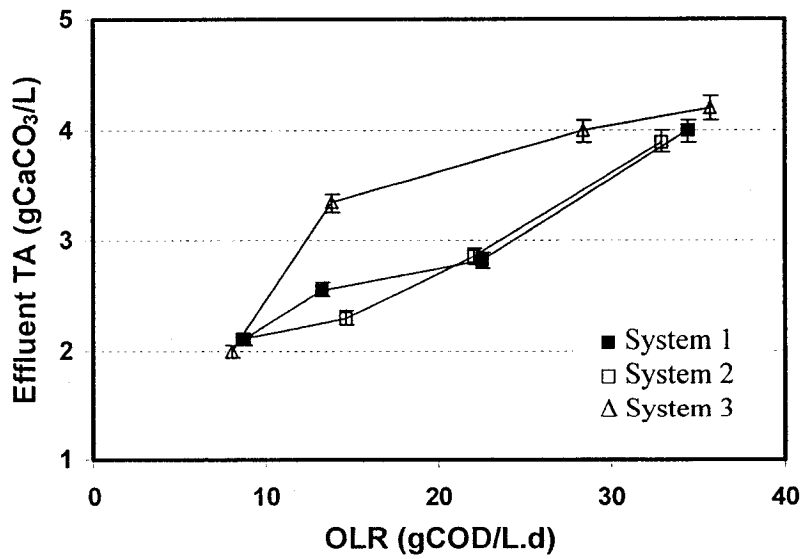

Figure 4.27 Variation of effluent total alkalinity (TA) at different organic loading rates for three systems during continuous operation.

4.3.6 System efficiency

System efficiency for the continuous operation was calculated based on COD and CO_2 removals. Since the highest values for both were desired, it is better to consider their product as an overall efficiency (η_{ove}) and define it as below:

$$\eta_{ove} = \eta_1 . \eta_2 \qquad (4\text{-}10)$$

where;

η_1 = System efficiency based on actual and theoretical amounts of COD removal and methane production.

η_2 = System efficiency based on CO_2 removal.

4.3.6.1 Efficiency Trends for COD removal

Calculated values of methane production per amount of COD removal for all systems are shown in Figure 4.28. Also, system efficiency, η_1, is calculated for the three systems and the results are shown in Figure 4.29. Compared to the batch experiments, higher values are obtained in this section and the values are highest for the first system and higher for the second compared to the third, showing a better performance of methanogens to digest simpler fatty acid molecules than more complex ones.

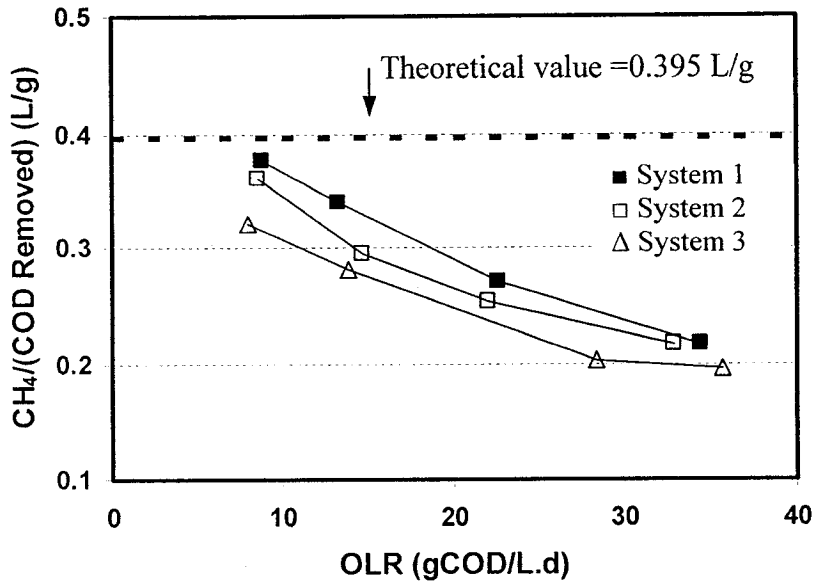

Figure 4.28 Theoretical and calculated values of methane production per COD removed at different organic loading rates for the three systems during continuous operation.

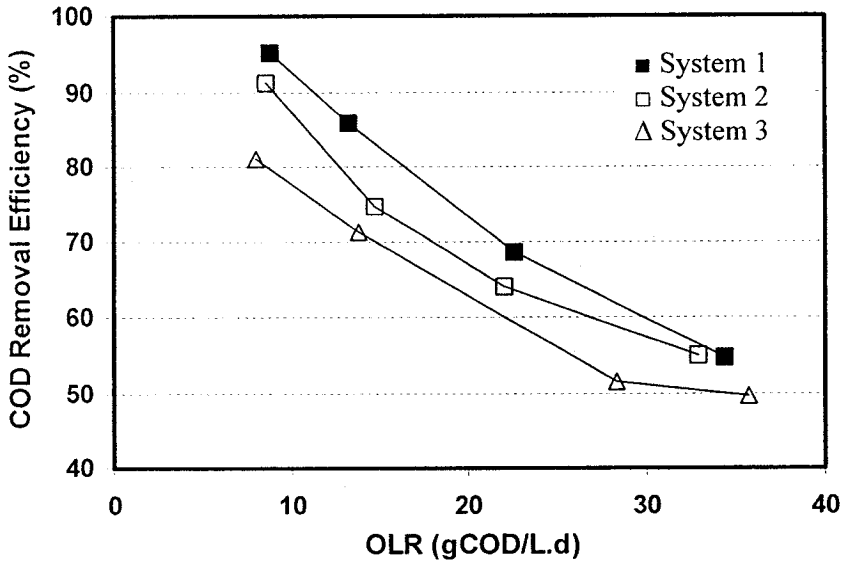

Figure 4.29 Efficiency values (η_1) at different organic loading rates for the three systems during continuous operation.

4.3.6.2 Efficiency trends for CO_2 removal

Values of the CO_2 removal efficiency (η_2) were calculated using the data in Table 4.8 and the following equation:

$$\eta_2 = \frac{(CO_2)_{rem}}{CO_2(aq)_i} = \frac{CO_2(aq)_i - CO_2(aq)_e - (CO_2)_b}{CO_2(aq)_i} \times 100 \qquad (4\text{-}11)$$

The results are shown in Figure 4.30. For the three systems, values of η_2 were between 68.7% and 85.7% and all trends were increasing, showing better removals for more concentrated solutions associated with higher loading rates.

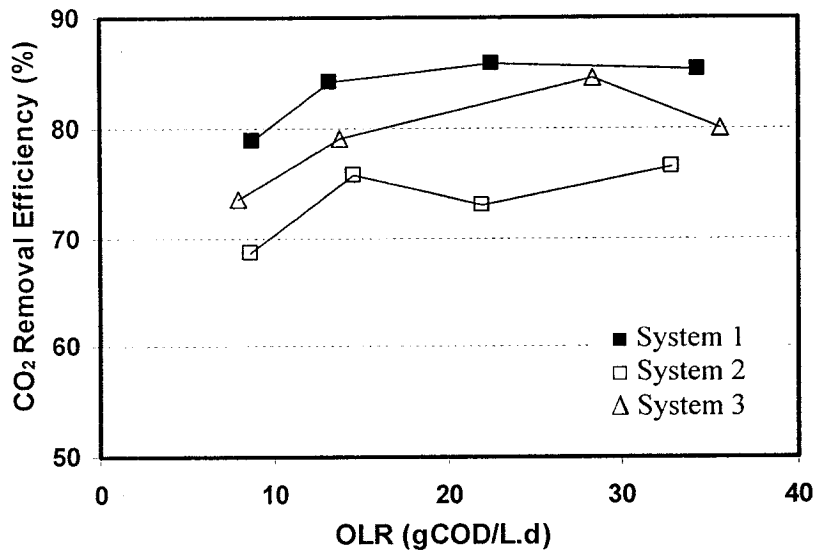

Figure 4.30 Values of CO_2 removal efficiency (η_2) for the three systems during continuous operation as a function of organic loading rate.

4.3.7 Overal Efficiency

Calculated values of the overall efficiency (η_{ove}) are shown in Figure 4.31. The first system showed the best performance in all organic loading rates and the results for the two others were in the same range. For higher organic loading rates, a lower rate of

decrease in values of overall efficiency is seen (especially for the second and third systems) which can be due to better CO_2 removal at higher loadings and better adaptation of the biomass to the continuous operation.

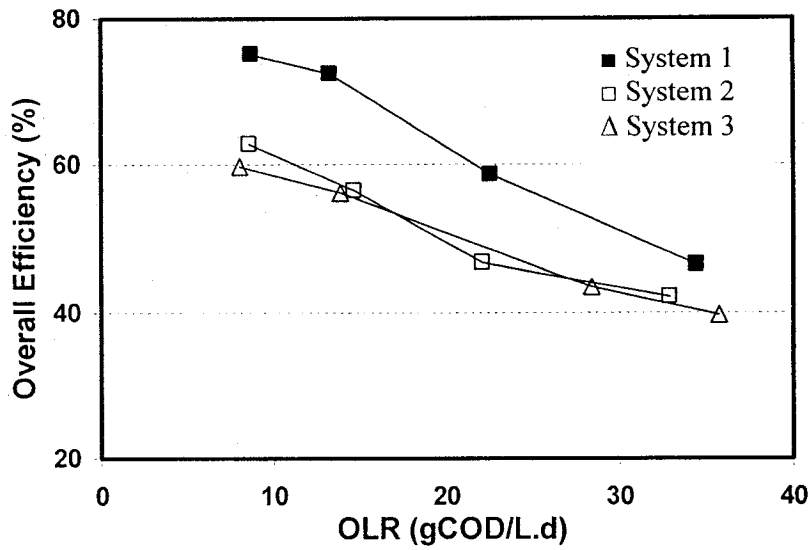

Figure 4.31 Values of overall efficiency (η_{ove}) as a function of organic loading rates for the three systems during continuous operation.

4.4 The reactor sludge

The amount and quality of the reactor biomass were monitored through analytical and microscopic tests. Also the amount of wasted sludge in the reactor effluent, the sludge height in the reactor, value of TSS and VSS were measured throughout the experiments.

4.4.1 Washed-out sludge

Every week, the amount of washed-out sludge during the discharge and refill process for the batch runs was measured and at the same time, and sludge height in the

reactor was recorded. The results are shown in Figure 4-32. It can be seen that biomass wash-out was at its highest value for the first weeks as a result of increasing rate of the biogas and its upflow velocity, but as the granulation and settling characteristics of the reactor sludge were improved, the amount of washed-out sludge decreased and the amount of sludge remaining in the reactor became more stable.

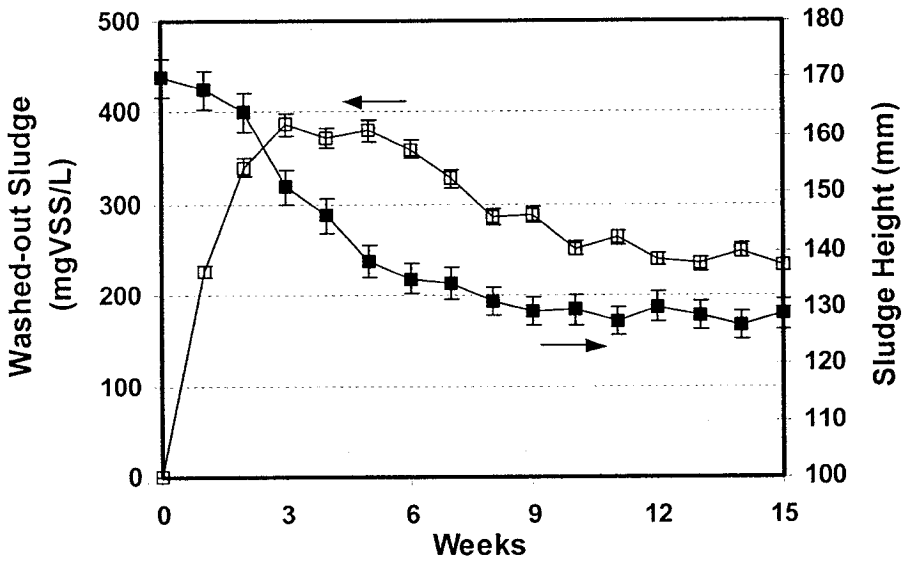

Figure 4.32 Progress curve for the amount of washed-out sludge and sludge height in the reactor.

4.4.2 Volatile and Suspended Solids of the Sludge (VSS and TSS)

The VSS, TSS and VSS/TSS ratio for the sludge in the reactor was measured and monitored in each stage of the work. Each time, three samples were taken and tested according to the method illustrated in section 3.3.5. It was realized that for all samples, the maximum difference between the average and the lowest or highest values was about 3%, so 3% error was considered with the data. Figure 4.33 shows these results for working weeks of the activation period and batch experiments.

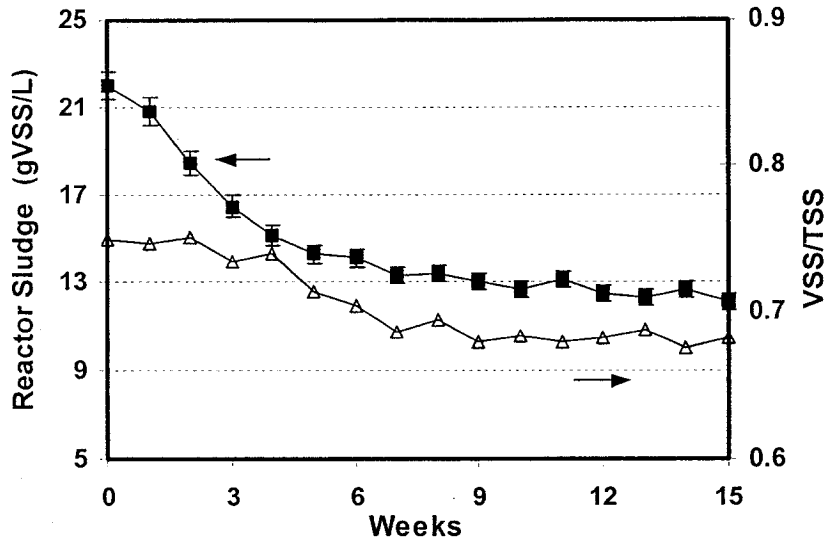

Figure 4.33 Progress curve for amounts and VSS/TSS ratios of the reactor sludge during the batch experiments.

As the results show, there was a sharp decrease in the amount of VSS in the reactor especially for the beginning weeks due to biomass wash-out and upflow gas bubbles in the reactor. Part of the biomass wash-out was due to erosion wash-out as mentioned by De Zeeuw (1984), which is usually the case for UASB reactors during the first weeks of start-up. The loss rate was decreased from week 6 which could be due to the improvement of the sludge settleability. The results for VSS and VSS/TSS ratio of the reactor sludge for the continuous operation are shown in Figure 4.34. Here, less variation in the amount of reactor biomass was observed and a more stationary biomass seemed to be established in the reactor.

The ratio of VSS/TSS for the initial biomass was 0.75 and it showed a decreasing trend during the first weeks after the reactor start-up, due to possibly loss of the lighter fraction, but seemed to be more stable after seven weeks. During the continuous operation, this ratio was gradually increased and a final value of 0.723 was measured for the sludge.

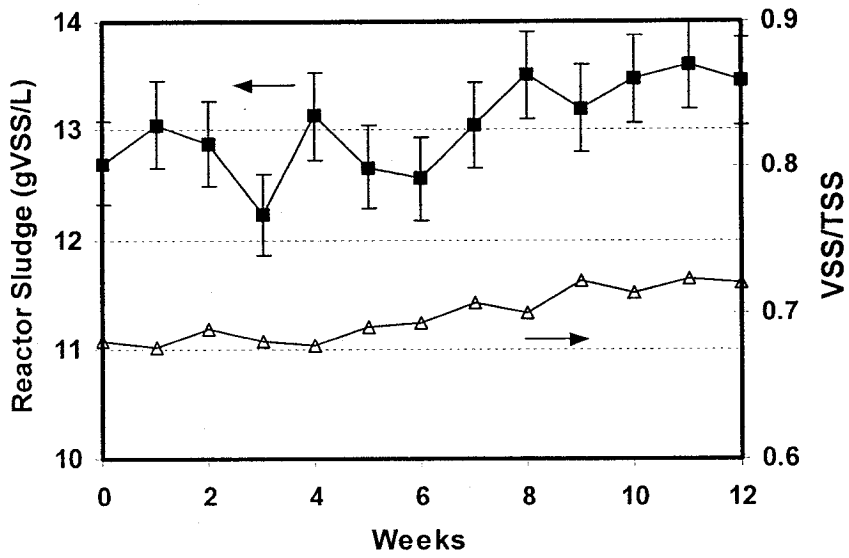

Figure 4.34 Progress curve for VSS and VSS/TSS ratio of the reactor sludge in the continuous operation.

These variations are related to structural changes of the biomass particles, which in turn are influenced by multiple factors as discussed in section 2.3.1, including influent composition. Higher VSS/TSS shows that the amount of insoluble organic or inorganic particulates contributing to TSS is less compared to organic constituents. This is usually the case for biomass particles treating soluble substrates. In a study by Dolfing *et al.* (1985) on granular methanogenic sludge grown on wastewater of a liquid sugar factory, values of 10 to 20% were reported for ash content of the biomass. The ash content of the initial and final biomass in this study was 25% and 27.7 % respectively. Zehnder *et al.* (1991) reported a minimum value of 45.4% for ash content of granular sludge grown on propionate in an UASB reactor. Gonzalez *et al.* (2001) reported an ash content of 15%, which did not vary significantly during one year of reactor operation. Fang (2003) reported the formation of granules of 1.6 mm in diameter, 1.038 g/ml in density and 11% in ash content for H_2-producing acidogenic sludge in a stirred reactor treating sucrose-rich wastewater at 26°C and pH 5.5 with 6 hours of hydraulic retention.

Figure 4.35 shows the amount of biomass wash-out during the continuous operation. For this part, the reactor sludge was more stable since the amount of biomass loss due to wash-out, is less than that for the batch experiments.

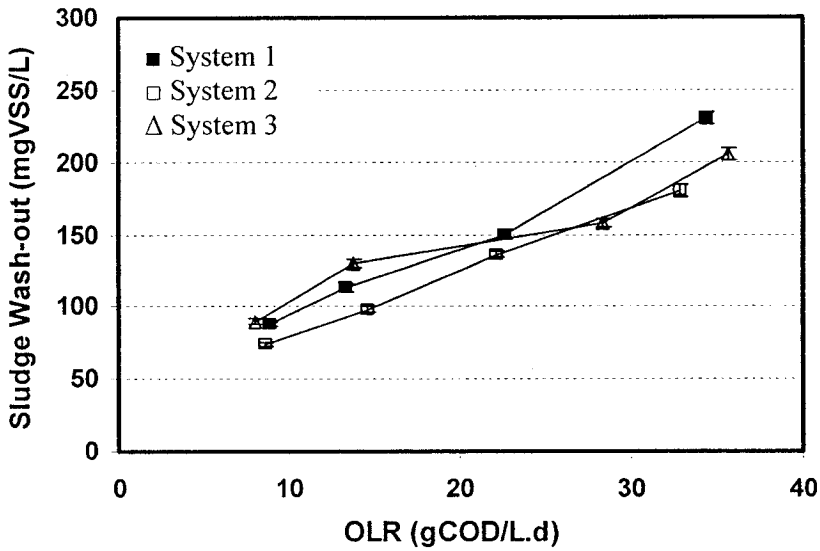

Figure 4.35 Results for sludge wash-out as a function of organic loading rate for three systems in the continuous operation.

4.4.3 Microscopic observations

Figure 4.36 shows pictures taken at different time intervals. Picture (a) shows the initial biomass from the whey-treating unit, consisted of particles covered with a grayish layer. As the experiments were going on, the appearance of the biomass particles changed indicating a structural change: In picture (b), the grayish layer seems to become thinner and pictures (c) and (d) show black spherical particles which are very different from the first ones and contain whitish spots on their surfaces probably due to inorganic compounds, e.g., Na^+ salts as discussed by Peinemann *et al.* (1988) or inorganic precipitates, e.g., $CaCO_3$ or calcium phosphate. Since bicarbonate is produced during anaerobic conversion of acetate, calcium precipitates can form within the sludge, even at

reactor calcium concentrations as low as 200 mg/liter (Guiot *et al.*, 1992, Uemura *et al.* 1995).

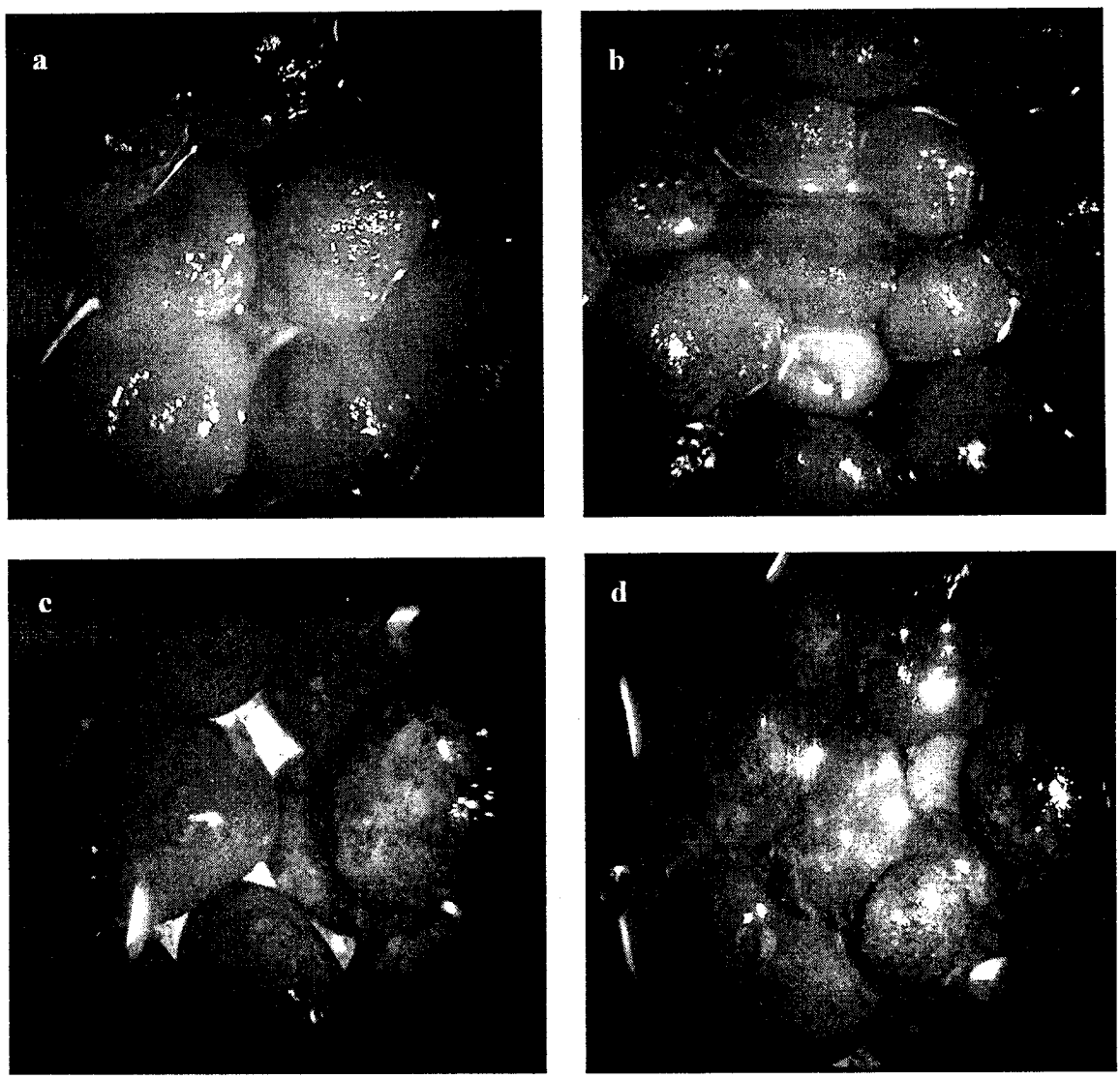

Figure 4.36 (a) Inactive sludge before the reactor start-up (b) Active Sludge after 10 weeks (c) & (d) Active Sludge after the end of the continuous runs (scales: b,c: 12X, a,c: 25X).

Final biomass particles were mostly in the size range of 1.5-2.5 mm, which was not very different from the initial ones, but some particles with diameters of 3.5 mm were observed. As mentioned before in section 2.3.1, many factors affect the granulation process in anaerobic treatment. More specifically, the granule's bacterial profile, and its

microstructure, depends on the concentration profile of the substrates and metabolites, such as VFA, acetate, hydrogen, etc., inside the granule (Fang *et al*, 1995). Zehnder *et al.* (1991) reported that for granules grown on propionate as a sole carbon and energy source, larger granules were obtained by using high substrate concentrations. The schematic shown in Figure 4.37, was proposed by Fang *et al.* (1995) for granules treating soluble hydrocarbons.

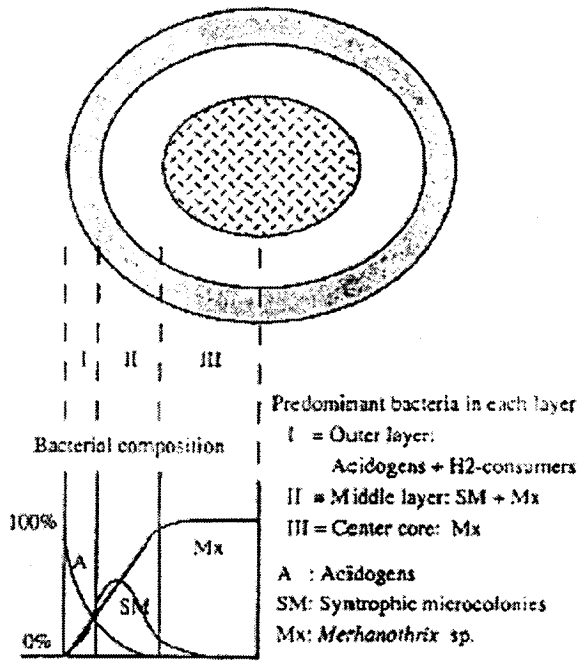

Figure 4.37 Proposed layered structure and bacterial composition for the granules treating soluble carbohydrates (Fang *et al.*, 1995).

As can be seen in the above structure, acidogens which are responsible for breaking down macromolecules in a complex substrate, are concentrated in the outer layer of the granule and they can be part of constituents of the grayish layer for the initial biomass in this study. As there were no polymeric macromolecules in the solutions prepared in this study, the population of acidogens might have been decreasing resulting in a change in the microstructure of biomass particles.

Microscopic observations towards the other microbial and activity tests can show the gradual changes in the microbial population and help interpretation of the results.

CHAPTER 5

CONCLUSIONS AND RECOMMENDATIONS

5.1 Conclusions

From the results of the research carried out in this work, the following conclusions are drawn:

1- A new method to convert carbon dioxide to methane was developed. All the systems showed high removal values (more than about 70%) for dissolved CO_2 in all organic loadings for which the values of above 75% were obtained for COD removal.

2- The solutions made in this work, were capable to capture CO_2 and the amount of captured carbon dioxide increased with the solution concentration and alkalinity. It was also possible to first treat a CO_2-containing gas stream with fresh water and then use this acidified water to make solutions.

3- It is better to use lower-chain fatty acids in the solutions since they are easier to digest for the methanogens and in turn will increase the methane production efficiency and therefore overall efficiency of the system.

4- The kinetic behavior of a system was investigated. A numerical method was developed to estimate kinetic parameters of the system. The results of the numerical method showed a good consistency with the experimental data, especially for less concentrated solutions. These parameters can be used to design anaerobic reactors.

5- It is important to select suitable materials with certain amounts for solution making. For each purpose, a different medium may be required which should be made according to the reference values for different microorganisms.

6- Acclimation of the biomass to the consumed material and operating conditions is very important. It is better to use the same materials and run the system under a steady operating condition, i.e., constant flow and temperature in order to have a steady condition with maximum efficiency.

7- Regarding the above mentioned comment, it is better to operate the system in a constant mode from the beginning. Since all UASB reactors operate in a continuous mode, it is better to run the lab-scale UASB reactors in the same mode, unless there is a need to study the kinetics of the system, for which a batch mode should be employed.

8- Increasing the organic loading rate should be done step-wise with a gradual acclimation of the biomass and regarding its activity, in order to avoid shock loadings which have negative effects on the system.

9- In batch operations, it is better to load low to medium strength solutions (here, less than 6 g/L for 1 L working volume) to the reactor, since the highly concentrated solutions, will make higher turbulence in the reactor, especially when the biomass is highly active. This will cause the biomass particles to collide and crash with each other and will result in production of more fine particles and higher washout rates.

10- Inhibitory conditions, i.e., high concentrations of inorganic materials, too high or low pH values, dissolved oxygen and toxic materials can significantly decrease the system efficiency. Care should be taken to avoid them.

11- Since the values of 50%-95.2% and 84.5%-92.2% were obtained for the COD and CO_2 removals respectively, it appears that to increase the overall efficiency, more efforts should be done to increase the former while keeping the latter at its highest values.

12- The UASB model reactor was a good prototype of a real one. It had an effective hydraulic characteristic regarding inflow distribution and its uniformity. The bottom distributor, made a plug-flow type pattern for the liquid flow which is a very important factor for an ideal UASB reactor. This design can be scaled up for the real reactors.

5.2 Recommendations

The following items may be further investigated in order to continue with the refinement and development of this work:

1- Since aqueous solutions containing CO_2 are treatable in this system, it is possible to design a system to treat aqueous solutions from CO_2 scrubbers as shown in the following schematic diagram.

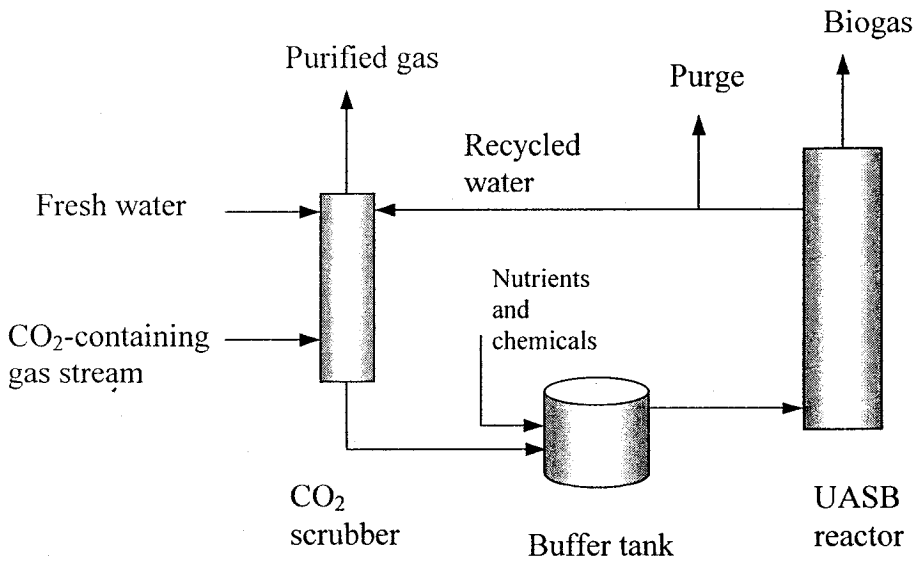

Figure 5.1 Flowsheet of the overall system to remove CO_2 from a gas stream.

2- There is a potential to do a similar study focusing on hydrogentrophic methanogens which are able to directly convert CO_2 to methane according to the following reaction:

$$CO_2 + 4H_2 \longrightarrow CH_4 + 2H_2O \qquad \Delta G^\circ = -130.4 \text{ kJ/mole } CH_4$$

The reaction is thermodynamically favorable and no further carbon dioxide is produced, but a source of hydrogen, i.e., a hydrogen generator may be needed which may question the feasibility of the method.

3- It would be better to work with a custom-made lab-scale UASB reactor with a minimum capacity of two liters or more to overcome some operating problems encountered with the one used in this work, i.e., fluctuations in low flow rates or limitations in sampling from the reactor solution or biomass. Furthermore, controlling instruments can be mounted more effectively on the bigger reactors. In these reactors, it is also possible to do a study on the sludge blanket itself by having multiple sample points along this zone.

4- There is a potential to develop the method for the existing wastewater treatment plants and investigate the dissolution of sequestered CO_2 into the influent streams or in the similar synthetic wastewaters. There is also a possibility to introduce methanogens to the underground storage areas containing captured CO_2 and provide them with necessary materials in order to convert CO_2 to methane. This seems to be more practical for sequestered CO_2 in coal beds or oil fields, since many natural gas fields were created this way.

REFERENCES

Ahring, B. K., and Westermann, P. (1987) Kinetics of butyrate, acetate and hydrogen methabolism in thermophilic, anaerobic butyrate-degrading triculture. *Appl. Environ. Microbiol.* **53**:434-439.

Alexander, M. (1994) *Biodegradation and bioremediation*, p. 71-98. Academic Press, A division of Harcourt Brace & Company, New York.

Archer, P. B. and Powell, G. E. (1985) Dependence of the specific growth rate of methanogenic mutualistic cocultures on the methanogen. *Arch. Microbiol.* **141**:133-137.

Archer, D. B. (1983) The microbial basis of process control in methanogenic fermentation of soluble wastes. *Enzyme Microbial Technology* **5**:162-169.

Atlas, M. (1997) *Handbook of Microbiological Media*. Florida, USA. CRC Press, Inc. pp. 898-901, p. 911.

Bachu, S., Gunter, W.D, and Perkins, E. H. (1994) Aquifer disposal of CO_2: hydrodynamic and mineral trapping. *Energy Conversion and Management* **34**(4):269-279.

Bergy, H. J. G., Krieg N. R., Sneath P. H. A., Stanley J. T. (1994) *Bergey's manual of determinative bacteriology.* Lippincott, Williams & Wilkins; 9th edition.

Björnsson, L. (2000). Intensification of the biogas process by improved process monitoring and biomass retention. *Doctoral Dissertation*, Department of Biotechnology, Lund University Sweden.

Bleicher, K., Zeller G., and Winter J. (1989) Growth of methanogens on cyclopentanol/ CO_2 and specificity of alcohol dehydrogenase. *FEMS Microbiol. Lett.* **59**:307-312.

Blotevogel, K. H., Gahl-JanBen R., Jannsen S., Fischer U., Pilz F., Auling G., Macario A. J. L, and Tindall B. J. (1991) Isolation and characterization of a novel mesophilic, fresh-water methanogen from river sediment *Methanoculleuse oldenburgensis* sp. nov. *Arch. Microbiol.* **157**:54-59.

Blotevogel, K. H., Fischer U., Mocha M., and Jannsen S. (1985) *Methanobacterium thermoalcaliphilium* spec. nov., a new moderately alkaliphilic and thermophilic autotrophic methanogen. *Arch. Microbial.* **142**:211-217.

Boone, D. R., Johnson R. L., and Liu Y. (1989) Diffusion of the interspecies electron carriers H_2 and formate in methanogenic ecosystems and implications in the measurement of K_m for H_2 or formate uptake. *Appl. Environ. Microbiol.* **55**:1735-1741.

Cappenberg, T. E. (1975) A study of mixed continuous cultures of sulfate reducing and methane-producing bacteria. *Microb.Ecol.* **2**:61-67.

Chakma A. (1995) separation of CO_2 and SO_2 from flue gas streams by liquid membranes. *Energy Convers. Mgmt.* Vol. **36**, No. 6-9, pp. 405-410.

Clesceri L. S., Greenberg A. E. and Eaton A. D. (1998) Standard Methods for the Examination of Water and Wastewater, Published by the American Public Health Association, the American Water Works Association and the Water Environment Federation, New York.

Corbitt Robert A. (1999) *Sandard Handbook of Environmental Engineering*, 2nd edition, McGraw-Hill Handbooks, New York.

Danish Energy Agency. (1995) *Progress Report on the Economy of Centralized Biogas Plants*, Danish Energy Agency, Copenhagen, Denmark.

De Zeeuw, W. (1984) Granular sludge in UASB reactors. In: *Granular Anaerobic Sludge Microbiology and Technology Proceedings of the GAMSAT Workshop, Lunteren, The Netherlands.*

De Zeeuw W. (1984) Acclimation of Anaerobic Sludge for UASB Reactor Start-up. Ph.D. Thesis, Univ. of Wageningen, The Netherlands.

Fang H. H. P. (2003) Two stage anaerobic wastewater treatment (Website http://web.hku.hk/~hrechef/)

Ferry, J. G. (1993) *Methanogenesis: Ecology, Physiology, Biochemistry & Genetics.* Chapman and Hall, Inc. New York, NY.

Fukazaki, S., Nishio N., and Nagai S. (1990) Kinetics of the methanogenic fermentation of acetate. *Appl. Environ. Microbiol.* **56**:3158-3163.

Giraldo-Gomez, E., Parkhurst S., Goodwin S. and Switzenbaum M. S. (1991) Determination of the half-saturation constant for hydrogen uptake in a mixed-culture methane-producing enrichment. The influence of mass transfer limitations. Submitted to *Biotechnol. Bioeng.*

Gonzalez-GH G., Lenz P. N. L., Van Alest A., Van As H., Versprille. (2001) Cluster structure of Anaerobic Aggregates of an Expanded Granular Sludge Bed Reactor.*Appl. Environ. Microbiol.* P. 3683-3692.

Grotenhuis, J. T. C., Kiessel J. C., Plugge C. M., Stams A. J. M., and Zehnder A. J. B. (1991) Role of substrate concentration in particle size distribution of methanogenic granular sludge in UASB reactors. *Water Res.* Vol.25, No. 1, pp 21-27, 1991.

Guiot, S. R., Rochelau S., Hawari J., and Samson R. (1992) Induction of granulation by sulphonated-lignin and calcium in an upflow anaerobic sludge bed reactor. *J. Chem. Technol. Biotechnol.* **53**:45–56.

Gujer, W. and Zehnder, A. J. B. (1983) Conversion processes in anaerobic digestion. *Wat. Sci. Technol.* **15**(8/9):27-167.

Harley, J. P., D. Klein A., and Prescott L. M. (1990) Microbiology. Wm. C. Brown Publishers, Dubuque, IA.

Herzog, H., Golomb D., and Zemba S. (1991) Feasibility, modeling and economics of sequestering power plant CO_2 emissions in deep oceans. Environmental Progress **10**(1):64-74

Henze, M. and Harremoës, P. (1983). Anaerobic treatment of wastewater in fixed film reactors- a literature review. *Wat. Sci. Technol.* **15**(8/9):1-101.

Heyes, R. H. and Hall, R. J. (1983) Kinetics of two subgroups of propionate-using organisms in anaerobic digestion. *Appl. Environ. Microbiol.* **46**:710-715.

Hitchon, B. (1996) *Aquifer disposal of carbon dioxide: hydrodynamic and mineral trapping-proof of concept*: Sherwood Park, Alberta, Canada, Geoscience Publishing Ltd.

Hippe, H., Caspari D., Fiebig K., and Gottschalk G. (1979) Utilization of trimethylamine and other N-methyl compounds for growth and methane formation by *Methanosarcina bakeri. Proc. Natl. Acad. Sci. USA* **76**:494-498.

Hulshoff Pol L. W., De Zeeuw W. J., Velzeboer C. T. M. and Lettinga G. (1983) Granulation in UASB reactors. *Wat. Sci. Technol.* **15:**291-304.

Hulshof Pol, L. W. and Lettinga, G. (1986) New technologies for anaerobic wastewater treatment. *Water Science and Technology* **18:** 41-54.

Hulshof Pol, L. W., Heynekamp, K. and Lettinga, G. (1987) The selection pressure as driving force behind the granulation of sludge. In: *Proceedings of the GAMSAT Workshop, Lunteren, The Netherlands.*

Hungate, R. E., Smith W., Bauchop T., Yu I. K., and Rabinowitz J. C. (1970) Formate as an intermediate in the bovine rumen fermentation. *J. Bacteriol.* **102**:389-397.

Huser, A. A., Wuhrmann K., and Zehnder A. J. B. (1982) *Methanotrix soehngenii* gen. nov. sp. nov., a new acetotrophic non-hydrogen-oxidizing methane bacterium. *Arch. Microbiol.* **132**:1-9.

Ince O., Kasapgil Ince B. and Yenigün O. (2001) Determination of potential methane production capacity of a granular sludge from a pilot-scale upflow anaerobic sludge

blanket reactor using a specific methanogenic activity. *Journal of Chemical Technology and Biotechnology*, **76**:573-578

Ince O., Anderson G.K., and Kasapgil B. (1994) Use of the specific methanogenic activity test for controlling the stability performance in anaerobic digestion of brewery wastewater, in *Proc 49th Purdue Industrial Waste Conferenc*, Purdue University, Indiana, USA.

Ingraham, J. L., Painter P. R., Stanier R. Y., and Wheelis M. L. (1986) The Microbial World, Fifth Edition. Prentice-Hall, Englewood Cliffs, NJ.

International Energy Agency. (1996) *Biogas from Municipal Solid Waste: Overview of Systems and Market for Anaerobic Digestion of MSW,* Danish Energy Agency, Copenhagen, Denmark.

James A., Chernicharo C.A.L and Campos C.M.M. (1990) The development of a new methodology for the assessment of specific methanogenic activity. *Wat. Res.* **24**:813-825.

Jetten, M. S. M., Stams A. J. M., and Zehnder A. J. B. (1990) Acetate threshold values and acetate activating enzymes in methanogenic bacteria. *FEMS Microbial. Ecol.* **73**:339-344.

Jones, W. J., D. P. N. Jr., and Whitman W. B. (1987) Methanogens and the diversity of archaebacteria. *Microbiol. Rev.* **51**:135-177.

Kiener, A., and Leisinger T. (1983) Oxygen sensitivity of methanogenic bacteria. *Syst. Appl. Microbial.* **4**:305-312.

Kiene, R. P., Oremland R. S., Catena A., Miller L. G., Capone D. G. (1986) Methabolism of reduced methylated sulfur compounds in anaerobic sediments and by a pure culture of an estuarine methanogen. *Appl. Environ. Microbiol.* **52**:1037-1045.

Kiener, A., Orme-Johnson, W. H., and Walsh, C. T. (1988) Reversible conversion of coenzyme F420 to the 8-OH-AMP and 8-OH-GMP esters, F390-A and F390-G, on oxygen exposure and reestablishment of anaerobiosis in *Methanobacterium thermoautotrophicum. Arch. Microbiol.* **150**:249-253.

Kleerebezem R. and Macarie H. (2003) Anaerobic digestion comes of age, *Chemical Engineering,* **110**(4) PP.56-64.

Köberle. E. (1995) Animal Manure Digestion Systems in Central Europe. *Proceedings, Biomass Conference of the Americas II*, D.L. Klass, ed., National Renewable Energy Laboratory, Golden, CO.

Kosaric, N. And Blaszczyk, R. (1991) Advances in Biochemical Engineering, **41**, 28.

Kristjansson, J. K., Schönheit, P. and Thauer, R. K. (1982). Different K_S values for hydrogen of methanogenic bacteria and sulfate reducing bacteria: An explanation for the apparent inhibition of methanogens by sulfate. *Arch. Microbiol.*, **131**:278-282.

Kugelman, I. J. and Chin, K. K. (1971) Toxicity, synergism, and antagonism in anaerobic waste treatment processes. In: *Anaerobic Biological Treatment Processes*, F. G. Pohland (ed.) Advances in Chemical Series, **105**:55-90, American Chemical Society, Washington D. C.

Lawrence, A. W. and McCarty, P. L. (1969) Kinetics of methane fermentation in anaerobic treatment. *J. Wat. Poll. Cont. Fed*, **41**:R1-R17.

Lema J. M., Soto M., Veiga M. C. and Mendez R. (1987) Mesophilic and thermophilic anaerobic treatment of wastewater from industrial processing of mussel. *Biomass for energy and industry* (Edited by Grassi G. *et al.*), pp. 872-876. Elsevier, Amsterdam.

Leslie Grady C.P., Jr., Daigger Glen T., Lim Henry C. (1999) *Biological Wastewater Treatment,* Marcel Dekker Inc., New York.

Lettinga, G. (1978) *Proceedings of the 4th European Sewage and Refuge Symposium*, Munich, Germany.

Lettinga, G. and Van Haandel A.C. (1995) *Anaerobic Digestion for Energy Production and Environmental Protection: Renewable Energy: Sources for Fuels and Electricity* Island Press, Washington, DC, 1160 pp.

Liu, Y., Boone D. R., and Choy C. (1990) *Methanohalophilus oregonese* sp. nov., a methylotrophic methanogen from an alkaline, saline aquifer. *Internat. J. System. Bacteriol.* **40**:111-116.

Lin, C-Y., Sato, K., Noike, T. and Matsumoto, J. (1986) Methanogenic digestion using mixed substrate acetic, propionic and butyric acids. *Wat. Res.* **20**:385-394.

Lusk, P. (1996) *Deploying Anaerobic Digesters: Current Status and Future Possibilities.* This report was prepared for the National Renewable Energy Laboratory under NREL Subcontract No. CAE-6-13383-01 and sponsored by the Regional Biomass Energy Program of the US Department of Energy.

Lusk, P. (1995) *Methane Recovery from Animal Manures: A Current Opportunities Casebook,* U.S. Department of Energy, Washington, DC, DOE/EE-0062.

Lusk, P. (1996) *Methane Recovery from Industrial Wastes: A Current Opportunities Casebook.*

Madigan, M.T., Martinko J.M., and Parker J. (2000) *Brock biology of microorganisms.* 9th. Prentice Hall, Upper Saddle River, N.J.

Maestrojuan, G. M., Boone D. R., Xun L., Mah R. A., and Zhang L. (1990) Transfer of *Methanogenium bourgense, Methanogenium marisnigri, Methanogenium olentangyi, and Methanoculleus gen. Nov., emendation of Methanoculleuse marisnigri and methanogenium*, and description of new strains of *Methanoculleus bourgense* and *Methanoculleus marisnigri. Int. J. Syst. Bacterio.* **40**:117-122.

Mathrani, I. M., Boone D. R., Mah R. A., Fox G. E., and Lau P. P. (1988) Methanohalophilus zhilinae sp. nov. an alkaliphilic, halophilic methyltrophic methanogen. *Int. J. Syst. Bacteriol.* **38**:139-142.

Min, H., and Zinder S. H. (1989) Kinetics of acetate utilization by two thermophilic acetotrophic methanogens: *Methanosarcina* sp. strain CALS-1 and *Methanotrix* sp. strain CALS-1. *Appl. Environ. Microbiol.* **55**:488-491.

Monod, J. (1950) La technique de culture continue: theorie et applications. *Annals Institute Pasteur* **79**, 390 [in French].

Noike, T., Endo G. Chang J-E., Yaguchi J-I. and Matsumoto J-I. (1985) Characteristics of carbohydrate degradation and the rate-limiting step in anaerobic digestion. *Biotechnol. Bioeng.* **27**:1482-1488.

Ohtsubo, S., Demizu K., Kohno S., Miura I., Ogawa T., and Fukuda H. (1992) Comparison of acetate utilization among strains of an aceticlastic methanogen, *Methanotrix soehngenii. Appl. Environ. Microbiol.* **58**:703-705.

Oremland, R. S., Kiene R. P., Mathrani I. M., Whiticar M. J., and Boone D. R. (1989) Description of an estuarine methyltrophic methanogen which grows on dimethyl sulfide. Appl. Environ. Microbiol. **55**:994-1002.

Pal, Niropam (1999) Microbial Sequestration of Carbon Dioxide and Subsequent conversion to Methane, California Polytechnic State University San Luis Obispo, CA USA.

Patel, G. B. (1992) A contrary view of the proposal to assign a neotype strain for *Methanothrix soehngenii. Internat. J. System. Bacteriol.* **42**:324-326.

Pavolstathis S. G., Miller T. I. and Wolin M. J. (1990) Cellulose fermentation by continuous culture of *Ruminococcus albus and Methanobrevibacter smithii. Appl. Microbiol. Biotechnol.* **33**:109-116.

Peinemann, S., Müller V., Blaut M. and Gottschalk G. (1988) Bioenergetics of Methanogenesis from Acetate by Methanosarcina barkeri. *Journal of Bacteriology*, p. 1369-1372.

Praveen, V.V. and Ramachandran, K.B. (1993) *Proceedings of the Ninth National Convention of Institution of Engineers*, C.Ayyanna (Ed.), Vishakhapatnam, India.

Qasim, Syed R. (1999) *Wastewater treatment plants: planning, design, and operation*, Lancaster, Pa., Technomic Pub. Co.

Reeve, D.A. (2000) The Capture and Storage of Carbon Dioxide Emissions P.24, *office of Energy Research and Development Natural Resources*, Ottawa, Canada.

Riemer, P.W.F, and Ormerod, W.G. (1995) International perspectives and the results of carbon dioxide capture, disposal, and utilization studies. *Energy Conversion and Management.* **36**(6-9): 813-818

Robinson, J. A. and Tiedje, J. M. (1984) Competition between sulfate-reducing and methanogenic bacteria for H_2 under resting and growing conditions. *Arch. Microbial.* **137**:26-32.

Robinson, J. A. and Tiedje, J. M. (1982) Kinetics of hydrogen consumption by rumen fluid, anaerobic digester sludge and sediment. *Appl. Environ. Microbiol.* **44**:1374-1384.

Roh, Y., McMillan A.D., Lauf R.J. and Phelps T.J. (2000) Utilization of biomineralization processes for carbon sequestration. Abstract for *Annual meeting American Geophysical Union*, December 15-19, San Francisco, CA.

Sax and Lusk. (1995) Anaerobic Digestion of Municipal, Industrial, and Livestock Wastes for Energy Recovery and Disposal. *Proceedings, Biomass Conference of the Americas II*, D.L. Klass, ed., National Renewable Energy Laboratory, Golden, CO.

Schnellen, C. G. T. P. (1947) Onderzoekingen over de methaangisting, pp. 1-137. Ph.D. thesis, Delft.

Shao, Y. and Golomb D. (1997) Power plants with CO_2 capture using integrated air separation and flue gas recycling. *Energy Convers. Mgmt.* **37**, No. 6-8, pp. 903-908.

Smith, M. R. and Mah, R. A. (1978) Growth and methanogenesis by methanosarsina strain 227 on acetate and methanol. *Appl. Environ. Microbial.* **36**:870-879.

Soto, M., Mendez, R. and Lema, J. M. (1993) Methanogenic and non-Methanogenic activity tests. Theoretical basis and experimental set up *Wat. Res.* **27**, No 8, pp. 1361-1376.

Sowers, K. R., Nelson M. J., and Ferry J. G. (1984) Growth of acetotrophic, methane-producing bacteria in a pH auxostat, *Curr. Microbiol.*, **11,** 227.

Sowers, K. R., and Gunsalus R. P. (1988) Adaptation for growth at various saline concentrations by the archaebacterium *Methanosarcina thermophila. J. Bacteriol.* **170**:998-1002.

Suflita, J. M. and Concannon F. (1995) Screening tests for assessing the anaerobic biodegradation of pollutant chemicals in subsurface environments. *Journal of Microbiological Methods* **21**:267-281

Tchobanoglous G., Burton Franklin L., and Stensel David. H. (2003) *Wastewater Engineering; Treatment and Reuse.* Metcalf and Eddy, Inc. McGraw-Hill 4th ed.

Thauer, R. K., Jungermann K., and Decker K. (1977) Energy conservation in chemotrophic anaerobic bacteria. *Bacteriol. Rev.* **41**:100-180.

Thiele, J. H., and Zeikus J. G. (1988) Control of interspecies electron flow during anaerobic digestion: significance of formate transfer versus hydrogen transfer during synthrophic methanogenesis in flocs. *Appl. Environ. Microbiol.* **54**:20-29.

Tontiwachwuthikul, P. (1996) Research and development activities on high efficiency separation process technologies for carbon dioxide removal from industrial sources at University of Regina, Canada. *Energy Convers. Mgmt.* **37**, No. 6-8, pp. 93-940.

Uemura, S., and Harada H. (1995) Inorganic composition and microbial characteristics of methanogenic granular sludge grown in a thermophilic upflow anaerobic sludge blanket reactor. *Appl. Microbiol. Biotechnol.* **43**:358–364.

VanderWiel, D.P. Zilka-Marco J.L., Wang Y., Tonkovich A. Y., Wegeng R.S. (1999) Carbon Dioxide Conversions in Microreactors, Pacific Northwest National Laboratory, WA, USA.

Van den Berg, L. (1977) Effect of temperature on growth and activity of a methanogenic culture using acetate. *Can. J.Microbiol.*, **23**:898-902.

Van Haandel, A. C. and Lettinga, G. (1994). *Anaerobic sewage treatment. A practical guide for regions with a hot climate.* Chichester, England. John Wiley & Sons Ltd. 226 pp.

Wandrey, C. and Aviasidis A. (1983) Continuous anaerobic digestion with *Methanosarcina barkeri, Ann. N. Y.Acad. Sci.*, 413, 489.

Westermann, P., Ahring B. K., and Mah R. A. (1989) Temperature compensation in *Methanosarsina bakeri* by modulation of hydrogen and acetate affinity. *Appl. Environ. Microbiol.* **55**:1262-1266.

Widdel, F. (1986) Growth of methanogenic bacteria in pure culture with 2-propanol and other alcohols as hydrogen donors. *Appl. Environ. Microbiol.* **51**:1056-1062.

Widdel, F., Rouviére, P. E., and Wolfe, R. S. (1988) Classification of secondary alcohol-utilizing methanogens including a new thermophilic isolate. *Arch. Microbiol.* **150**:477-481.

Wolin, M. J. (1976) Interactions between H_2-producing and methane producing species. *In Microbial formation and utilization of gases (H_2, CH_4, CO),* Sclegel H. G., Gottsschalk G., and Pfennig N. (eds.), pp. 141-150.

Yadava, L. S. and Hesse P. R. (1981) The Development and Use of Biogas Technology in Rural Areas of Asia (A Status Report 1981). Improving Soil Fertility through Organic Recycling, FAO/UNDP Regional Project RAS/75/004, Project Field Document No. 10.

Zehnder, A. J. B., Husser, B. A., Brock, T. D. and Wuhrmann, K. (1980) Characteristics of an decarboxylating, non-hydrogen-oxidizing methane bacterium. *Arch. Microbiol.* **124**:1-11.

Zinder, S. H. and Mah R. A. (1979) Isolation and characterization of a thermophilic strain of *Methanosarsina* unable to use H_2-CO_2 for methanogenesis. *Appl. Environ. Microbiol.* **38**:996-1008.

Zellner, G. and Winter J. (1987a) Secondary alcohols as hydrogen donors for CO_2-reduction by methanogens. *FEMS Microbiol. Lett.* **44**:323-328.

Websites used:

- Biogas technology. (1996) A training manual for extension Food and Agriculture Organization/Consolidated Management Services Kathmandu. (http://www.fao.org/sd/EGdirect/EGre0022.htm)

- Frenkel, Gerald. (2004) Michaelis-Menten Model of Enzyme Kinetics (http://tecn.rutgers.edu/bio301s/michaelismenten_kinetics.htm)

- Takle, Eugene S. (1996) Atmospheric composition, carbon dioxide (http://www.iitap.iastate.edu/gcp/chem/gases/gases_lecture.html)

- US Environmental Protection Agency (EPA). (2004) Global Warming: Climate (http://yosemite.epa.gov/oar/globalwarming.nsf/content/Climate.html)

-U.S. Department of Energy, National Energy Technology Laboratory. (2004) Pilot experiment for geological sequestration of carbon dioxide in saline aquifer brine formation. (2004) (http://www.netl.doe.gov/coalpower/sequestration/index.html)

- University of Waterloo. (2004) Environmental Microbiology (http://wvlc.uwaterloo.ca/biology447/modules/module7/7b4_s1.htm)

-Woster, Patrick M. (2004) Enzymes - Kinetics and Catalysis

(http://wiz2.pharm.wayne.edu/biochem/enz.html)

- White, Chris. (2004) Anaerobic Digestion, Biotank Ltd. Radar House Willingale Road Fyfield Ongar Essex. CM5 0SD UK

(http://www.biotank.co.uk/anaerobic_digestion.htm)

APPENDIX

A-Reference curve for measuring methane content of the biogas

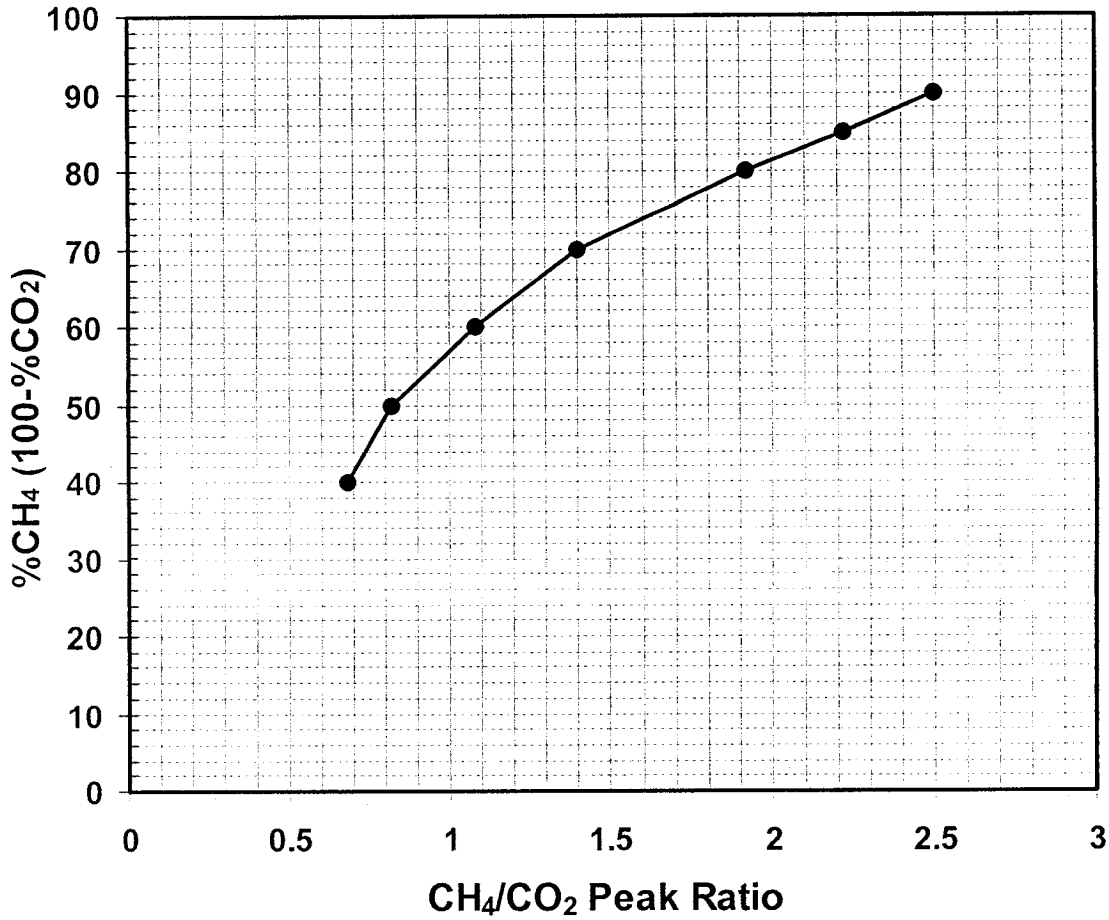

Figure A.1 The reference curve prepared in this work to determine the biogas purity.

B- Calculation table for concentration of dissolved carbon dioxide programmed in this work using Microsoft Excel.

When the values of the input data are entered, the values of output data are automatically calculated. The related equations are described in Section 3.3.4 and the results for a sample calculation are shown in Table A.1.

Table B.1 Sample calculation for the amount of dissolved carbon dioxide.

Input Data	
Parameter	**Value**
$T\ (^{\circ}C)$	25
PH	7
$Alk\ (\frac{g}{L} CaCO_3)$	1
Calculated Values	
Parameter	**Value**
$T(^{\circ}K)$	298.15
$*\ Pk_1$	6.351
$*\ Pk_2$	10.329
k_1	4.46 E-07
k_2	4.69 E-11
$[HCO_3^-]$(M)	9.99 E-3
$[CO_3^{2-}]$(M)	4.68 E-6
$[CO_2](\frac{g}{L})$	9.86 E-2
$[CO_2](\frac{L}{L(H_2O)})$	5.48 E-2

* Pk = -Log k. Correlations for values of Pk at different temperatures are from " Handbook of Chemistry and Physics: Lide David L. (2002-2003), Sec. 7-12, CRC Press, LLC.

C- Simpson's rule to calculate the area under a curve

In this method, in order to calculate the surface area under a curve with the equation Y= f(x) between two points (x = a) and (x = b), f(x) is approximated by a parabola.

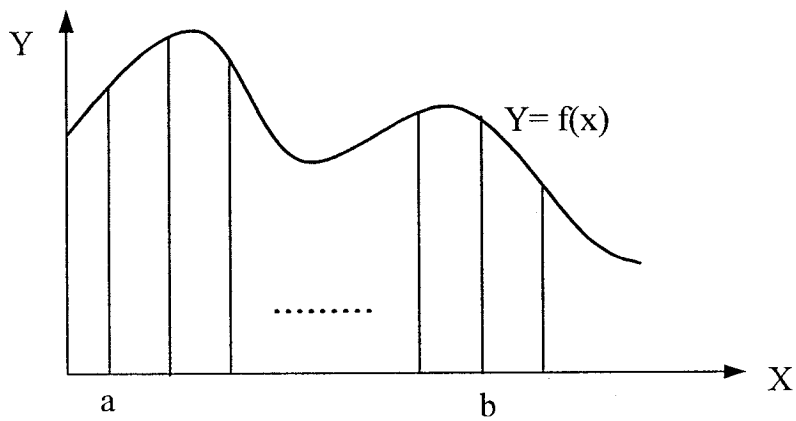

Figure C.1 Numerical integration of function Y=f(x) over the interval [a,b].

For "even" numbers of subintervals, n, the area under f(x) was calculated using the following formula:

$$\int_a^b f(x)dx \approx \frac{\Delta x}{3}\left[f(x_0)+4f(x_1)+2f(x_2)+4f(x_3)+2f(x_4)+....+4f(x_{n-1})+f(x_n)\right]$$

where; $\Delta X = \frac{b-a}{n}$

Here, Y = biogas rate (L/d) and x = time (d).

D- Glossary and abbreviations

Archaea

Archaea are prokaryotes that do not incorporate muramic acid into their cell walls, and represent a highly diverse group of organisms living at environmental extremes that represent one of the three taxonomic kingdoms.

Anabolism

Also referred to as 'constructive' metabolism. It is the process of converting simple molecules to more complex molecules. An example include the *de novo* synthesis of precursors, or building blocks, used for the synthesis of macromolecules such as proteins and nucleic acids. The assembly of the precursors into macromolecules would also be an example of anabolism. The antonym is catabolism.

ATP

Adenosine triphosphate. The primary source of energy for cells. The third phosphate is hydrolyzed by enzymes called ATPases resulting in the formation of ADP (adenosine diphosphate) and phosphate. The energy stored in the hydrolyzed phosphate bond is captured and used to carry out a function associated with that particular ATPase.

Catabolism

Also referred to as 'destructive' metabolism. It is the opposite of anabolism and involves breakdown of molecules into simpler components. For example, the breakdown and oxidation of glucose to carbon dioxide and the capture of the released energy in the form of ATP is a catabolic process. Catabolism also includes the breakdown of macromolecules into their monomeric units.

Coenzyme

A molecule that binds to an enzyme and is essential for its activity, but is not permanently altered by the reaction. Many coenzymes are derived from vitamins.

Enzyme

A protein which accelerates a biochemical reaction without being modified or just temporarily.

Fatty acid

An organic acid molecule consisting of a chain of carbon molecules and a carboxylic acid (COOH) group. Fatty acids are found in fats, oils, and as components of a number of essential lipids and can be burned by the body for energy.

Hydrogenase

An enzyme of various microorganisms that promotes the formation and utilization of gaseous hydrogen.

Inoculum

A substance or organism that is introduced into surroundings suited to cell growth.

Metabolism

All biochemical reactions in a cell, both anabolic and catabolic.

Methanogens

Methane-producing prokaryotes, which are members of the Archaea.

Minerals

Nutritionally significant elements. Elements are composed of only one kind of atom. Minerals are inorganic and they do not contain carbon as do vitamins and other organic compounds.

PPm

Part per million. It is a unit for expressing small concentrations.

Prokaryote

An organism whose cells lack a membrane-bound, structurally discrete nucleus and other subcellular compartments.

Respiration

An energy-yielding metabolic process in which electrons from an oxidizable substrate are transferred by a series of oxidatin-reduction reactions to a terminal electron acceptor such as oxygen, nitrate, etc.

Respirometer

A device to determine the microbial activity by measuring the volume of biogas produced in anaerobic digestion.

Stock solution

Stock solution is a concentrated solution of certain components, which is prepared as a way of avoiding frequent solution making. The working solutions are made by diluting the stock solutions.

Substrate

A molecule that binds to an enzyme and undergoes a chemical change during the ensuing enzymatic reaction.

Syntrophy

Syntrophy is the name given to the association between two species of microorganisms (which are called syntrophic cultures), growing in the same culture environment, where each exhibits growth characteristics that depend on the presence of the other organism. (http://lpi.oregonstate.edu/infocenter/glossary.html)

Total Suspended Solids (TSS)

A measure of the total suspended solids in water, both organic and inorganic.

Volatile Suspended Solids (VSS)

The portion of the TSS that is lost after ignition. This represents the organic part of the TSS.

(http://www.tnrcc.state.tx.us/admin/topdoc/gi/252/appb.pdf)

E-Indexes

0 = initial

1,2,3...= reaction constant indices indicating the reaction orders

a = actual

abs = absorbed

b = biogas

d = death

e = effluent

g = growth

i = influent

m = methane

max = maximum

ove. = overall

r = reference

rem. = removed

s = sample

t = total